



Differential cross-section measurements of coherent production of singly and doubly resonant top-quark in $WWbb$ events with one lepton at $\sqrt{s} = 13$ TeV with the ATLAS detector

The ATLAS Collaboration

This paper presents differential cross-section measurements of events containing a charged lepton, missing transverse momentum, two b -jets, and two light jets, consistent with the $W^+W^-b\bar{b}$ final state. The analysis is based on 140 fb^{-1} of proton–proton collision data at $\sqrt{s} = 13$ TeV recorded with the ATLAS detector during Run 2 of the Large Hadron Collider (2015–2018). Differential cross-sections are unfolded at particle level for a range of kinematic observables and in three kinematic regions. Both regions and observables are optimised for sensitivity to the interference between $W^+W^-b\bar{b}$ produced with singly and doubly resonant top quarks. Results are compared with various theoretical predictions. Significant discrepancies are observed in regions sensitive to the interference between singly and doubly resonant top-quark production. The unfolded results provide new information about the modelling of interference and off-shell effects of the $W^+W^-b\bar{b}$ final state, improving the understanding of top-quark production mechanisms and providing new inputs for future Monte Carlo generator development.

1 Introduction

The study of the top quark is a cornerstone of the Large Hadron Collider (LHC) [1] physics programme. At the LHC, top quarks are predominantly produced in top–antitop-quark pairs. This process is referred to as doubly resonant top-quark production, or $t\bar{t}$, in the following. Additionally, top quarks can be produced individually via singly resonant top-quark production, which occurs through three main channels: the t -, s -, and tW -channels. The t -channel involves the exchange of a virtual W boson and is characterised by the scattering of a light quark, making it the most abundant single-top production mode. The s -channel proceeds through the production of a virtual W boson that decays into a top-quark and a bottom quark. Lastly, the tW -channel involves the production of a single top quark in association with a W boson. The top quark decays into a W boson and a bottom quark (b) with a branching fraction of approximately 100%. When considering all processes at next-to-leading (NLO) accuracy in quantum chromodynamics (QCD), the associated production of a single resonant top-quark and a W boson, or tWb , has the same final state as doubly resonant top-quark production. Traditionally these processes have been treated separately in theory calculations and experimental measurements, due to their large cross-section differences and the non-trivial interplay between leading order (LO) and NLO between the two processes¹.

Differential cross-sections for $t\bar{t}$ production have been measured by the ATLAS [2–6] and CMS [7–10] Collaborations and accurate theory calculations have been performed [11–13]. Differential cross-sections for tW production have also been measured by the two LHC experiments [14–20]. A dedicated procedure [21–25] is used to define single-top-quark cross-sections and Monte Carlo predictions not including the doubly resonant top-quark production. The separation of single and double top-quark production is subject to a certain degree of arbitrariness, related to the treatment of interferences and off-shell top-quark (finite-width) effects. This theory approximation provides a significant source of uncertainty for many measurements [3, 26–28] and searches for physics beyond the Standard Model (BSM) [29–39]. For this reason, a coherent treatment of singly and doubly top resonant production is desirable. This can be achieved considering the complete process $pp \rightarrow W^+W^-b\bar{b}$. The $W^+W^-b\bar{b}$ topology can arise from doubly resonant top-quark processes (Figure 1(a)), singly resonant top-quark processes (Figure 1(b)), non-resonant diagrams without intermediate top quarks (Figure 1(c)) and their interference. The consistent calculation of the $W^+W^-b\bar{b}$ process was performed up to NLO order in QCD [40] and supplemented with parton showers [41, 42]. A calculation of the process $pp \rightarrow \ell\nu b\bar{b}jj$ was performed up to NLO in Ref. [43]. The only existing measurements to assess these predictions in a region sensitive to the interplay between singly and doubly resonant top-quark processes have been performed in final states with two light charged leptons [6, 44, 45].

This paper considers events with at least one leptonically decaying W boson. The final state is characterised by a light charged lepton (e or μ), missing transverse momentum, and three or four jets, of which two identified as originating from b -quarks (b -jets). The focus of this measurement is singly and doubly resonant top quark production: $t\bar{t}$ and tWb . Differential cross-sections on key top-quark physics observables are extracted using an unfolding procedure at particle level. The analysis selections, fiducial volumes and observables are optimised to probe a kinematic phase space where the interplay (and interference) between the two processes is enhanced, using dedicated requirements to actively suppress the pure doubly resonant top-quark production. The non-resonant $W^+W^-b\bar{b}$ production is not explicitly enhanced in these selections and has therefore a negligible contribution to the analysis selections. In comparison with measurements requiring two light charged leptons in the final state, the single-lepton channel provides the opportunity to

¹ At NLO, the $g\bar{b} \rightarrow WWb$ process receives radiative corrections that include contributions overlapping with the LO $g\bar{g} \rightarrow W^+W^-b\bar{b}$ process ($t\bar{t}$). The contribution of the latter, being $t\bar{t}$ mediated, is much larger than the former.

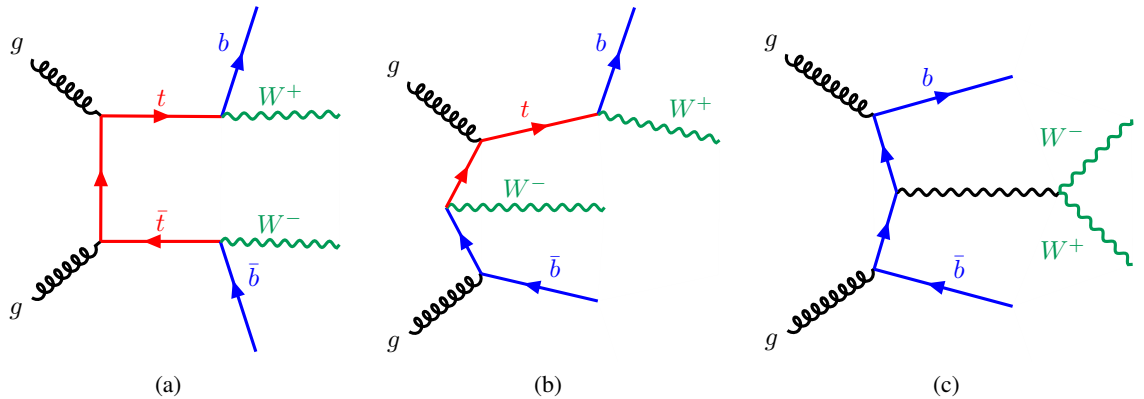


Figure 1: Feynman diagram of the $W^+W^-b\bar{b}$ production. The $W^+W^-b\bar{b}$ topology can arise from (a) doubly resonant top-quark processes, (b) singly resonant top-quark processes, (c) diagrams without intermediate top-quarks, and their interference.

measure the W boson kinematic properties directly, since the hadronically decaying W boson can be fully reconstructed. In addition, the larger branching ratio gives access to kinematic regions of the phase space characterised by more extreme momenta. The analysis therefore focusses on three kinematic regions. The inclusive region (IR), designed to study both single and double top-quark processes and their interference in the broadest possible phase space; the W -hadronic region (WR), which directly probes the $W^+W^-b\bar{b}$ process by studying the kinematic properties of the W boson and b -jet kinematic observables and thus provides constraints on higher-order corrections or the modelling of real emissions; and the search-like region (SLR), which takes inspiration from a number of BSM searches [29–32, 46, 47] that probe less inclusive corners of the phase space where the interference effects between $t\bar{t}$ and tWb processes are found to be enhanced.

The results of this paper are compared with various state-of-the-art simulations and can be used in the development of new predictions. The full data sample collected with the ATLAS detector between 2015 and 2018 at centre-of-mass energy $\sqrt{s} = 13$ TeV with an integrated luminosity of $\mathcal{L} = 140 \text{ fb}^{-1}$ is used for the measurement.

2 Experimental and simulation setups

2.1 The ATLAS experiment

The ATLAS experiment [48] at the LHC is a multi-purpose particle detector with a forward–backward symmetric cylindrical geometry and a near 4π coverage in solid angle.² It consists of an inner tracking detector surrounded by a thin superconducting solenoid providing a 2 T axial magnetic field, electromagnetic and hadronic calorimeters, and a muon spectrometer. The inner tracking detector (ID) covers the pseudorapidity range $|\eta| < 2.5$. It consists of silicon pixel, silicon microstrip, and transition radiation

² ATLAS uses a right-handed coordinate system with its origin at the nominal interaction point (IP) in the centre of the detector and the z -axis along the beam pipe. The x -axis points from the IP to the centre of the LHC ring, and the y -axis points upwards. Polar coordinates (r, ϕ) are used in the transverse plane, ϕ being the azimuthal angle around the z -axis. The pseudorapidity is defined in terms of the polar angle θ as $\eta = -\ln \tan(\theta/2)$. Angular distance is measured in units of $\Delta R \equiv \sqrt{(\Delta\eta)^2 + (\Delta\phi)^2}$.

tracking detectors. Lead/liquid-argon (LAr) sampling calorimeters provide electromagnetic (EM) energy measurements with high granularity within the region $|\eta| < 3.2$. A steel/scintillator-tile hadronic calorimeter covers the central pseudorapidity range ($|\eta| < 1.7$). The endcap and forward regions are instrumented with LAr calorimeters for EM and hadronic energy measurements up to $|\eta| = 4.9$. The muon spectrometer surrounds the calorimeters and is based on three large superconducting air-core toroidal magnets with eight coils each. The field integral of the toroids ranges between 2.0 and 6.0 T m across most of the detector. The muon spectrometer includes a system of precision tracking chambers up to $|\eta| = 2.7$ and fast detectors for triggering up to $|\eta| = 2.4$. The luminosity is measured mainly by the LUCID-2 [49] detector which is located close to the beampipe. A two-level trigger system is used to select events [50]. The first-level trigger is implemented in hardware and uses a subset of the detector information to accept events at a rate close to 100 kHz. This is followed by a software-based trigger that reduces the accepted rate of complete events to 1.25 kHz on average depending on the data-taking conditions. A software suite [51] is used in data simulation, in the reconstruction and analysis of real and simulated data, in detector operations, and in the trigger and data acquisition systems of the experiment.

2.2 Object reconstruction

Each physics object included in the event selection is defined by a collection of detector information and is reconstructed using dedicated algorithms. These reconstructed particles are referred to as detector-level objects in the following text.

Electron candidates are reconstructed from energy deposits (clusters) in the electromagnetic calorimeter associated with reconstructed tracks in the inner detector [52]. Candidates that have a transverse momentum $p_T > 10$ GeV and $|\eta| < 2.47$ are selected, excluding the calorimeter transition region $1.37 < |\eta| < 1.52$. Electrons in this measurement must satisfy the *Tight* likelihood-based identification criterion [52]. Muon candidates are reconstructed from track segments in the various layers of the muon spectrometer, and matched with tracks from the inner detector [53]. The final muon candidates are refitted using the complete track information from both detector systems, and required to satisfy $p_T > 10$ GeV and $|\eta| < 2.5$. Muons are required to satisfy the *Medium* identification requirements. Both electrons and muons are required to meet the tight working point of the prompt-lepton isolation discriminant [54], trained to separate prompt and non-prompt leptons. Electrons (muons) are further required to have $|z_0 \sin(\theta)| < 0.5$ mm and $|d_0/\sigma(d_0)| < 5$ (3), where the longitudinal and transverse impact parameters d_0 and z_0 are computed relative to the primary vertex, and $\sigma(d_0)$ is the resolution of the track transverse impact parameter d_0 [55]. Calibrations of the electron and muon energy scale and resolution, as well as corrections to the reconstruction, identification and isolation efficiencies are applied following Refs. [52, 53, 56, 57]. A secondary set of (fake) electrons and muons candidates is used in the estimate of background arising from misidentified and non-prompt lepton sources. Electron candidates in the fakes category are required to fulfil all kinematic requirements of standard electrons. They are additionally required to satisfy the *Loose* likelihood-based identification criterion but fail to meet either the tight identification requirement or the isolation requirements. Muon candidates in the fakes category are required to fulfil all kinematic and identification requirements of standard muons, but fail to satisfy the isolation requirements.

Jets are reconstructed using the anti- k_r algorithm [58] as implemented in FastJet [59] with a jet radius parameter $R = 0.4$. The inputs to this algorithm are particle flow (PFlow) objects [60], which combine measurements from the ATLAS inner detector and calorimeters [61] to improve the jet energy resolution and increase the jet reconstruction efficiency, especially at low jet p_T . Jets are required to have $p_T > 25$ GeV and $|\eta| < 2.5$. Jets originating from pile-up interactions are rejected using the *jet vertex tagger* (JVT)

tool [62], which uses a combination of track-based variables providing discrimination against pile-up jets. The Tight working point is used for jets in the momentum range $20 < p_T < 60$ GeV and $|\eta| < 2.4$. Calibrations (and their associated uncertainties) are applied in the measurement to the jet energy scale (JES) and resolution (JER) [63], which include components derived both from simulation and in situ measurements. The identification of b -jets is made using the DL1r b -tagging algorithm [64], a high-level tagger based on a deep neural network and it is applied to jets satisfying the selections stated above. In this measurement, a working point with a b -tagging efficiency of 77% is used, as evaluated in simulated $t\bar{t}$ events. The corresponding rejection factors are 6 for charm-jets and 134 for light-jets, respectively. Correction factors are applied to the simulated event samples to compensate for differences between data and simulation in the b -tagging efficiency for b -, c - and light-jets.

The missing transverse momentum, with magnitude E_T^{miss} , is defined as the negative vector sum of the transverse momenta of all selected and calibrated electrons, muons and jets in the event, with an extra track-based term added to account for energy in the event that is not associated with any of these objects [65].

To avoid double-counting in the analysis due to reconstruction ambiguities, objects are removed based on the distance $\Delta R_y = \sqrt{(\Delta y)^2 + (\Delta\phi)^2}$, where y is rapidity. If an electron and a muon overlap within $\Delta R_y = 0.1$, the muon is removed if it is reconstructed only from an ID track and calorimeter energy deposits consistent with a minimum-ionising particle, otherwise the electron is removed. Then, jets within $\Delta R_y = 0.2$ of an electron are removed. If a jet within $\Delta R_y = 0.4$ survives, the electron is discarded. Muons are removed if $\Delta R_y < 0.4$ from a jet, but if the jet has fewer than three tracks, the jet is removed instead, ensuring efficient selection of high-energy muons affected by calorimeter energy loss.

2.3 Modelling and simulation of Standard Model processes

Monte Carlo (MC) simulated event samples of all major Standard Model (SM) processes are used to aid in the estimation of the differential cross-sections and the unfolding procedure. They are additionally used to estimate systematic uncertainties arising from the theory modelling of such processes. The ATLAS detector response is simulated using a detailed description of the detector geometry and response [66] based on Geant4 [67] or through a fast simulation using a parameterisation of the calorimeter response and Geant4 for the other parts of the detector. Detector-level objects are reconstructed in simulated events using the same algorithms used to process the data, with appropriate performance corrections and calibrations applied. The matrix element (ME) generator, parton shower (PS), cross-section accuracy (CS) and specific tools used for their calculation, parton distribution function (PDF) set and the set of tuned parameters (tune) for these samples are given in Table 1, and more details of the generator configurations can be found in Refs. [25, 68–70] and are briefly summarised in the following text. All simulation samples, except for SHERPA, use EVTGEN [71] to model the decays of bottom and charm hadrons. The effect of multiple interactions in the same and neighbouring bunch crossings (pile-up) is modelled by overlaying the simulated hard-scattering event with inelastic proton–proton (pp) events generated with PYTHIA 8.186 [72] using the NNPDF2.3LO set of PDFs [73] and the A3 set of tuned parameters [74]. Events are weighted to reproduce the distribution of the average number of interactions per bunch crossing ($\langle\mu\rangle$) observed in the data. The $\langle\mu\rangle$ value in data is rescaled by a factor of 1.03 ± 0.04 to improve agreement between data and simulation in the visible inelastic pp cross-section [75].

Modelling of the signal processes This measurement targets singly and doubly resonant top quark production: $tW(b)$ and $t\bar{t}$. Simulation samples of these processes are used to estimate the unfolding parameters needed to extract fiducial differential cross-sections at particle-level and to estimate the systematic uncertainties associated with the modelling of these processes. These simulation samples are also used to construct the pseudo-data sample used to estimate the closure and robustness of the unfolding procedure.

The production of both final states is modelled using the POWHEG BOX v2 [76–79] generator, which provides MEs at NLO in the strong coupling constant α_s , and is interfaced with PYTHIA 8.2 [80] for the parton shower and hadronisation according to the settings described in Table 1. The generation of both processes uses the five-flavour scheme. The top quark mass, m_{top} , is set to 172.5 GeV. The h_{damp} parameter, which controls the matching in POWHEG and effectively regulates the high- p_T radiation against which the $t\bar{t}$ or tW system recoils, is set to $1.5 m_{\text{top}}$ [25]. The functional form of the renormalisation and factorisation scales is set to the default dynamic scale $\sqrt{m_{\text{top}}^2 + p_T^2}$. The definition of the tW sample is chosen to enable combination with the corresponding $t\bar{t}$ calculation. This is non-trivial at NLO, where care must be taken to avoid double-counting tWb events with $m_{bW} \sim m_{\text{top}}$. The default scheme for combining the $t\bar{t}$ and tW processes at NLO adopted here is diagram removal (DR) [22] in which all doubly resonant amplitudes are removed from the tW sample. Other choices exist (see Ref. [24] for a review), for example the case where doubly resonant contributions are canceled out by gauge-invariant subtraction terms (diagram subtraction, DS) [22, 25]. The $t\bar{t}$ sample is normalised to a cross-section of $831.8_{-36.5}^{+29.3}$ pb. The cross-section prediction is calculated at next-to-next-to-leading-order (NNLO) in QCD including the resummation of next-to-next-to-leading logarithmic (NNLL) soft-gluon terms calculated using TOP++ 2.0 [11, 81–86]. The tW sample is normalised to a cross-section of $79.3_{-2.8}^{+2.9}$ pb. This cross-section prediction is calculated at NLO in QCD with NNLL soft-gluon corrections [87–89].

Additional uncertainties associated with the modelling of $t\bar{t}$ and $tW(b)$ processes have been considered using alternative simulation samples.

The impact of using a different parton shower and hadronisation model is evaluated with a simulation sample produced with an alternative shower generator (HERWIG [90–93]), see Table 1. Furthermore, effects associated with the parameters that regulate the matching between ME and PS generators are estimated by varying the $p_{T,\text{hard}}$ parameter according to the studies in Ref. [94]. The top-quark recoil model is also varied in such a way that the parton shower of the nominal $t\bar{t}$ sample employs the recoiling against the top-quark instead of b -quarks. Uncertainties from missing higher orders are evaluated [95] using two-point variations of the QCD factorisation and renormalisation scales in the matrix elements by factors of 0.5 and 2.

To assess the uncertainties related to the modelling of the initial-state radiation (ISR), the sample is reweighted using the Var3c up variation from the A14 tune, which changes the scales in the ISR shower in PYTHIA. The impact of final-state radiation (FSR) is evaluated by varying the renormalisation scale for emissions from the parton shower up and down by a factor of two. The uncertainties in the cross-section due to the PDF and α_s are calculated using the PDF4LHC15 prescription [96] and are added in quadrature to the effect of the scale uncertainty. Alternative simulation samples with varied h_{damp} parameter ($3 m_{\text{top}}$) value and varied top-quark mass values (equivalent to a variation of $\pm 0.5 m_{\text{top}}$) were also used to estimate the impact of these parameters on the modelling of the $t\bar{t}$ and tW processes. An alternative tW sample generated with the DS scheme is used to estimate the impact of the double-counting removal procedure used to generate $tW(b)$ events. It is also used as an alternative prediction when comparing to the final result.

Finally, a sample aims to model $t\bar{t}$ processes at NNLO QCD and incorporates all-order radiative corrections through parton-shower simulations as detailed in Ref. [97]. This sample is generated using a procedure that consists of three steps. In the first step $t\bar{t}$ pairs plus one light parton are generated using the POWHEG BOX v2 program, which performs an NLO calculation and includes a second light parton. The second step involves computing the limit in which the emitted light partons become collinear with the $t\bar{t}$ system. This step incorporates Sudakov form factors and relevant higher-order corrections to ensure the result remains well-behaved and accurate at NNLO for inclusive $t\bar{t}$ production. The third step explicitly generates the kinematic properties of the second radiated parton using POWHEG BOX v2, since this was only treated inclusively in the initial stage. This ensures that the NLO accuracy of the $t\bar{t}$ +jet cross-section is maintained. Following this step, additional radiation is simulated using the PS method of Pythia. This sample is referred to as the “MiNNLOPS” sample in the paper and is used only in the final comparison with the unfolded results. The sample is normalised to the same cross-section at NNLO+NNLL in pQCD calculated with the Top++ 2.0 program, as previously mentioned.

Modelling of the background processes All relevant SM background processes, with the exception of the QCD multi-jet background, are estimated with the aid of MC simulation samples. The most important processes are the production of vector bosons in association with jets (V + jets), diboson production (VV), $t\bar{t}H$, $t\bar{t}V$ and single top (s - and t -channel) production. The production of single-boson and diboson processes is simulated using the SHERPA 2.2.1 [98]. The V + jets (VV) processes are simulated at NLO MEs for up to two (one) partons, and LO matrix elements for up to five (three) partons calculated with the COMIX [99] and OPENLOOPS [100–102] libraries. The matrix element calculations are matched and merged with the SHERPA parton shower based on Catani–Seymour dipole factorisation [99, 103] using the MEPS@NLO prescription [104–107]. The diboson simulation samples include off-shell effects and Higgs boson contributions, where appropriate. The V + jets simulation samples include electroweak virtual corrections [108, 109]. An additional data-driven normalisation correction is applied to the W + jets processes as described in Section 4. Single-top-quark (s - and t -channel) processes are simulated using the POWHEG BOX v2 generator interfaced with PYTHIA. The $t\bar{t}H$ and $t\bar{t}V$ processes are simulated using the POWHEG BOX v2 and MADGRAPH5_AMC@NLO [110] generators, respectively.

Table 1: Summary of the generator settings used for the Monte Carlo simulation samples. The columns indicate the physics process, the matrix element (ME) generator, the parton shower (PS) generator, the cross-section accuracy (CS), the parton distribution function (PDF) set, the tune used for the underlying event, and the program used for the b/c hadron decays. MADGRAPH5_AMC@NLO is here referred to as MG. See text for further details.

Process	ME	PS	CS	PDF	Tune	b/c decays
$t\bar{t}$	POWHEG BOX v2	PYTHIA 8.230	NNLO+NNLL (TOP++ 2.0)	NNPDF3.0NLO	A14 tune + NNPDF2.3LO	EvtGEN 1.6.0
tW	POWHEG BOX v2	PYTHIA 8.230	NLO+NNLL	NNPDF3.0NLO	A14 tune + NNPDF2.3LO	EvtGEN 1.6.0
$t\bar{t}$ (alt.)	POWHEG BOX v2	HERWIG 7.1.3	NNLO+NNLL	NNPDF3.0NLO	H7 def. + MMHT2014LO	EvtGEN 1.6.0
tW (alt.)	POWHEG BOX v2	HERWIG 7.2.3	NLO+NNLL	NNPDF3.0NLO	H7 def. + MMHT2014LO	EvtGEN 1.6.0
$t\bar{t}$ MiNNLOPS	MiNNLOPS + POWHEG BOX v2	PYTHIA 8.230	NNLO+NNLL	NNPDF3.0NLO	A14 tune + NNPDF2.3LO	EvtGEN 1.6.0
V +jets	SHERPA 2.2.11	SHERPA	NLO	NNPDF3.0NNLO	SHERPA tune	
VV	SHERPA 2.2.11	SHERPA	NLO	NNPDF3.0NNLO	SHERPA tune	
s and t -chan- nel single- t	POWHEG BOX v2	PYTHIA 8.230	NLO (HATHOR 2.1 [111, 112])	NNPDF3.0NLO	A14 tune + NNPDF2.3LO	EvtGEN 1.6.0
$t\bar{t}H$	POWHEG BOX v2	PYTHIA 8.230	NLO QCD & EW [113]	NNPDF3.0NLO	A14 tune + NNPDF2.3LO	EvtGEN 1.6.0
$t\bar{t}V$	MG 2.3.3	PYTHIA 8.210	NLO QCD & EW	NNPDF3.0NLO	A14 tune + NNPDF2.3LO	EvtGEN 1.2.0

The background arising from QCD multi-jets events containing misidentified or non-prompt leptons is estimated using a data-driven *fake-factor* method as described in Section 4. Simulation samples as described in this section are used to subtract the prompt-lepton contamination of the non-prompt estimation region and to estimate the systematic uncertainties, including the ones associated with the extrapolation to the phase space of this measurement.

3 Event selection

The results presented in this paper are based on data collected with the ATLAS experiment between 2015 and 2018 during Run 2 of the LHC. The data sample corresponds to an integrated luminosity of 140 fb^{-1} [49, 114] of pp collisions at a center-of-mass energy of 13 TeV. The measurement of the integrated luminosity is obtained using the LUCID-2 detector for the primary measurement and complemented by measurements in the inner detector and calorimeters. Every detector subsystem must have been in operation during data collection. Moreover, stringent data quality criteria are applied to ensure the reliability of the data [115]. Events are required to be triggered by a collection of single-electron or single-muon triggers [50, 116, 117] operating at different thresholds of transverse momentum and identification criteria through the data-taking periods. Events are required to contain at least one collision vertex with two or more associated tracks with $p_T > 500 \text{ MeV}$, and the vertex with the highest p_T^2 sum of the associated tracks is taken as the primary vertex (PV) [118] of the event.

Table 2: Summary of the selections used in the three measurement regions: inclusive region (IR), W -hadronic region (WR) and search-like region (SLR). Details on the definition of the hadronic W candidate, $W_{\text{had.}}$, and the invariant mass quantities m_T^ℓ and $m_{b\ell}^{\text{min}}$ are given in the text.

Requirements		
<i>preselection</i>	$N_{b\text{-jets}}$	≥ 2
	$N_\ell(p_T > 10 \text{ GeV})$	$= 1$
	$E_T^{\text{miss}} + m_T^\ell$	$\geq 60 \text{ GeV}$
	$p_T(\ell)$	$\geq 30 \text{ GeV}$
<i>IR</i>	N_{jets}	≥ 4
<i>WR</i>	N_{jets}	≥ 3
	$p_T(W_{\text{had.}})$	$\geq 80 \text{ GeV}$
	$60 < m(W_{\text{had.}}) < 100 \text{ GeV}$	
<i>SLR</i>	N_{jets}	≥ 4
	$m_{b\ell}^{\text{min}}$	$\geq 150 \text{ GeV}$
	$p_T(j_1), p_T(j_2)$	$\geq 50 \text{ GeV}$
	$p_T(b_1), p_T(b_2)$	$\geq 160, 50 \text{ GeV}$
	$1.4 < \Delta R(b_1, b_2)$	
	$E_T^{\text{miss}} \geq -0.625 p_T(\ell) + 270 \text{ GeV}$	

The target topology of this measurement are events containing two W bosons, one decaying leptonically

and one hadronically, and two b -jets, arising from $t\bar{t}$ or tWb production. To select this topology, the events are required to contain exactly one light charged lepton (ℓ , either an electron or a muon) with $p_T > 30$ GeV, which ensures the full efficiency of the triggers. Any event containing an additional lepton with $p_T > 10$ GeV is rejected. Events are also required to have at least four jets, of which at least two are b -jets. An additional requirement on the sum of the E_T^{miss} and the m_T^ℓ , the transverse mass between the E_T^{miss} and the lepton³, of greater than 60 GeV is applied to suppress contaminations from the misidentified and non-prompt lepton background.

As introduced before, three kinematic regions are used in this measurement: the inclusive region IR, the W -hadronic region WR and the search-like region SLR. The selection criteria described so far define the IR.

The WR is defined by explicitly requiring a hadronically decaying W boson in the final state. A W boson reconstruction algorithm is optimised to maximize the overall W identification purity with a procedure that is equally easy to apply on detector-level objects and particle-level objects. This procedure identifies the W candidate as either the leading jet, the subleading jet, or their vectorial sum, with b -jets excluded from this procedure. This approach aims to increase the purity of W identification in the high- p_T region, where the boosted W boson decay products are collimated and the W boson is reconstructed as a single jet. The candidate with a mass closest to the W mass is selected. The mass of the candidate is required to be between $60 < m_W < 100$ GeV and its p_T is required to be at least 80 GeV. These requirements ensure a signal purity of at least 75%, which becomes larger than 90% for events with a W boson transverse momentum larger than 180 GeV.

The SLR is optimised for an extreme phase space and it takes inspiration from BSM physics searches that probed phase spaces where the interference modelling between $t\bar{t}$ and tWb processes resulted in large systematic uncertainties. The unfolded results in this peculiar phase space are very sensitive to the modelling of interference effects. To optimise the selection, the tWb purity and the yield difference between the tW DR and DS simulation samples are used as key metrics. The optimisation aims to minimise this yield difference while maintaining high tWb purity. The minimum invariant mass obtained by pairing the lepton with each of the b -jets in the event, $m_{b\ell}^{\text{min}}$, is an important observable to enhance topologies where at least one top quark is produced off-shell, where interference effects between $t\bar{t}$ and tWb can be probed best. A requirement of $m_{b\ell}^{\text{min}} \geq 150$ GeV exploits the characteristic kinematic endpoint of $t\bar{t}$ events and suppresses events with an on-shell semileptonically decaying top quark. Further requirements are embedded into the selection to suppress on-shell $t\bar{t}$ events: the transverse momentum of the leading (subleading) b -jet is required to be greater than 160 (50) GeV. The leading and subleading b -jets are required to have a relatively large spatial separation ($\Delta R(b_1, b_2) > 1.4$). Finally, E_T^{miss} and $p_T(\ell)$ are required to satisfy the following condition in the SLR:

$$E_T^{\text{miss}} \geq -0.625p_T(\ell) + 270 \text{ GeV}.$$

This requirement is chosen to maximise the overall $t\bar{t} + tWb$ acceptance, while enhancing the interference effects in this phase space using easily-interpretable observables. The selection criteria for the three measurement regions are summarised in Table 2.

In the WR selection, observables are chosen study the kinematic properties of the hadronically decaying W boson. These are:

- $p_T(W_{\text{had.}})$: the transverse momentum of the hadronically decaying W boson candidate.

³ This transverse mass is defined as $m_T^\ell = \sqrt{(E_T^{\text{miss}} + E_{T,\ell})^2 - (\vec{p}_T^{\text{miss}} + \vec{p}_{T,\ell})^2}$.

- $y(W_{\text{had.}})$: the rapidity of the hadronically decaying W boson candidate.
- $m(W_{\text{had.}}bb\ell)$: the invariant mass of the $Wbb\ell$ system.
- m_{bW}^{minimax} : variation of the min-max variable from Ref. [44], which takes into account the different final state considered in this paper. The variable is defined using the hadronic W candidate ($W_{\text{had.}}$) and the two leading b -jets as:

$$m_{bW}^{\text{minimax}} = \min(\max(m_{W_{\text{had.}}b_1}, m_{\ell b_2}), \max(m_{\ell b_1}, m_{W_{\text{had.}}b_2})).$$

This observable considers all possible pairings of the two b -jets with either $W_{\text{had.}}$ or the lepton. It exhibits a kinematic endpoint at

$$m_{bW}^{\text{minimax}} < \sqrt{m_{\text{top}}^2 - m_W^2}$$

for doubly resonant top-quark topologies, where m_{top} and m_W denote the top-quark and W masses, respectively. This makes it sensitive to regions of phase space enriched in singly resonant processes, where this endpoint is exceeded.

- $m_{b\ell}^{\text{selected}}$: a variation of the $m_{b\ell}^{\text{min}}$ observable which uses the b -jets assignment from the m_{bW}^{minimax} observable to calculate the invariant mass between the lepton and the selected b -jet.

A variation of the $m_{b\ell}^{\text{min}}$ observable, $m_{\text{T}}^{\text{min}}(b\ell)$, is studied in the IR and SR selections. It considers also the $E_{\text{T}}^{\text{miss}}$ information to constrain the mass of the leptonically decaying top. This is defined as the minimum transverse invariant mass between the $E_{\text{T}}^{\text{miss}}$, the lepton and the b -jet.

The total yields observed in data and predicted from the simulation in each region are shown in Table 3. The breakdown by SM process is also shown.

Table 3: Summary of the contributions of all SM processes and observed data in the three measurement regions. All statistical and systematic uncertainties are included, with the exception of the signal modelling, in the total uncertainty in the yields and are summed in quadrature. Both diagram removal (DR) and diagram subtraction (DS) yields are shown for the tW process for comparison.

Physics process	IR		WR		SLR	
tW DR	139 000	+8000 -8000	34 000	+1900 -1900	1680	+100 -80
tW DS (alt.)	120 000	+8000 -8000	28 400	+1900 -1900	234	+15 -15
$t\bar{t}$	4 000 000	+200 000 -200 000	850 000	+40 000 -40 000	1170	+80 -80
W + jets	120 000	+22 000 -18 000	10 300	+2000 -1600	344	+90 -56
Other t	91 000	+24 000 -24 000	9300	+2400 -2400	104	+27 -27
Other V	25 000	+4000 -16 000	2210	+230 -1600	61	+4 -61
Mis-ID lep.	20 000	+8000 -14 000	1900	+1300 -700	45	+33 -34
Total MC w/ DR	4 400 000	+230 000 -220 000	910 000	+50 000 -50 000	3400	+210 -190
Data	4 303 650		849 115		2403	

In addition to the detector-level objects, corresponding particle-level objects are defined using generator-level information from stable particles, identified as those with a proper lifetime $c\tau > 10$ nm. These objects

are identified without simulating their interactions with the detector and are used to define the fiducial phase-space regions and observables of interest in the measurement.

Particle-level electrons and muons are required not to originate from hadrons, either directly or through intermediate τ -lepton decays. A lepton is retained if it arises from a τ -lepton that itself originates directly from a W boson. The lepton four-momenta are corrected for final-state radiation from photons not originating from hadron decays and located within $\Delta R = 0.1$ of the lepton direction. The same transverse momentum and pseudorapidity requirements as for detector-level leptons are applied.

Particle-level jets are reconstructed by clustering all stable particles, excluding those identified as leptons or as neutrinos from electroweak boson decays, using the anti- k_r algorithm with a radius parameter of $R = 0.4$. The identification of b -jets is performed via the ghost-association technique: all b -hadrons are included in the jet clustering with their momentum set to a negligible value, and jets containing a b -hadron with $p_T > 5$ GeV are classified as b -tagged.

The particle-level missing transverse momentum is computed as the negative vector sum of the transverse momenta of all neutrinos, excluding those originating from hadron decays, either directly or via τ -leptons.

An overlap removal is applied among particle-level objects where electrons and muons located within $\Delta R = 0.4$ of any jet are removed.

The particle-level selections for the three measurement regions used for the differential measurements are constructed to match the detector-level regions by applying the same selection criteria.

4 Unfolding procedure

The differential cross-section measurement is performed in each of the three measurement regions (IR, WR and SLR), using the fiducial volumes definitions described in the previous section. An unfolding procedure is applied to extract the results at particle-level, following the methodology outlined in Refs. [119, 120]. The unfolding is performed using the TUnfold package [121].

The differential cross-section for a variable X at particle-level is defined as follows:

$$\frac{d\sigma_{\text{fid}}}{dX_i} = \frac{1}{\mathcal{L}_{\text{int}} \cdot \Delta X_i} \cdot \frac{1}{\epsilon_i} \cdot \sum_j M_{i,j}^{-1} f_{\text{acc}}^j (N_{d,j} - N_{b,j}).$$

The index i runs over all the bins of the particle-level definition of the variable X while the index j runs over all the bins of the reconstructed-level definition of the variable X . \mathcal{L}_{int} is the integrated luminosity. The differential cross-section is obtained from the data distribution $N_{d,j}$ after subtracting the background contribution $N_{b,j}$. The unfolding efficiency ϵ_i and the unfolding acceptance f_{acc}^j are obtained from the simulation of the target processes of the analysis ($t\bar{t} + tWb$). The efficiency is defined as the fraction of particle-level events that satisfy the detector-level selections and corrects for detector inefficiencies in the fiducial phase space. The acceptance is defined as the fraction of detector-level signal simulated events that satisfy the particle-level selection in each bin and corrects for events that are generated outside the fiducial phase-space but satisfy the detector-level selection. The migration matrix $M_{i,j}$, or normalised response matrix, is derived from the simulation and it describes the fraction of events that migrate from particle-level bin i to reconstructed bin j . The bin width is indicated by ΔX_i . The bin boundaries are chosen such that, in most cases, the diagonal of the migration matrix contains at least 60% of particle-level events of a row. The

number of reconstructed distribution bins is chosen to be twice the number of particle-level bins, according to the TUnfold default configuration [121]. The migration matrix inversion, M^{-1} , is estimated using a Tikhonov-Phillips regularisation scheme [122, 123], which reduces the statistical uncertainty associated with the inversion at the price of a possible deviation from the true value (bias). The bias is quantified with a closure test and found to be negligible.

Typical efficiency values across the three measurement regions range between 20 and 30% for most of the phase space and observables considered in the unfolding results. The acceptance values exhibit stronger variability across regions and phase space. In the IR and WR selections, typical acceptance values range between 60 and 80%, while in the SLR selections, the acceptance values are lower, with typical values around 40%. The migration matrix is almost diagonal for observables with small reconstruction uncertainties, such as the lepton p_T , while it is more off-diagonal for observables with larger reconstruction uncertainties, such as the (b) -jet momenta or the $m_{b\ell}^{\min}$ observable.

The unfolding is performed in each of the three measurement regions and the results are compared with the predictions of the simulation on key observables that allow for a thorough assessment of the data and its comparison with the MC models across all relevant kinematic phase space.

All SM processes other than $t\bar{t}$ and tWb are subtracted from data as the first step of the unfolding procedure. The dominant processes are $W + \text{jets}$, $Z + \text{jets}$ and diboson (referred to as “Other V ”), $t\bar{t}V$, $t\bar{t}H$ and sub-dominant single-top channels (referred to as “Other t ”) and QCD multi-jets processes with fake and non-prompt leptons (referred to as “Mis ID. lep.”). $W + \text{jets}$ is an important background for the IR and SLR selections. Its normalisation is constrained in a dedicated control region, WCR, enriched in this process with the purpose of better controlling the impact of systematic uncertainties related to this background. Events in the WCR are required to fulfil all requirements of the IR selection, except for the jet multiplicity requirement that is reduced to exactly three jets to ensure orthogonality. The overlap with the WR is removed by vetoing events that fulfil the WR selection, which is a small fraction of the total events in WCR. The $W + \text{jets}$ contribution is further enhanced by requiring $40 \text{ GeV} < m_T^\ell < 100 \text{ GeV}$ and $m_{b\ell}^{\min} > 180 \text{ GeV}$. A purity of 50% is achieved, with a contamination of 39% from $t\bar{t} + tWb$ events. The normalisation of the $W + \text{jets}$ background is estimated by means of a likelihood fit in the WCR, where detector and modelling uncertainties of all processes are treated as nuisance parameters in the fit. The resulting normalisation factor is 1.10 ± 0.10 . The data is within the uncertainty in the expected yields after the fit. The normalisation factor is used to correct the $W + \text{jets}$ process in all measurement regions (and is applied also in Table 3).

Misidentified and non-prompt leptons are estimated by using a data-driven method called *fake-factor method* that estimates the non-prompt contamination from a control region rich in this background and with high statistical power as described in detail in Ref. [124]. This process is found to be the smallest source of background in every region of the analysis. The electron and muon requirements used to select this fakes control region are described in Section 2.2. The prediction is validated in a dedicated and statistically independent validation region selecting events failing the requirement on $E_T^{\text{miss}} + m_T^\ell$ and applying looser requirements on the jet multiplicity. All other backgrounds are estimated from simulation.

The unfolding procedure is tested using pseudo-experiments and the self-consistency of the procedure (closure) is quantified. The unfolding is found to be stable and the bias is found to be negligible. In addition, stress tests are performed to verify that the unfolding is able to recover an alternative truth-level distribution. The stress tests include the reweighting of the unfolding observable with a linear function, the reweighting of the unfolding observable to match the data distribution, and the reweighting of the unfolding observable with a histogram of the ratio of observed-to-expected signal in the unfolded variable at detector

level. The unfolding is able to recover an alternative distribution in all cases, with discrepancies always consistent with the statistical precision of the test.

5 Systematic uncertainties

The sources of systematic uncertainties that affect the measurements of the differential cross-sections include the detector-related uncertainties that affect the calibration and the reconstruction efficiency of detector-level particles, the background and signal modelling, and the size of the data and MC samples. All systematic uncertainties related to the detector performance and calibration and the modelling of the SM processes (as described in Section 2) are propagated through the unfolding procedure.

The integrated luminosity has an uncertainty of 0.83% [114], which is propagated as a systematic uncertainty in the measurement to all physics processes other than the QCD multi-jet background. The pile-up uncertainty is assessed through the uncertainty on the factor used for the μ reweighting.

Charged leptons have uncertainties in the efficiency of the reconstruction, identification, isolation requirements, and trigger, which are derived from studies using $Z \rightarrow ee$ and $Z \rightarrow \mu\mu$ events [52, 53, 116, 117]. The impact of the lepton energy scale and resolution uncertainty is evaluated using resonance decays [56, 57]. The JER and JES uncertainties are derived using a combination of data and MC samples, using measurements of (for example) the jet p_T balance in dijet, Z +jet and γ +jet events [63]. Further jet-related uncertainties originate from efficiency corrections for tagging pile-up jets [62] and the identification of b -jets [125–127]. Uncertainties in the E_T^{miss} are estimated by propagating the uncertainties in the energy and momentum scale of each of the objects entering the calculation of E_T^{miss} , with additional terms taking into account the uncertainty in the resolution and scale of the soft term [65].

Modelling uncertainties are considered for both signal and background processes. Uncertainties associated with the modelling of $t\bar{t}$ and $tW(b)$ processes have been considered using alternative simulation samples as described in Section 2.3. The most important uncertainty is found to be the one related to different schemes used as double-counting removal procedure in the generation of $tW(b)$ events (DS versus DR removal schemes), followed by those related to the use of a different parton shower and hadronisation model and to variations of ISR and FSR. Additional uncertainties include factorisation and renormalisation scale variations, effects associated with the parameters that regulate the matching between ME and PS generators ($p_{T,\text{hard}}$ parameter), top-quark recoil model, and PDF choice. Since the $t\bar{t}$ and $tW(b)$ cross-sections are known at different perturbative orders in QCD and the two processes are treated here coherently, the modelling uncertainties in the two processes are treated consistently at NLO in QCD. The impact of the assumed value of the top quark mass on the results is evaluated using additional simulation samples with varied top-quark mass values of 172 GeV and 173 GeV. The resulting uncertainty is usually found to be negligible, but can grow up to 5% in the most extreme regions of phase space. Furthermore, uncertainties related to the flavour composition of extra jets radiated in association with top pairs are estimated and found to be negligible.

All signal modelling uncertainties are treated as correlated between the two processes. A dedicated uncertainty is included to account for the approximations used to model the shape of the top-quark mass with a proper width and high off-shell behaviours. This uncertainty is estimated by comparing two existing implementations from POWHEG and MADGRAPH5_AMC@NLO [128]. Uncertainties related to the modelling of additional $b\bar{b}$ or $c\bar{c}$ pairs in the parton shower are estimated by varying their respective contributions in the nominal $t\bar{t}$ sample and found to be negligible. The cross-section uncertainties are

treated as anti-correlated for the $t\bar{t}$ and tW samples, which is the most conservative approach for a result that is sensitive to the relative normalisation of the two processes. The results are also found to be insensitive to whether the $t\bar{t}$ samples are normalised using NLO+NNLL or NNLO+NNLL cross-sections.

The full uncertainty in the $W + \text{jets}$ normalisation, as obtained from the profile likelihood fit, is propagated to the unfolding. In addition, the shape component of all systematic uncertainties associated with the $W + \text{jets}$ background are propagated individually to the unfolding using the corresponding variations.

For all background samples, cross-section uncertainties are estimated by taking into account scales and PDF variations. The uncertainties due to missing higher-order corrections are evaluated by varying the renormalisation and factorisation scales by factors of 2.0 and 0.5. The PDF uncertainties are estimated by using the PDF4LHC15 prescription. Electroweak correction uncertainties are estimated for single and multi boson processes [108, 109].

The uncertainties related to the modelling of the QCD multi-jet background are estimated by varying the control region selection criteria used in the fake-factor method and by varying the Monte Carlo predictions by 10% around their nominal values. These procedures result in a conservative uncertainty of 50% to 70% in the total yield of this background, which does not affect the final results because of the small contribution of this background in all regions.

Detector and modelling uncertainties in backgrounds are propagated from detector to particle level by calculating varied unfolding corrections ($M_{i,j}$, ϵ_i and f_{acc}^j). The data is then unfolded with these varied corrections and the difference to the nominal unfolded data defines the uncertainty. Modelling uncertainties in signal are treated differently. Pseudo-data built using alternative predictions are unfolded using the nominal setup. These results are compared with the alternative simulation sample at particle-level and the difference defines the uncertainty.

Overall, small uncertainties are observed for the variables that are reconstructed only from leptons or dominated by $t\bar{t}$ only, thanks to the large number of data events and small migrations between the bins. The more statistically limited SLR results in unfolded observables with relatively large statistical uncertainties.

One of the dominant uncertainties is the uncertainty in the modelling of the interference between $t\bar{t}$ and tWb arising from using the alternative tWb DS MC sample in the unfolding procedure. This comparison estimates whether the unfolding is able to recover an alternative truth-level distribution and it is particularly important when no simulation is available that models the data well, as in this case. This uncertainty particularly strongly affects the SLR selection, where the large difference both in acceptance and normalisation of the two simulation approaches changes the relative fractions of $t\bar{t}$ and tWb processes in the unfolding and affects the unfolded result in a significant way. This uncertainty is presented separately in all unfolded cross-sections in Section 6 as it is the one with the largest potential for reduction in the future.

The uncertainties of the unfolded distributions range approximately from 5% to 20% in the higher statistics regions and from 20% to 80% in extreme phase spaces. The more extreme phase spaces, especially in the SLR selection, are strongly affected by the DR-DS uncertainty. The results for these selections achieve a precision at the level of 20% or better overall when the DS-DR uncertainty is not taken into account.

A detailed breakdown of systematic uncertainties is presented in Figures 2 to 4 for all observables discussed in this paper. Depending on the region and observable the dominant systematic uncertainties are found to be detector systematic uncertainties related to jet tagging and calibration, and modelling of the signal processes. Observables that exhibit end-points, e.g. $m_{b\ell}^{\text{min}}$, $m_{\text{T}}^{\text{min}}(b\ell)$, $m_{b\ell}^{\text{selected}}$ and m_{T}^{ℓ} , are particularly sensitive to variations of the jet energy scale and resolution, which create sharp increases in the uncertainties

around the top-quark mass in Figures 2(a), 2(c), 3(a) and 3(b). Uncertainties related to the modelling of the $t\bar{t}$ signal processes are also significant around those end-points, where different modelling of the parton shower or the initial and final state radiation can lead to different shaping of the distributions.

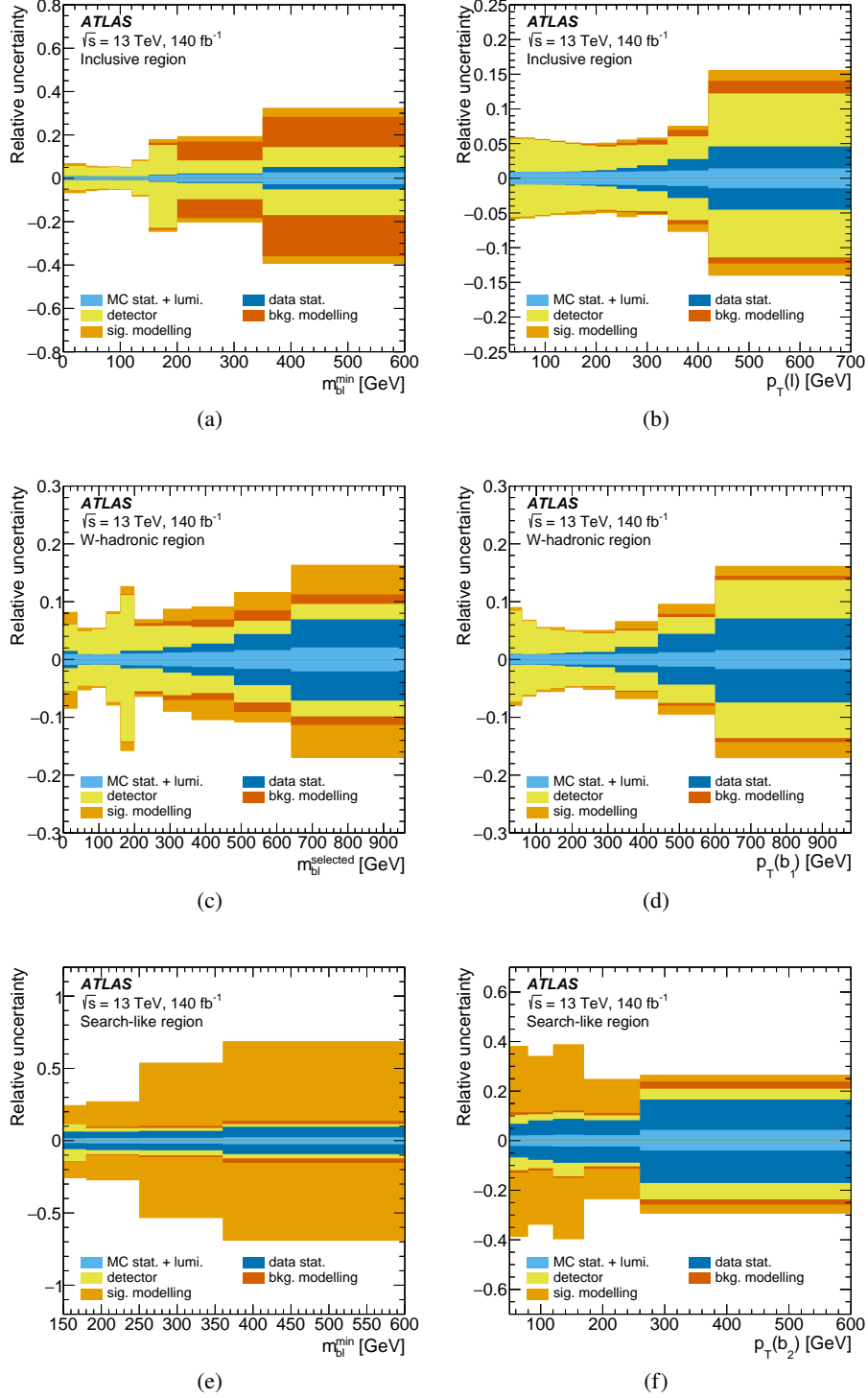


Figure 2: Breakdown of the systematic uncertainties in the unfolded differential cross-section measurement for (a) $m_{b\ell}^{\text{min}}$ for the inclusive region, (b) the lepton p_{T} for the inclusive region, (c) $m_{b\ell}^{\text{selected}}$ for the W-hadronic region, (d) leading b -jet p_{T} for the W-hadronic region, (e) $m_{b\ell}^{\text{min}}$ for the search-like region, and (f) the subleading b -jet p_{T} for the search-like region. The coloured bands represent each individual source of systematic uncertainty. The envelope of the coloured band represents the total systematic uncertainty, where each component is added in quadrature.

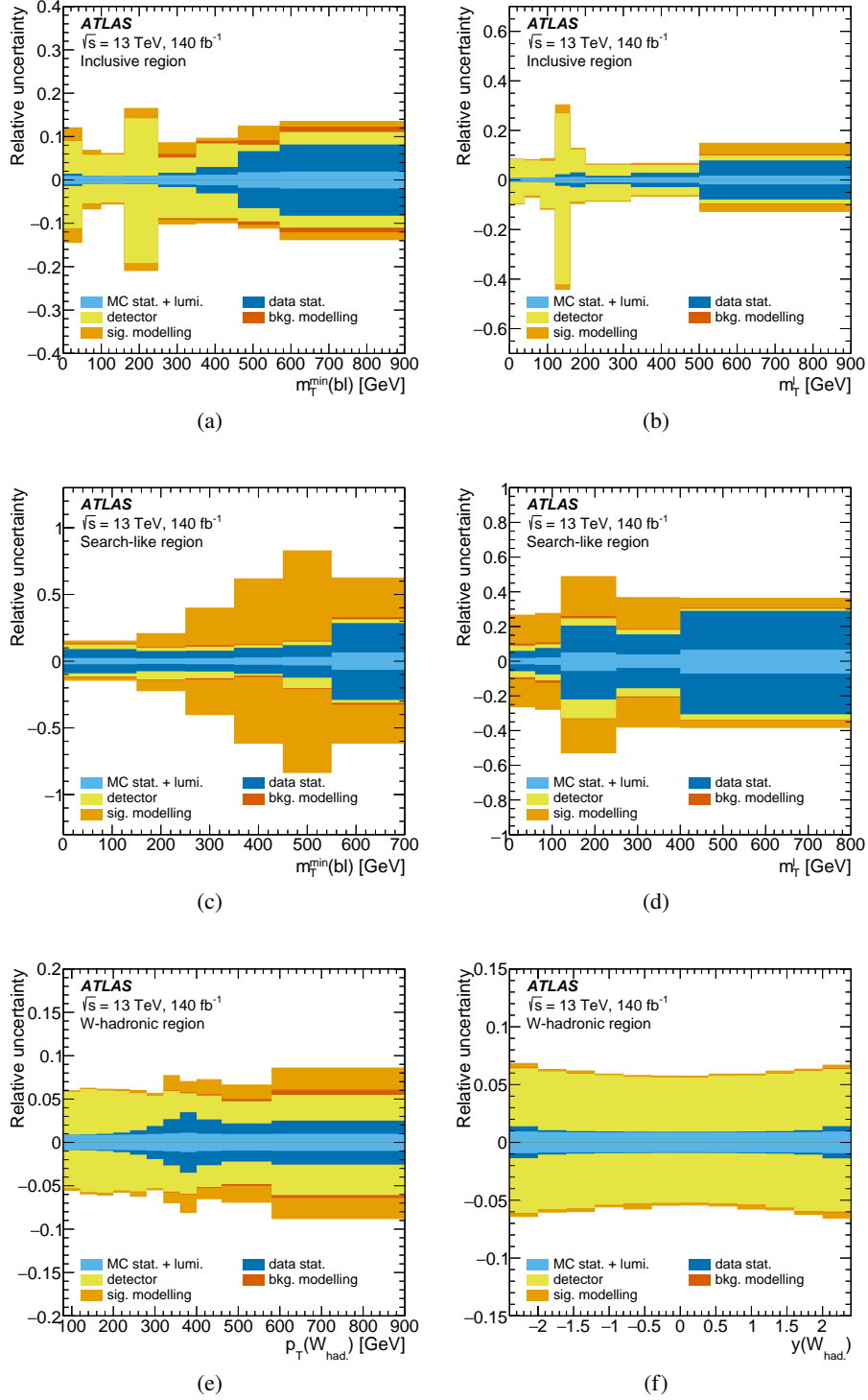


Figure 3: Breakdown of the systematic uncertainties in the unfolded differential cross-section measurement for (a) $m_T^{\min}(b\ell)$ for the inclusive region, (b) the transverse mass of the lepton, m_T^ℓ , for the inclusive region, (c) $m_T^{\min}(b\ell)$ for the search-like region, (d) the transverse mass of the lepton, m_T^ℓ , for the search-like region. (e) the hadronic W candidate transverse momentum for the W -hadronic region, and (f) the rapidity $y(W_{\text{had.}})$ for the W -hadronic region. The coloured bands represent each individual source of systematic uncertainty. The envelope of the coloured band represents the total systematic uncertainty, where each component is added in quadrature.

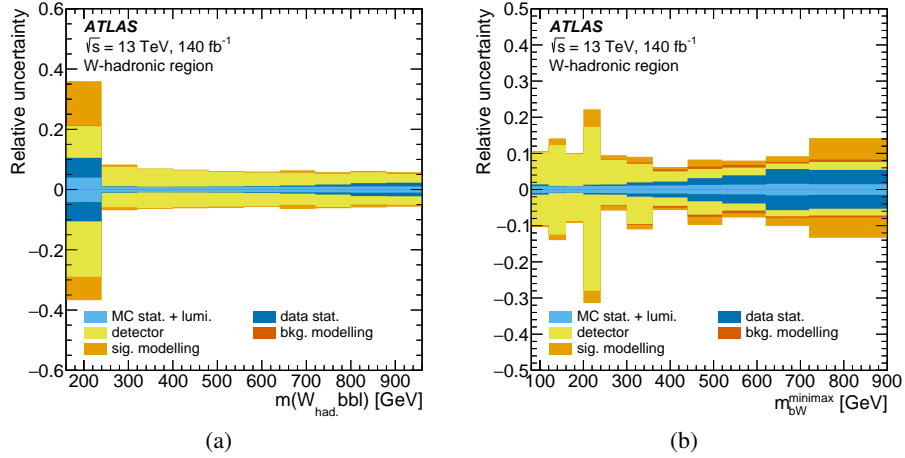


Figure 4: Breakdown of the systematic uncertainties in the unfolded differential cross-section measurement for (a) the invariant mass of the $Wbb\ell$ system and (b) m_{bW}^{minimax} for the W -hadronic region. The coloured bands represent each individual source of systematic uncertainty. The envelope of the coloured band represents the total systematic uncertainty, where each component is added in quadrature.

6 Differential cross-section results

The differential cross-sections are measured in the three measurement regions (IR, WR and SLR) for a set of kinematic variables. The variables are chosen to probe the phase space where the interference effects between $t\bar{t}$ and tWb processes are most prominent. In the WR region, the observables are chosen to represent all relevant kinematic quantities of the $W^+W^-b\bar{b}$ process. The variables are defined at particle level and are unfolded from the detector level using the procedure described in the previous sections. Selected unfolded differential cross-section results as a function of $m_{b\ell}^{\text{min}}$ and characteristic kinematic observables for the three measurement regions are presented in Figures 5 and 6, together with their detector-level distributions. Cross-sections in the IR and SLR as a function of the minimum transverse invariant mass between the E_T^{miss} , the lepton and the b -jets, $m_T^{\text{min}}(b\ell)$, and as a function of the transverse mass between the lepton and the E_T^{miss} , m_T^ℓ , are presented in Figures 7 and 8.

The observable presenting the largest overall disagreement between the unfolded data and the simulation is $m_{b\ell}^{\text{min}}$. This observable is a proxy for the invariant mass of the leptonically decaying top quark and is particularly sensitive to effects related to processes with virtual top contributions in the $t\bar{t} + tWb$ production. Detector-level and particle-level distributions are presented in Figure 5 for IR, WR and SLR selections. The ratio panel of each figure compares the reconstructed or unfolded data with the prediction from simulation. The full set of systematic uncertainties, arising from detector and modelling sources, is presented as a shaded band. In the detector-level results, only the nominal simulation prediction is shown, which includes tWb processes simulated with the DR approach. Various unfolded $t\bar{t} + tW$ differential cross-section predictions are shown in the figures. The details of each prediction are given in Section 2.3. They are: PH+PY8 DR (nominal prediction which includes the tWb process with DR treatment), PH+PY8 DS (prediction with the tWb process simulated with DS treatment), MiNNLOPS (using NNLO QCD description for the $t\bar{t}$ process), and PH+H7 DR (using HERWIG as shower model).

The unfolded results in Figure 5 show that none of the available predictions are well suited to simultaneously describe all the kinematic properties of the phase space under investigation. The various predictions exhibit

a varying level of agreement in different observables and regions of the phase space. The disagreement is particularly enhanced in those parts of the kinematic phase space that are not dominated exclusively by doubly resonant top production, such as the tails of the $m_{b\ell}^{\min}$ observable for the IR and WR selection. Additionally, a discrepancy is observed across the entire phase space and with a more pronounced deviation in the SLR selection, because of the interference-dominated phase space selected by this region. This discrepancy is about one standard deviation if all systematic uncertainties are considered. The uncertainties in these selections are dominated by the modelling of the singly resonant top quark production (DS/DR uncertainty). Recent progress in event generators [42] will contribute to future studies of the modelling in this region. The PH+PY8 DR and PH+PY8 DS predictions enclose the unfolded data distributions, with discrepancies at the level of approximately one standard deviation.

The modelling of the lepton and the b -jets' momenta in the event crucially characterises the phase space kinematic properties, as they are directly linked to the modelling of the boost of the tWb or $t\bar{t}$ systems. In the three representative distributions shown for the three measurement regions in Figure 6 it can be observed that no prediction is within one sigma of the unfolded data in the p_T spectrum of the lepton and the b -jets for highly energetic objects ($p_T \gtrsim 200$ GeV). In the IR the discrepancy can be mitigated by $t\bar{t}$ higher order corrections (MiNNLOPS prediction) when doubly resonant top-quark production dominates in the phase space. This is however not true everywhere, as for example the MiNNLOPS prediction exhibits slightly worse modelling of the data than the nominal prediction for events with leading b -jet momenta < 200 GeV in the WR selection (Figure 6(d)) and the MiNNLOPS prediction is very similar to the nominal PH+PY8 DR prediction in the SLR selection (Figure 6(f)). Observables related to the invariant mass of the leptonic W , like m_T^ℓ , which are instead independent of the boost of the tWb or $t\bar{t}$ system, are well modelled in the inclusive (IR) phase space (see Figure 7). The $m_T^{\min}(b\ell)$ observable is presented in Figure 8 for IR and SLR selections, as a proxy for the transverse component of the invariant mass of the leptonically decaying top quark. Such an observable exploits the E_T^{miss} information from the neutrino and is less sensitive to contaminations from the W + jets background in the interference-enhanced phase space of the regions and therefore overall affected by smaller systematic uncertainties. Despite the overlap between events in the tail of the $m_{b\ell}^{\min}$ and $m_T^{\min}(b\ell)$ distributions in the inclusive region (Figure 5(b) and Figure 8(b)), the two distributions exhibit opposite trends in terms of agreement between unfolded data and predictions. The nominal PH+PY8 DR prediction models best the unfolded data for the $m_{b\ell}^{\min}$ observable. By contrast, the unfolded data for the $m_T^{\min}(b\ell)$ observable is best described by the PH+PY8 DS prediction. In the SLR instead, the PH+PY8 DR and PH+PY8 DS predictions enclose the unfolded data distributions in similar ways across the $m_{b\ell}^{\min}$ and $m_T^{\min}(b\ell)$ observables, with differences of about one standard deviation.

Figure 9 presents the transverse momentum and rapidity of the hadronic W candidate in the WR selection. None of the prediction shows a good modelling of all the unfolded data, with the exception of the alternative PH+H7 DR model. The discrepancy between the predictions and the unfolded data is particularly enhanced for large W boson transverse momenta and central rapidity. The MiNNLOPS prediction exhibits particularly large disagreements, especially in the overall normalisation in this selection. The m_{bW}^{minimax} and $m(W_{\text{had.}} b b \ell)$ observables are presented in Figure 10. The former allows to probe the transition region of the relative abundance of singly versus doubly resonant top-quark processes (at the kinematic endpoint $m_{bW}^{\text{minimax}} < \sqrt{m_t^2 - m_W^2}$). The latter allows to study the modelling of the entire $W^+W^- b\bar{b}$ system. Also in this case, the alternative PH+H7 DR model seems to provide the best description of the unfolded data, while PH+PY8 DS exhibits a worse modelling, especially in the region that is most sensitive to the interference effects between $t\bar{t}$ and tWb processes.

The compatibility of the unfolded distributions and the predictions is quantitatively assessed by calculating χ^2 values, as presented in Tables 4 to 6. All uncertainties (statistical and systematic, both symmetrised)

Table 4: χ^2 and p -values for each variable (rows) for each prediction (columns) for the absolute differential cross-section in the IR. All systematic uncertainties described in Section 5 are included, with no additional uncertainties included on the predictions under test.

Inclusive region	PH+PY8 DR		PH+PY8 DS		PH+H7 DR		PH+PY8 DR (MiNNLOPS)	
	χ^2 / NDF	p -value	χ^2 / NDF	p -value	χ^2 / NDF	p -value	χ^2 / NDF	p -value
$m_{b\ell}^{\min}$	7.27 / 9	0.61	10.15 / 9	0.34	6.00 / 9	0.74	23.72 / 9	<0.01
$p_T(\ell)$	31.67 / 11	<0.01	19.70 / 11	0.05	13.11 / 11	0.29	7.54 / 11	0.75
m_T^ℓ	11.20 / 8	0.19	7.91 / 8	0.44	12.13 / 8	0.15	3.68 / 8	0.88
$m_T^{\min}(b\ell)$	21.17 / 8	0.01	7.49 / 8	0.48	16.54 / 8	0.04	17.34 / 8	0.03

Table 5: χ^2 and p -values for each variable (rows) for each prediction (columns) for the absolute differential cross-section in the WR. All systematic uncertainties described in Section 5 are included, with no additional uncertainties included on the predictions under test.

W-hadronic region	PH+PY8 DR		PH+PY8 DS		PH+H7 DR		PH+PY8 DR (MiNNLOPS)	
	χ^2 / NDF	p -value	χ^2 / NDF	p -value	χ^2 / NDF	p -value	χ^2 / NDF	p -value
$m_{b\ell}^{\text{selected}}$	15.65 / 10	0.11	26.84 / 10	<0.01	6.95 / 10	0.73	30.53 / 10	<0.01
$p_T(b_1)$	25.50 / 9	<0.01	20.56 / 9	0.01	10.19 / 9	0.34	13.62 / 9	0.14
$p_T(W_{\text{had.}})$	20.79 / 11	0.04	14.32 / 11	0.22	10.99 / 11	0.44	7.28 / 11	0.78
$y(W_{\text{had.}})$	14.81 / 12	0.25	14.13 / 12	0.29	7.96 / 12	0.79	11.99 / 12	0.45
m_{bW}^{minimax}	22.37 / 11	0.02	44.24 / 11	<0.01	12.72 / 11	0.31	34.33 / 11	<0.01
$m(W_{\text{had.}}, bb\ell)$	5.37 / 10	0.87	7.83 / 10	0.65	2.08 / 10	1.00	4.54 / 10	0.92

Table 6: χ^2 and p -values for each variable (rows) for each prediction (columns) for the absolute differential cross-section in the SLR. All systematic uncertainties described in Section 5 are included, with no additional uncertainties included on the predictions under test.

Search-like region	PH+PY8 DR		PH+PY8 DS		PH+H7 DR		PH+PY8 DR (MiNNLOPS)	
	χ^2 / NDF	p -value	χ^2 / NDF	p -value	χ^2 / NDF	p -value	χ^2 / NDF	p -value
$m_{b\ell}^{\min}$	9.57 / 4	0.05	7.57 / 4	0.11	9.21 / 4	0.06	10.73 / 4	0.03
$p_T(b_2)$	17.11 / 5	<0.01	4.12 / 5	0.53	14.72 / 5	0.01	13.00 / 5	0.02
m_T^ℓ	0.41 / 4	0.98	4.24 / 4	0.38	0.30 / 4	0.99	0.58 / 4	0.96
$m_T^{\min}(b\ell)$	11.54 / 6	0.07	2.76 / 6	0.84	10.01 / 6	0.12	10.45 / 6	0.11

associated with the unfolded distributions, described in Section 5 are included, taking into account their correlations, with no additional uncertainties included on the predictions under test.

The corresponding p -values are calculated inclusively for each distribution and reflect the various level of disagreement observed between the unfolded data and the simulation in the various observables and regions studied in this paper.

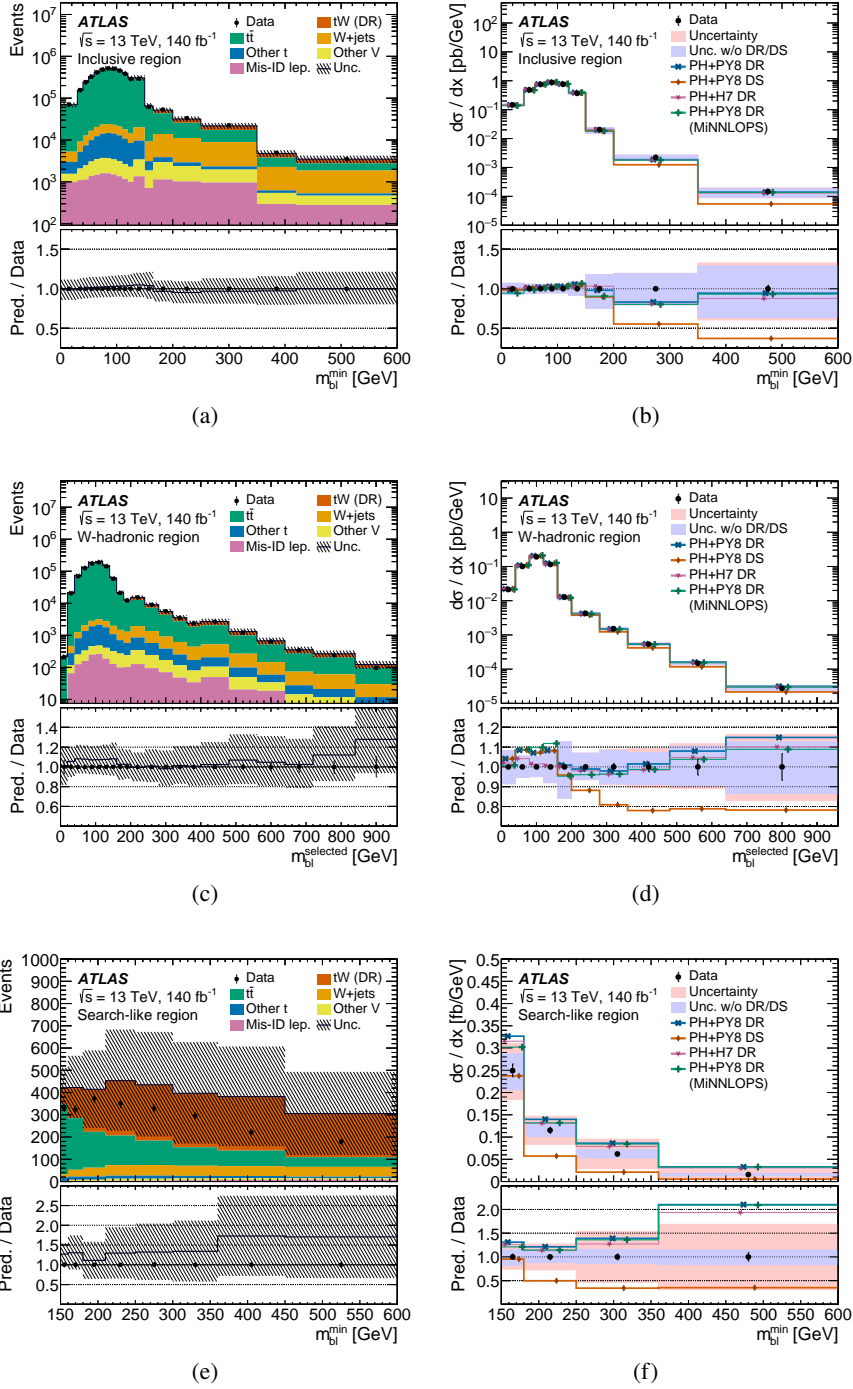


Figure 5: The ((a), (c), (e)) detector-level distributions and ((b), (d), (f)) unfolded differential cross-sections of the invariant mass between the lepton and the b -jets. The distributions are shown ((a) and (b)) in the inclusive region, ((c) and (d)) in the W -hadronic and ((e) and (f)) in the search-like region. In the bottom panel, the reconstructed or unfolded data are compared with the predictions. The markers representing the different predictions are shifted from the bin centre to improve readability. The data statistical uncertainty is shown as error bars. The total systematic uncertainty is shown as a shaded band. An additional band including all uncertainties except the DS/DR interference modelling is shown for the unfolded results. The unfolded $t\bar{t} + tW$ predictions are shown: PH+PY8 DR (nominal using DR tW), PH+PY8 DS (using DS tW), MiNNLOPS (using NNLO QCD $t\bar{t}$), and PH+H7 DR (using HERWIG shower model).

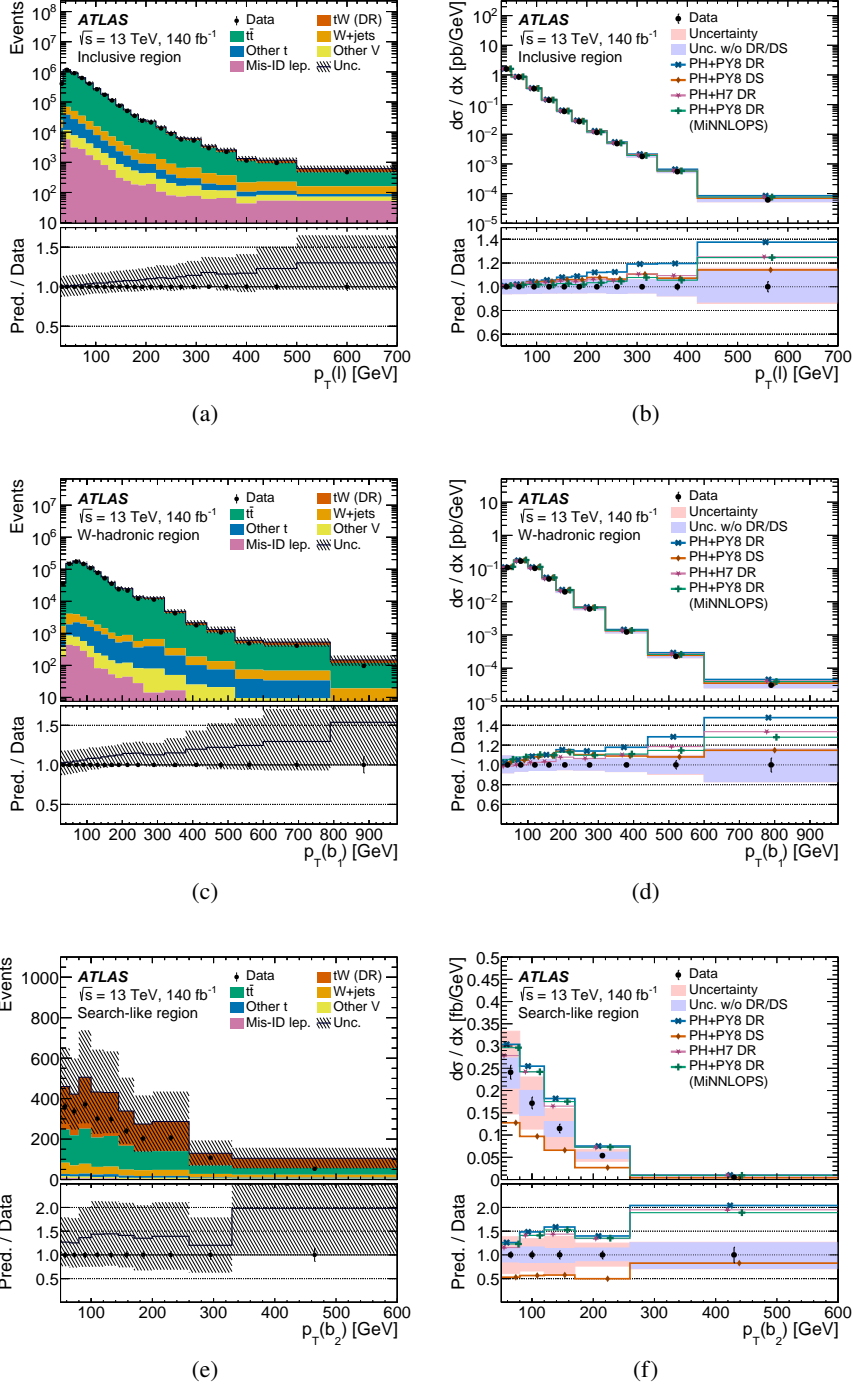


Figure 6: The ((a), (c), (e)) detector-level distributions and ((b), (d), (f)) unfolded differential cross-sections of ((a) and (b)) the lepton p_T for the inclusive region, ((c) and (d)) the leading b -jet p_T for the W -hadronic region and ((e) and (f)) the subleading b -jet p_T for the search-like region. In the bottom panel, the reconstructed or unfolded data are compared with the predictions. The markers representing the different predictions are shifted from the bin centre to improve readability. The data statistical uncertainty is shown as error bars. The total systematic uncertainty is shown as a shaded band. An additional band including all uncertainties except the DS/DR interference modelling is shown for the unfolded results. The unfolded $t\bar{t} + tW$ predictions are shown: PH+PY8 DR (nominal using DR tW), PH+PY8 DS (using DS tW), MiNNLOPS (using NNLO QCD $t\bar{t}$), and PH+H7 DR (using HERWIG shower model).

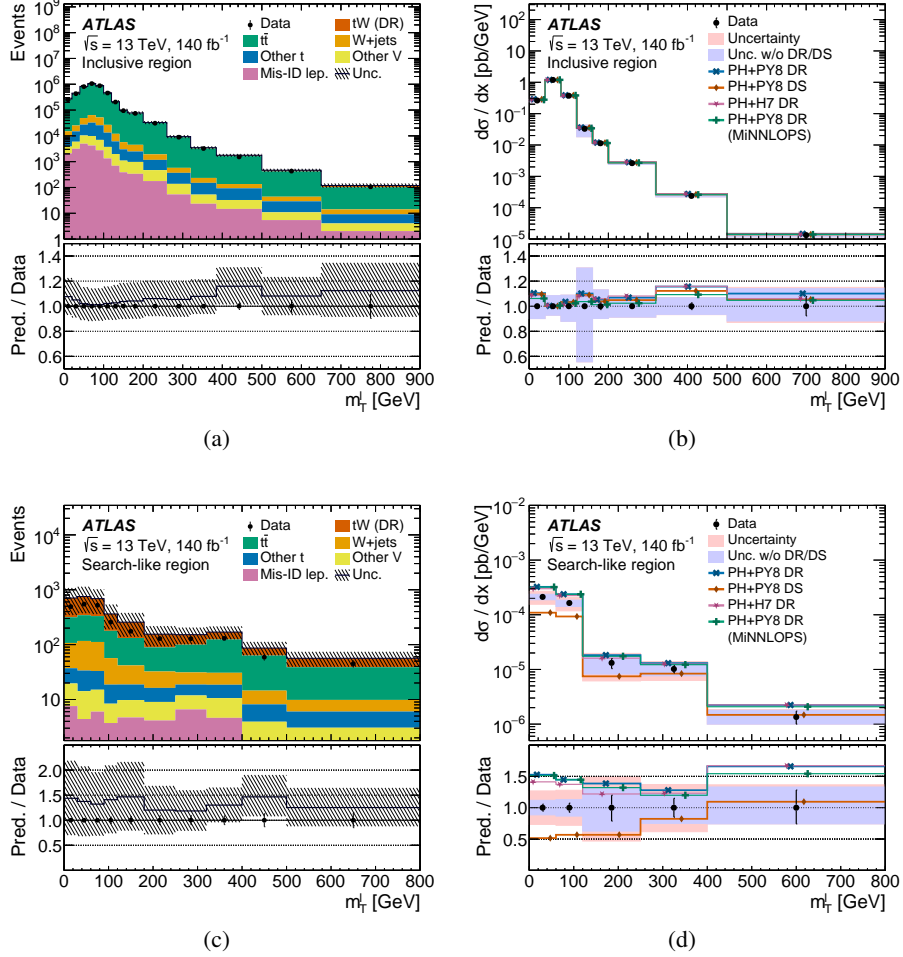


Figure 7: The ((a), (c)) detector-level distributions and ((b), (d)) unfolded differential cross-sections of the lepton transverse mass, m_T^ℓ . The distributions are shown ((a) and (b)) in the inclusive region and ((c) and (d)) in the search-like region. In the bottom panel, the reconstructed or unfolded data are compared with the predictions. The markers representing the different predictions are shifted from the bin centre to improve readability. The data statistical uncertainty is shown as error bars. The total systematic uncertainty is shown as a shaded band. An additional band including all uncertainties except the DS/DR interference modelling is shown for the unfolded results. The unfolded $t\bar{t} + tW$ predictions are shown: PH+PY8 DR (nominal using DR tW), PH+PY8 DS (using DS tW), MiNNLOPS (using NNLO QCD $t\bar{t}$), and PH+H7 DR (using HERWIG shower model).

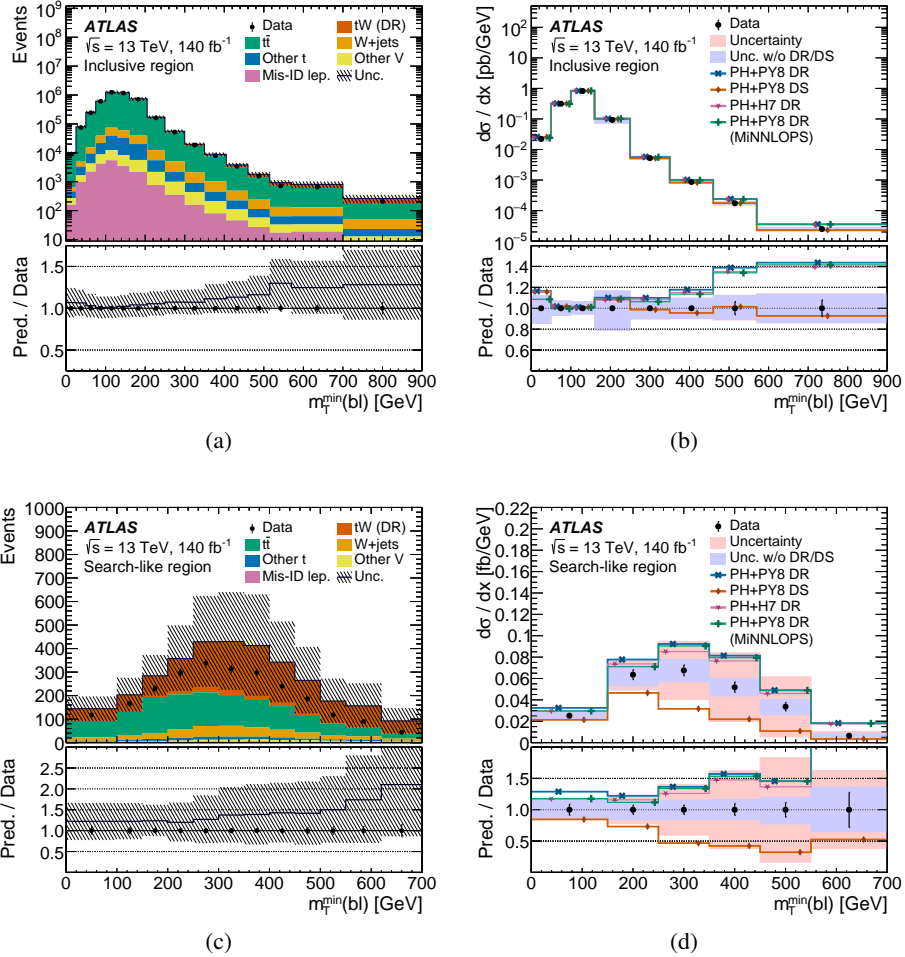


Figure 8: The ((a), (c)) detector-level distributions and ((b), (d)) unfolded differential cross-sections of the transverse component of the minimal transverse mass between the E_T^{miss} , the lepton and the b -jets in the event, $m_T^{\min}(b\ell)$. The distributions are shown ((a) and (b)) in the inclusive region and ((c) and (d)) in the search-like region. In the bottom panel, the reconstructed or unfolded data are compared with the predictions. The markers representing the different predictions are shifted from the bin centre to improve readability. The data statistical uncertainty is shown as error bars. The total systematic uncertainty is shown as a shaded band. An additional band including all uncertainties except the DS/DR interference modelling is shown for the unfolded results. The unfolded $t\bar{t} + tW$ predictions are shown: PH+PY8 DR (nominal using DR tW), PH+PY8 DS (using DS tW), MiNNLOPS (using NNLO QCD $t\bar{t}$), and PH+H7 DR (using HERWIG shower model).

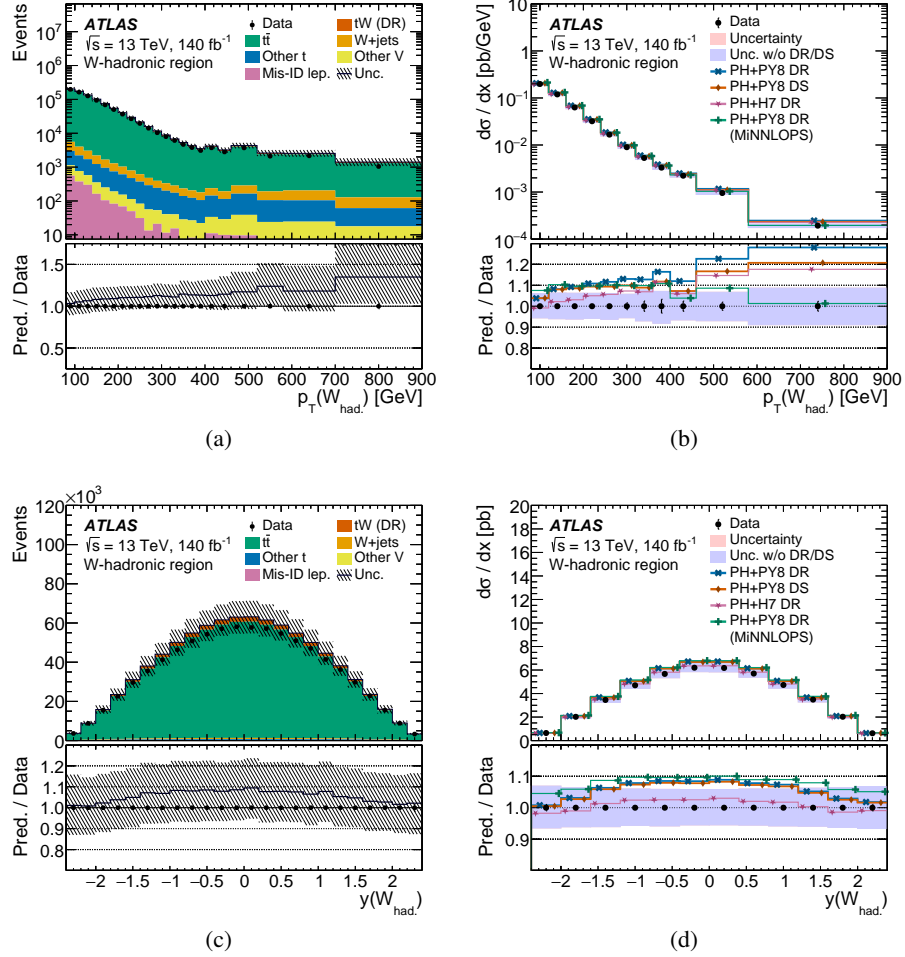


Figure 9: The ((a), (c)) detector-level distributions and ((b), (d)) unfolded differential cross-sections in the W -hadronic region. The distributions are shown for ((a) and (b)) the hadronic W candidate momentum $p_T(W_{had.})$ and ((c) and (d)) rapidity $y(W_{had.})$. In the bottom panel, the reconstructed or unfolded data are compared with the predictions. The markers representing the different predictions are shifted from the bin centre to improve readability. The data statistical uncertainty is shown as error bars. The total systematic uncertainty is shown as a shaded band. An additional band including all uncertainties except the DS/DR interference modelling is shown for the unfolded results. The unfolded $t\bar{t} + tW$ predictions are shown: PH+PY8 DR (nominal using DR tW), PH+PY8 DS (using DS tW), MiNNLOPS (using NNLO QCD $t\bar{t}$), and PH+H7 DR (using HERWIG shower model).

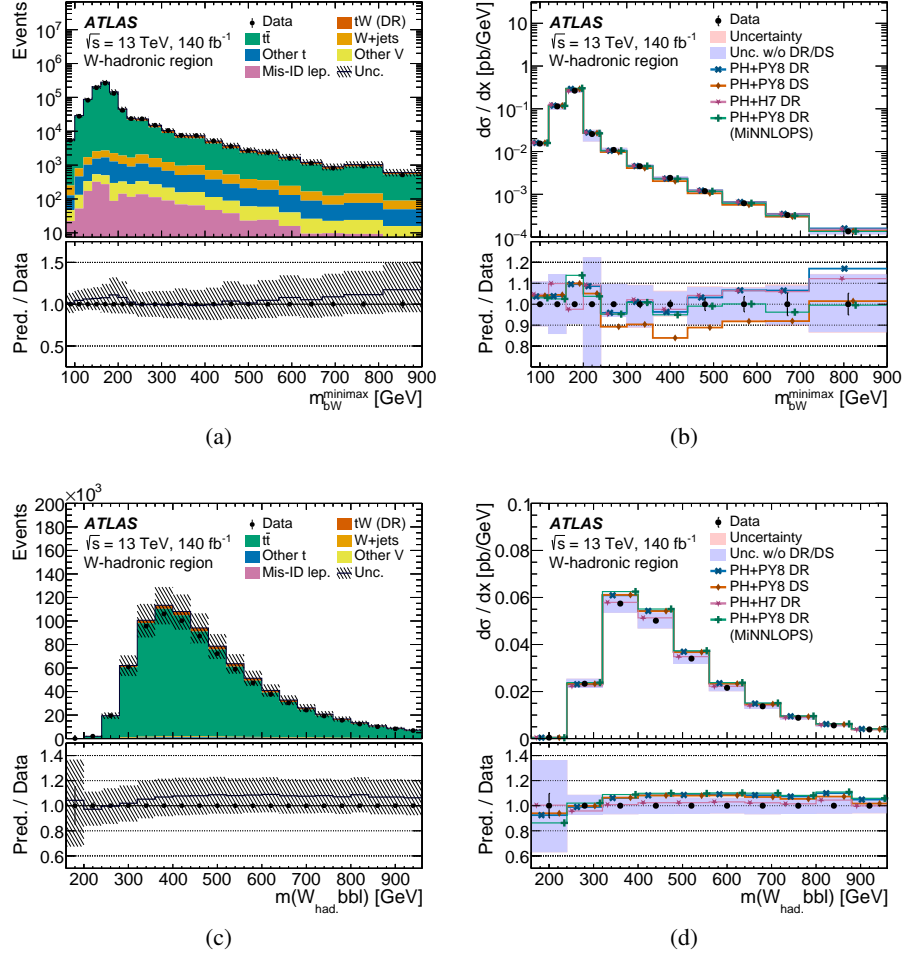


Figure 10: The ((a), (c)) detector-level distributions and ((b), (d)) unfolded differential cross-sections in the W -hadronic region. The distributions are shown for ((a) and (b)) m_{bW}^{minimax} and ((c) and (d)) the invariant mass of the $Wbbl$ system. In the bottom panel, the reconstructed or unfolded data are compared with the predictions. The markers representing the different predictions are shifted from the bin centre to improve readability. The data statistical uncertainty is shown as error bars. The total systematic uncertainty is shown as a shaded band. An additional band including all uncertainties except the DS/DR interference modelling is shown for the unfolded results. The unfolded $t\bar{t} + tW$ predictions are shown: PH+PY8 DR (nominal using DR tW), PH+PY8 DS (using DS tW), MiNNLOPS (using NNLO QCD $t\bar{t}$), and PH+H7 DR (using HERWIG shower model).

7 Conclusions

This paper presented a differential cross-section measurement of the coherent production of singly and doubly resonant top quarks in $W^+W^-b\bar{b}$ events using 140 fb^{-1} of pp collisions at a center-of-mass energy of 13 TeV, collected with the ATLAS experiment in the years from 2015 to 2018 during Run 2 of the LHC. Events requiring one lepton, three or four jets, of which at least two b -jets, were considered. Three measurement regions were defined: the inclusive region, the W -hadronic region, and the search-like region. The analysis selections, fiducial volumes and observables were optimised to isolate a phase space that probes the kinematic properties of the $t\bar{t} + tWb$ processes and their interference, actively suppressing the pure doubly resonant top-quark production.

Differential cross-sections obtained at particle-level from unfolded data are derived for various observables. The results are compared with predictions from several simulations. The results indicate that none of the considered predictions can simultaneously accurately describe all observables in the fiducial phase-space. For most of the phase space, observables connected to the transverse momentum of the $tW/t\bar{t}$ system are described better by the MiNNLOPS prediction, which describes $t\bar{t}$ processes at NNLO QCD accuracy. These observations are compatible with the findings of other recent analyses targeting dileptonic final states [6, 45].

The measurement is limited by the uncertainties in the signal modelling, in particular those related to the treatment of the $t\bar{t} + tWb$ interference, uncertainties related to the calibration of jets and b -jets. When comparing with the measurement performed in the dilepton channel [45], a larger number of observables sensitive to interference effects has been studied. The overall findings are consistent, with discrepancies between data and predictions at the level of one standard deviation when the comparison between the DS and DR removal schemes is included as modelling uncertainty, increasing to two to three standard deviations when excluding it. Furthermore, statistical uncertainties in the single-lepton measurement are significant only in the tails of the distributions. This measurement represents the first differential cross-section measurement of the coherent production of singly and doubly resonant top-quarks in final states with exactly one lepton. The results of this study provide valuable insights into the modelling of the $W^+W^-b\bar{b}$ process in the fiducial phase-space and can be used to assess the modelling accuracy of future Monte Carlo simulation developments.

Acknowledgements

We thank CERN for the very successful operation of the LHC and its injectors, as well as the support staff at CERN and at our institutions worldwide without whom ATLAS could not be operated efficiently.

The crucial computing support from all WLCG partners is acknowledged gratefully, in particular from CERN, the ATLAS Tier-1 facilities at TRIUMF/SFU (Canada), NDGF (Denmark, Norway, Sweden), CC-IN2P3 (France), KIT/GridKA (Germany), INFN-CNAF (Italy), NL-T1 (Netherlands), PIC (Spain), RAL (UK) and BNL (USA), the Tier-2 facilities worldwide and large non-WLCG resource providers. Major contributors of computing resources are listed in Ref. [129].

We gratefully acknowledge the support of ANPCyT, Argentina; YerPhI, Armenia; ARC, Australia; BMWFW and FWF, Austria; ANAS, Azerbaijan; CNPq and FAPESP, Brazil; NSERC, NRC and CFI, Canada; CERN; ANID, Chile; CAS, MOST and NSFC, China; Minciencias, Colombia; MEYS CR, Czech Republic; DNRf and DNSRC, Denmark; IN2P3-CNRS and CEA-DRF/IRFU, France; SRNSFG, Georgia; BMFTR, HGF

and MPG, Germany; GSRI, Greece; RGC and Hong Kong SAR, China; ICHEP and Academy of Sciences and Humanities, Israel; INFN, Italy; MEXT and JSPS, Japan; CNRST, Morocco; NWO, Netherlands; RCN, Norway; MNiSW, Poland; FCT, Portugal; MNE/IFA, Romania; MSTDI, Serbia; MSSR, Slovakia; ARIS and MVZI, Slovenia; DSI/NRF, South Africa; MICIU/AEI, Spain; SRC and Wallenberg Foundation, Sweden; SERI, SNSF and Cantons of Bern and Geneva, Switzerland; NSTC, Taipei; TENMAK, Türkiye; STFC/UKRI, United Kingdom; DOE and NSF, United States of America.

Individual groups and members have received support from BCKDF, CANARIE, CRC and DRAC, Canada; CERN-CZ, FORTE and PRIMUS, Czech Republic; COST, ERC, ERDF, Horizon 2020, ICSC-NextGenerationEU and Marie Skłodowska-Curie Actions, European Union; Investissements d’Avenir Labex, Investissements d’Avenir Idex and ANR, France; DFG and AvH Foundation, Germany; Herakleitos, Thales and Aristeia programmes co-financed by EU-ESF and the Greek NSRF, Greece; BSF-NSF and MINERVA, Israel; NCN and NAWA, Poland; La Caixa Banking Foundation, CERCA Programme Generalitat de Catalunya and PROMETEO and GenT Programmes Generalitat Valenciana, Spain; Göran Gustafssons Stiftelse, Sweden; The Royal Society and Leverhulme Trust, United Kingdom.

In addition, individual members wish to acknowledge support from CERN: European Organization for Nuclear Research (CERN DOCT); Chile: Agencia Nacional de Investigación y Desarrollo (FONDECYT 1230812, FONDECYT 1240864, Fondecyt 3240661, Fondecyt Regular 1240721); China: Chinese Ministry of Science and Technology (MOST-2023YFA1605700, MOST-2023YFA1609300), National Natural Science Foundation of China (NSFC - 12175119, NSFC 12275265); Czech Republic: Czech Science Foundation (GACR - 24-11373S), Ministry of Education Youth and Sports (ERC-CZ-LL2327, FORTE CZ.02.01.01/00/22_008/0004632), PRIMUS Research Programme (PRIMUS/21/SCI/017); EU: H2020 European Research Council (ERC - 101002463); European Union: European Research Council (BARD No. 101116429, ERC - 948254, ERC 101089007), European Regional Development Fund (SMASH COFUND 101081355, SLO ERDF), European Union, Future Artificial Intelligence Research (FAIR-NextGenerationEU PE00000013), Italian Center for High Performance Computing, Big Data and Quantum Computing (ICSC, NextGenerationEU); France: Agence Nationale de la Recherche (ANR-21-CE31-0022, ANR-22-EDIR-0002, ANR-24-CE31-0504-01); Germany: Deutsche Forschungsgemeinschaft (DFG - 469666862, DFG - CR 312/5-2); China: Research Grants Council (GRF); Italy: Istituto Nazionale di Fisica Nucleare (ICSC, NextGenerationEU), Ministero dell’Università e della Ricerca (NextGenEU 153D23001490006 M4C2.1.1, NextGenEU I53D23000820006 M4C2.1.1, NextGenEU I53D23001490006 M4C2.1.1, SOE2024_0000023); Japan: Japan Society for the Promotion of Science (JSPS KAKENHI JP22H01227, JSPS KAKENHI JP22H04944, JSPS KAKENHI JP22KK0227, JSPS KAKENHI JP24K23939, JSPS KAKENHI JP24KK0251, JSPS KAKENHI JP25H00650, JSPS KAKENHI JP25H01291, JSPS KAKENHI JP25K01023); Norway: Research Council of Norway (RCN-314472); Poland: Ministry of Science and Higher Education (IDUB AGH, POB8, D4 no 9722), Polish National Science Centre (NCN 2021/42/E/ST2/00350, NCN OPUS 2023/51/B/ST2/02507, NCN UMO-2019/34/E/ST2/00393, UMO-2022/47/O/ST2/00148, UMO-2023/49/B/ST2/04085, UMO-2023/51/B/ST2/00920, UMO-2024/53/N/ST2/00869); Portugal: Foundation for Science and Technology (FCT); Spain: Ministry of Science and Innovation (MCIN & NextGenEU PCI2022-135018-2, MICIN & FEDER PID2021-125273NB, RYC2019-028510-I, RYC2020-030254-I, RYC2021-031273-I, RYC2022-038164-I); Sweden: Carl Trygger Foundation (Carl Trygger Foundation CTS 22:2312), Swedish Research Council (Swedish Research Council 2023-04654, VR 2021-03651, VR 2022-03845, VR 2022-04683, VR 2023-03403, VR 2024-05451), Knut and Alice Wallenberg Foundation (KAW 2018.0458, KAW 2022.0358, KAW 2023.0366); Switzerland: Swiss National Science Foundation (SNSF - PCEFP2_194658); United Kingdom: Royal Society (NIF-R1-231091); United States of America: U.S. Department of Energy (ECA DE-AC02-76SF00515), Neubauer Family Foundation.

References

- [1] L. Evans and P. Bryant, *LHC Machine*, [JINST 3 \(2008\) S08001](#).
- [2] ATLAS Collaboration, *Measurements of top-quark pair differential cross-sections in the lepton+jets channel in pp collisions at $\sqrt{s} = 13$ TeV using the ATLAS detector*, [JHEP 11 \(2017\) 191](#), arXiv: [1708.00727 \[hep-ex\]](#).
- [3] ATLAS Collaboration, *Measurements of top-quark pair differential and double-differential cross-sections in the ℓ +jets channel with pp collisions at $\sqrt{s} = 13$ TeV using the ATLAS detector*, [Eur. Phys. J. C 79 \(2019\) 1028](#), arXiv: [1908.07305 \[hep-ex\]](#),
Erratum: [Eur. Phys. J. C 80 \(2020\) 1092](#).
- [4] ATLAS Collaboration, *Measurement of jet substructure in boosted $t\bar{t}$ events with the ATLAS detector using 140fb^{-1} of 13 TeV pp collisions*, [Phys. Rev. D 109 \(2024\) 112016](#),
arXiv: [2312.03797 \[hep-ex\]](#).
- [5] ATLAS Collaboration, *Measurement of differential cross-sections in $t\bar{t}$ and $t\bar{t}$ +jets production in the lepton+jets final state in pp collisions at $\sqrt{s} = 13$ TeV using 140fb^{-1} of ATLAS data*, [JHEP 08 \(2024\) 182](#), arXiv: [2406.19701 \[hep-ex\]](#).
- [6] ATLAS Collaboration, *Precise measurement of the $t\bar{t}$ production cross-section and lepton differential distributions in $e\mu$ dilepton events from $\sqrt{s} = 13$ TeV pp collisions with the ATLAS detector*, (2025),
arXiv: [2509.15066 \[hep-ex\]](#).
- [7] CMS Collaboration, *Measurement of normalized differential $t\bar{t}$ cross sections in the dilepton channel from pp collisions at $\sqrt{s} = 13$ TeV*, [JHEP 04 \(2018\) 060](#), arXiv: [1708.07638 \[hep-ex\]](#).
- [8] CMS Collaboration, *Measurements of differential cross sections of top quark pair production as a function of kinematic event variables in proton–proton collisions at $\sqrt{s} = 13$ TeV*, [JHEP 06 \(2018\) 002](#), arXiv: [1803.03991 \[hep-ex\]](#).
- [9] CMS Collaboration, *Measurement of differential cross sections for the production of top quark pairs and of additional jets in lepton+jets events from pp collisions at $\sqrt{s} = 13$ TeV*, [Phys. Rev. D 97 \(2018\) 112003](#), arXiv: [1803.08856 \[hep-ex\]](#).
- [10] CMS Collaboration, *Measurement of $t\bar{t}$ normalised multi-differential cross sections in pp collisions at $\sqrt{s} = 13$ TeV, and simultaneous determination of the strong coupling strength, top quark pole mass, and parton distribution functions*, [Eur. Phys. J. C 80 \(2020\) 658](#),
arXiv: [1904.05237 \[hep-ex\]](#).
- [11] M. Czakon and A. Mitov, *Top++: A program for the calculation of the top-pair cross-section at hadron colliders*, [Comput. Phys. Commun. 185 \(2014\) 2930](#), arXiv: [1112.5675 \[hep-ph\]](#).
- [12] M. Czakon, D. Heymes and A. Mitov, *High-precision differential predictions for top-quark pairs at the LHC*, [Phys. Rev. Lett. 116 \(2016\) 082003](#), arXiv: [1511.00549 \[hep-ph\]](#).
- [13] M. Czakon, D. Heymes and A. Mitov, *Dynamical scales for multi-TeV top-pair production at the LHC*, [JHEP 04 \(2017\) 071](#),
arXiv: [1606.03350 \[hep-ph\]](#).

- [14] ATLAS Collaboration, *Measurement of the cross-section for producing a W boson in association with a single top quark in pp collisions at $\sqrt{s} = 13$ TeV with ATLAS*, *JHEP* **01** (2018) 063, arXiv: [1612.07231 \[hep-ex\]](#).
- [15] ATLAS Collaboration, *Measurement of differential cross-sections of a single top quark produced in association with a W boson at $\sqrt{s} = 13$ TeV with ATLAS*, *Eur. Phys. J. C* **78** (2018) 186, arXiv: [1712.01602 \[hep-ex\]](#).
- [16] ATLAS Collaboration, *Measurement of single top-quark production in association with a W boson in pp collisions at $\sqrt{s} = 13$ TeV with the ATLAS detector*, *Phys. Rev. D* **110** (2024) 072010, arXiv: [2407.15594 \[hep-ex\]](#).
- [17] CMS Collaboration, *Measurement of the production cross section for single top quarks in association with W bosons in proton–proton collisions at $\sqrt{s} = 13$ TeV*, *JHEP* **10** (2018) 117, arXiv: [1805.07399 \[hep-ex\]](#).
- [18] CMS Collaboration, *Observation of tW production in the single-lepton channel in pp collisions at $\sqrt{s} = 13$ TeV*, *JHEP* **11** (2021) 111, arXiv: [2109.01706 \[hep-ex\]](#).
- [19] CMS Collaboration, *Measurement of inclusive and differential cross sections for single top quark production in association with a W boson in proton–proton collisions at $\sqrt{s} = 13$ TeV*, *JHEP* **07** (2023) 046, arXiv: [2208.00924 \[hep-ex\]](#).
- [20] CMS Collaboration, *Measurement of differential cross sections and charge ratios for t-channel single top quark production in proton–proton collisions at $\sqrt{s} = 13$ TeV*, *Eur. Phys. J. C* **80** (2020) 370, arXiv: [1907.08330 \[hep-ex\]](#).
- [21] C. D. White, S. Frixione, E. Laenen and F. Maltoni, *Isolating Wt production at the LHC*, *JHEP* **11** (2009) 074, arXiv: [0908.0631 \[hep-ph\]](#).
- [22] S. Frixione, E. Laenen, P. Motylinski, C. White and B. R. Webber, *Single-top hadroproduction in association with a W boson*, *JHEP* **07** (2008) 029, arXiv: [0805.3067 \[hep-ph\]](#).
- [23] W. Hollik, J. M. Lindert and D. Pagani, *NLO corrections to squark-squark production and decay at the LHC*, *JHEP* **03** (2013) 139, arXiv: [1207.1071 \[hep-ph\]](#).
- [24] F. Demartin, B. Maier, F. Maltoni, K. Mawatari and M. Zaro, *tWH associated production at the LHC*, *Eur. Phys. J. C* **77** (2017) 34, arXiv: [1607.05862 \[hep-ph\]](#).
- [25] ATLAS Collaboration, *Studies on top-quark Monte Carlo modelling for Top2016*, ATL-PHYS-PUB-2016-020, 2016, URL: <https://cds.cern.ch/record/2216168>.
- [26] ATLAS Collaboration, *Inclusive and differential cross-sections for dilepton $t\bar{t}$ production measured in $\sqrt{s} = 13$ TeV pp collisions with the ATLAS detector*, *JHEP* **07** (2023) 141, arXiv: [2303.15340 \[hep-ex\]](#).
- [27] ATLAS Collaboration, *Evidence for the charge asymmetry in $pp \rightarrow t\bar{t}$ production at $\sqrt{s} = 13$ TeV with the ATLAS detector*, *JHEP* **08** (2023) 077, arXiv: [2208.12095 \[hep-ex\]](#).
- [28] ATLAS Collaboration, *Measurement of double-differential charged-current Drell–Yan cross-sections at high transverse masses in pp collisions at $\sqrt{s} = 13$ TeV with the ATLAS detector*, *JHEP* **07** (2025) 026, arXiv: [2502.21088 \[hep-ex\]](#).

- [29] ATLAS Collaboration, *Search for direct top squark pair production in final states with two leptons in $\sqrt{s} = 13$ TeV pp collisions with the ATLAS detector*, *Eur. Phys. J. C* **77** (2017) 898, arXiv: [1708.03247 \[hep-ex\]](#).
- [30] ATLAS Collaboration, *ATLAS Run 1 searches for direct pair production of third-generation squarks at the Large Hadron Collider*, *Eur. Phys. J. C* **75** (2015) 510, arXiv: [1506.08616 \[hep-ex\]](#).
- [31] ATLAS Collaboration, *Search for bottom squark pair production in proton–proton collisions at $\sqrt{s} = 13$ TeV with the ATLAS detector*, *Eur. Phys. J. C* **76** (2016) 547, arXiv: [1606.08772 \[hep-ex\]](#).
- [32] ATLAS Collaboration, *Search for gluinos in events with an isolated lepton, jets and missing transverse momentum at $\sqrt{s} = 13$ TeV with the ATLAS detector*, *Eur. Phys. J. C* **76** (2016) 565, arXiv: [1605.04285 \[hep-ex\]](#).
- [33] ATLAS Collaboration, *Search for top-squark pair production in final states with one lepton, jets, and missing transverse momentum using 36fb^{-1} of $\sqrt{s} = 13$ TeV pp collision data with the ATLAS detector*, *JHEP* **06** (2018) 108, arXiv: [1711.11520 \[hep-ex\]](#).
- [34] ATLAS Collaboration, *Search for a scalar partner of the top quark in the all-hadronic $t\bar{t}$ plus missing transverse momentum final state at $\sqrt{s} = 13$ TeV with the ATLAS detector*, *Eur. Phys. J. C* **80** (2020) 737, arXiv: [2004.14060 \[hep-ex\]](#).
- [35] ATLAS Collaboration, *Search for new phenomena in pp collisions in final states with tau leptons, b -jets, and missing transverse momentum with the ATLAS detector*, *Phys. Rev. D* **104** (2021) 112005, arXiv: [2108.07665 \[hep-ex\]](#).
- [36] ATLAS Collaboration, *Search for pair-produced scalar and vector leptoquarks decaying into third-generation quarks and first- or second-generation leptons in pp collisions with the ATLAS detector*, *JHEP* **06** (2023) 188, arXiv: [2210.04517 \[hep-ex\]](#).
- [37] ATLAS Collaboration, *Search for pair-produced vector-like top and bottom partners in events with large missing transverse momentum in pp collisions with the ATLAS detector*, *Eur. Phys. J. C* **83** (2023) 719, arXiv: [2212.05263 \[hep-ex\]](#).
- [38] ATLAS Collaboration, *Search for excited τ -leptons and leptoquarks in the final state with τ -leptons and jets in pp collisions at $\sqrt{s} = 13$ TeV with the ATLAS detector*, *JHEP* **06** (2023) 199, arXiv: [2303.09444 \[hep-ex\]](#).
- [39] ATLAS Collaboration, *Search for supersymmetry in final states with missing transverse momentum and three or more b -jets in 139fb^{-1} of proton–proton collisions at $\sqrt{s} = 13$ TeV with the ATLAS detector*, *Eur. Phys. J. C* **83** (2023) 561, arXiv: [2211.08028 \[hep-ex\]](#).
- [40] A. Denner, S. Dittmaier, S. Kallweit and S. Pozzorini, *Next-to-Leading-Order QCD corrections to $W^+W^-b\bar{b}$ production at Hadron Colliders*, *Phys. Rev. Lett.* **106** (2011) 052001, arXiv: [1012.3975 \[hep-ph\]](#).
- [41] T. Ježo, J. M. Lindert, P. Nason, C. Oleari and S. Pozzorini, *An NLO+PS generator for $t\bar{t}$ and Wt production and decay including non-resonant and interference effects*, *Eur. Phys. J. C* **76** (2016) 691, arXiv: [1607.04538 \[hep-ph\]](#).

- [42] T. Ježo, J. M. Lindert and S. Pozzorini, *Resonance-aware NLOPS matching for off-shell $t\bar{t} + tW$ production with semileptonic decays*, [JHEP **10** \(2023\) 008](#), arXiv: [2307.15653 \[hep-ph\]](#).
- [43] A. Denner and M. Pellen, *Off-shell production of top-antitop pairs in the lepton+jets channel at NLO QCD*, [JHEP **02** \(2018\) 013](#), arXiv: [1711.10359 \[hep-ph\]](#).
- [44] ATLAS Collaboration, *Probing the Quantum Interference between Singly and Doubly Resonant Top-Quark Production in pp Collisions at $\sqrt{s} = 13$ TeV with the ATLAS Detector*, [Phys. Rev. Lett. **121** \(2018\) 152002](#), arXiv: [1806.04667 \[hep-ex\]](#).
- [45] ATLAS Collaboration, *Measurements of differential cross-sections of $WbWb$ production in the dilepton channel in pp collisions at $\sqrt{s} = 13$ TeV using the ATLAS detector*, (2025), arXiv: [2506.14700 \[hep-ex\]](#).
- [46] ATLAS Collaboration, *Search for top squarks in final states with one isolated lepton, jets, and missing transverse momentum in $\sqrt{s} = 13$ TeV pp collisions with the ATLAS detector*, [Phys. Rev. D **94** \(2016\) 052009](#), arXiv: [1606.03903 \[hep-ex\]](#).
- [47] ATLAS Collaboration, *Search for a scalar partner of the top quark in the jets plus missing transverse momentum final state at $\sqrt{s} = 13$ TeV with the ATLAS detector*, [JHEP **12** \(2017\) 085](#), arXiv: [1709.04183 \[hep-ex\]](#).
- [48] ATLAS Collaboration, *The ATLAS Experiment at the CERN Large Hadron Collider*, [JINST **3** \(2008\) S08003](#).
- [49] G. Avoni et al., *The new LUCID-2 detector for luminosity measurement and monitoring in ATLAS*, [JINST **13** \(2018\) P07017](#).
- [50] ATLAS Collaboration, *Performance of the ATLAS trigger system in 2015*, [Eur. Phys. J. C **77** \(2017\) 317](#), arXiv: [1611.09661 \[hep-ex\]](#).
- [51] ATLAS Collaboration, *Software and computing for Run 3 of the ATLAS experiment at the LHC*, [Eur. Phys. J. C **85** \(2025\) 234](#), arXiv: [2404.06335 \[hep-ex\]](#).
- [52] ATLAS Collaboration, *Electron and photon performance measurements with the ATLAS detector using the 2015–2017 LHC proton–proton collision data*, [JINST **14** \(2019\) P12006](#), arXiv: [1908.00005 \[hep-ex\]](#).
- [53] ATLAS Collaboration, *Muon reconstruction and identification efficiency in ATLAS using the full Run 2 pp collision data set at $\sqrt{s} = 13$ TeV*, [Eur. Phys. J. C **81** \(2021\) 578](#), arXiv: [2012.00578 \[hep-ex\]](#).
- [54] ATLAS Collaboration, *Evidence for the associated production of the Higgs boson and a top quark pair with the ATLAS detector*, [Phys. Rev. D **97** \(2018\) 072003](#), arXiv: [1712.08891 \[hep-ex\]](#).
- [55] C. Magliocca, *Measurement of the track impact parameters resolution with the ATLAS experiment at LHC using 2016-2018 data*, [Nuovo Cim. C **44** \(2021\) 55](#).
- [56] ATLAS Collaboration, *Electron and photon energy calibration with the ATLAS detector using LHC Run 2 data*, [JINST **19** \(2024\) P02009](#), arXiv: [2309.05471 \[hep-ex\]](#).
- [57] ATLAS Collaboration, *Studies of the muon momentum calibration and performance of the ATLAS detector with pp collisions at $\sqrt{s} = 13$ TeV*, [Eur. Phys. J. C **83** \(2023\) 686](#), arXiv: [2212.07338 \[hep-ex\]](#).

- [58] M. Cacciari, G. P. Salam and G. Soyez, *The anti- k_t jet clustering algorithm*, *JHEP* **04** (2008) 063, arXiv: [0802.1189 \[hep-ph\]](#).
- [59] M. Cacciari, G. P. Salam and G. Soyez, *FastJet user manual*, *Eur. Phys. J. C* **72** (2012) 1896, arXiv: [1111.6097 \[hep-ph\]](#).
- [60] ATLAS Collaboration, *Jet reconstruction and performance using particle flow with the ATLAS Detector*, *Eur. Phys. J. C* **77** (2017) 466, arXiv: [1703.10485 \[hep-ex\]](#).
- [61] ATLAS Collaboration, *Topological cell clustering in the ATLAS calorimeters and its performance in LHC Run 1*, *Eur. Phys. J. C* **77** (2017) 490, arXiv: [1603.02934 \[hep-ex\]](#).
- [62] ATLAS Collaboration, *Performance of pile-up mitigation techniques for jets in pp collisions at $\sqrt{s} = 8$ TeV using the ATLAS detector*, *Eur. Phys. J. C* **76** (2016) 581, arXiv: [1510.03823 \[hep-ex\]](#).
- [63] ATLAS Collaboration, *Jet energy scale and resolution measured in proton–proton collisions at $\sqrt{s} = 13$ TeV with the ATLAS detector*, *Eur. Phys. J. C* **81** (2021) 689, arXiv: [2007.02645 \[hep-ex\]](#).
- [64] ATLAS Collaboration, *ATLAS flavour-tagging algorithms for the LHC Run 2 pp collision dataset*, *Eur. Phys. J. C* **83** (2023) 681, arXiv: [2211.16345 \[physics.data-an\]](#).
- [65] ATLAS Collaboration, *The performance of missing transverse momentum reconstruction and its significance with the ATLAS detector using 140fb^{-1} of $\sqrt{s} = 13$ TeV pp collisions*, *Eur. Phys. J. C* **85** (2025) 606, arXiv: [2402.05858 \[hep-ex\]](#).
- [66] ATLAS Collaboration, *The ATLAS Simulation Infrastructure*, *Eur. Phys. J. C* **70** (2010) 823, arXiv: [1005.4568 \[physics.ins-det\]](#).
- [67] S. Agostinelli et al., *GEANT4 – a simulation toolkit*, *Nucl. Instrum. Meth. A* **506** (2003) 250.
- [68] ATLAS Collaboration, *Study of the double Higgs production channel $H(\rightarrow b\bar{b})H(\rightarrow \gamma\gamma)$ with the ATLAS experiment at HL-LHC*, ATL-PHYS-PUB-2017-001, 2017, URL: <https://cds.cern.ch/record/2243387>.
- [69] ATLAS Collaboration, *Multi-Boson Simulation for 13 TeV ATLAS Analyses*, ATL-PHYS-PUB-2017-005, 2017, URL: <https://cds.cern.ch/record/2261933>.
- [70] ATLAS Collaboration, *Improvements in $t\bar{t}$ modelling using NLO+PS Monte Carlo generators for Run 2*, ATL-PHYS-PUB-2018-009, 2018, URL: <https://cds.cern.ch/record/2630327>.
- [71] D. J. Lange, *The EvtGen particle decay simulation package*, *Nucl. Instrum. Meth. A* **462** (2001) 152.
- [72] T. Sjöstrand, S. Mrenna and P. Skands, *A brief introduction to PYTHIA 8.1*, *Comput. Phys. Commun.* **178** (2008) 852, arXiv: [0710.3820 \[hep-ph\]](#).
- [73] NNPDF Collaboration, R. D. Ball et al., *Parton distributions with LHC data*, *Nucl. Phys. B* **867** (2013) 244, arXiv: [1207.1303 \[hep-ph\]](#).
- [74] ATLAS Collaboration, *The Pythia 8 A3 tune description of ATLAS minimum bias and inelastic measurements incorporating the Donnachie–Landshoff diffractive model*, ATL-PHYS-PUB-2016-017, 2016, URL: <https://cds.cern.ch/record/2206965>.

- [75] ATLAS Collaboration, *Measurement of the Inelastic Proton–Proton Cross Section at $\sqrt{s} = 13$ TeV with the ATLAS Detector at the LHC*, *Phys. Rev. Lett.* **117** (2016) 182002, arXiv: [1606.02625 \[hep-ex\]](#).
- [76] S. Frixione, G. Ridolfi and P. Nason, *A positive-weight next-to-leading-order Monte Carlo for heavy flavour hadroproduction*, *JHEP* **09** (2007) 126, arXiv: [0707.3088 \[hep-ph\]](#).
- [77] P. Nason, *A new method for combining NLO QCD with shower Monte Carlo algorithms*, *JHEP* **11** (2004) 040, arXiv: [hep-ph/0409146](#).
- [78] S. Frixione, P. Nason and C. Oleari, *Matching NLO QCD computations with parton shower simulations: the POWHEG method*, *JHEP* **11** (2007) 070, arXiv: [0709.2092 \[hep-ph\]](#).
- [79] S. Alioli, P. Nason, C. Oleari and E. Re, *A general framework for implementing NLO calculations in shower Monte Carlo programs: the POWHEG BOX*, *JHEP* **06** (2010) 043, arXiv: [1002.2581 \[hep-ph\]](#).
- [80] T. Sjöstrand et al., *An introduction to PYTHIA 8.2*, *Comput. Phys. Commun.* **191** (2015) 159, arXiv: [1410.3012 \[hep-ph\]](#).
- [81] M. Beneke, P. Falgari, S. Klein and C. Schwinn, *Hadronic top-quark pair production with NNLL threshold resummation*, *Nucl. Phys. B* **855** (2012) 695, arXiv: [1109.1536 \[hep-ph\]](#).
- [82] M. Cacciari, M. Czakon, M. Mangano, A. Mitov and P. Nason, *Top-pair production at hadron colliders with next-to-next-to-leading logarithmic soft-gluon resummation*, *Phys. Lett. B* **710** (2012) 612, arXiv: [1111.5869 \[hep-ph\]](#).
- [83] P. Bärnreuther, M. Czakon and A. Mitov, *Percent-Level-Precision Physics at the Tevatron: Next-to-Next-to-Leading Order QCD Corrections to $q\bar{q} \rightarrow t\bar{t} + X$* , *Phys. Rev. Lett.* **109** (2012) 132001, arXiv: [1204.5201 \[hep-ph\]](#).
- [84] M. Czakon and A. Mitov, *NNLO corrections to top-pair production at hadron colliders: the all-fermionic scattering channels*, *JHEP* **12** (2012) 054, arXiv: [1207.0236 \[hep-ph\]](#).
- [85] M. Czakon and A. Mitov, *NNLO corrections to top pair production at hadron colliders: the quark-gluon reaction*, *JHEP* **01** (2013) 080, arXiv: [1210.6832 \[hep-ph\]](#).
- [86] M. Czakon, P. Fiedler and A. Mitov, *Total Top-Quark Pair-Production Cross Section at Hadron Colliders Through $O(\alpha_S^4)$* , *Phys. Rev. Lett.* **110** (2013) 252004, arXiv: [1303.6254 \[hep-ph\]](#).
- [87] N. Kidonakis and N. Yamanaka, *Higher-order corrections for tW production at high-energy hadron colliders*, *JHEP* **05** (2021) 278, arXiv: [2102.11300 \[hep-ph\]](#).
- [88] N. Kidonakis, *Two-loop soft anomalous dimensions for single top quark associated production with a W^- or H^-* , *Phys. Rev. D* **82** (2010) 054018, arXiv: [1005.4451 \[hep-ph\]](#).
- [89] N. Kidonakis, ‘Top Quark Production’, *Proceedings, Helmholtz International Summer School on Physics of Heavy Quarks and Hadrons (HQ2013)* (JINR, Dubna, Russia, 15th–28th July 2013) 139, arXiv: [1311.0283 \[hep-ph\]](#).

- [90] M. Bähr et al., *Herwig++ physics and manual*, *Eur. Phys. J. C* **58** (2008) 639, arXiv: [0803.0883 \[hep-ph\]](#).
- [91] J. Bellm et al., *Herwig 7.0/Herwig++ 3.0 release note*, *Eur. Phys. J. C* **76** (2016) 196, arXiv: [1512.01178 \[hep-ph\]](#).
- [92] J. Bellm et al., *Herwig 7.1 Release Note*, (2017), arXiv: [1705.06919 \[hep-ph\]](#).
- [93] J. Bellm et al., *Herwig 7.2 release note*, *Eur. Phys. J. C* **80** (2020) 452, arXiv: [1912.06509 \[hep-ph\]](#).
- [94] S. Höche, S. Mrenna, S. Payne, C. T. Preuss and P. Skands, *A Study of QCD Radiation in VBF Higgs Production with Vincia and Pythia*, *SciPost Phys.* **12** (2022) 010, arXiv: [2106.10987 \[hep-ph\]](#).
- [95] E. Bothmann, M. Schönherr and S. Schumann, *Reweighting QCD matrix-element and parton-shower calculations*, *Eur. Phys. J. C* **76** (2016) 590, arXiv: [1606.08753 \[hep-ph\]](#).
- [96] J. Butterworth et al., *PDF4LHC recommendations for LHC Run II*, *J. Phys. G* **43** (2016) 023001, arXiv: [1510.03865 \[hep-ph\]](#).
- [97] J. Mazzitelli et al., *Next-to-Next-to-Leading Order Event Generation for Top-Quark Pair Production*, *Phys. Rev. Lett.* **127** (2021) 062001, arXiv: [2012.14267 \[hep-ph\]](#).
- [98] E. Bothmann et al., *Event generation with Sherpa 2.2*, *SciPost Phys.* **7** (2019) 034, arXiv: [1905.09127 \[hep-ph\]](#).
- [99] T. Gleisberg and S. Höche, *Comix, a new matrix element generator*, *JHEP* **12** (2008) 039, arXiv: [0808.3674 \[hep-ph\]](#).
- [100] F. Buccioni et al., *OpenLoops 2*, *Eur. Phys. J. C* **79** (2019) 866, arXiv: [1907.13071 \[hep-ph\]](#).
- [101] F. Cascioli, P. Maierhöfer and S. Pozzorini, *Scattering Amplitudes with Open Loops*, *Phys. Rev. Lett.* **108** (2012) 111601, arXiv: [1111.5206 \[hep-ph\]](#).
- [102] A. Denner, S. Dittmaier and L. Hofer, *COLLIER: A fortran-based complex one-loop library in extended regularizations*, *Comput. Phys. Commun.* **212** (2017) 220, arXiv: [1604.06792 \[hep-ph\]](#).
- [103] S. Schumann and F. Krauss, *A parton shower algorithm based on Catani–Seymour dipole factorisation*, *JHEP* **03** (2008) 038, arXiv: [0709.1027 \[hep-ph\]](#).
- [104] S. Höche, F. Krauss, M. Schönherr and F. Siegert, *A critical appraisal of NLO+PS matching methods*, *JHEP* **09** (2012) 049, arXiv: [1111.1220 \[hep-ph\]](#).
- [105] S. Höche, F. Krauss, M. Schönherr and F. Siegert, *QCD matrix elements + parton showers. The NLO case*, *JHEP* **04** (2013) 027, arXiv: [1207.5030 \[hep-ph\]](#).
- [106] S. Catani, F. Krauss, B. R. Webber and R. Kuhn, *QCD Matrix Elements + Parton Showers*, *JHEP* **11** (2001) 063, arXiv: [hep-ph/0109231](#).
- [107] S. Höche, F. Krauss, S. Schumann and F. Siegert, *QCD matrix elements and truncated showers*, *JHEP* **05** (2009) 053, arXiv: [0903.1219 \[hep-ph\]](#).

- [108] S. Kallweit, J. M. Lindert, P. Maierhöfer, S. Pozzorini and M. Schönherr, *NLO electroweak automation and precise predictions for W +multijet production at the LHC*, [JHEP **04** \(2015\) 012](#), arXiv: [1412.5157 \[hep-ph\]](#).
- [109] S. Kallweit, J. M. Lindert, P. Maierhöfer, S. Pozzorini and M. Schönherr, *NLO QCD+EW predictions for V + jets including off-shell vector-boson decays and multijet merging*, [JHEP **04** \(2016\) 021](#), arXiv: [1511.08692 \[hep-ph\]](#).
- [110] J. Alwall et al., *The automated computation of tree-level and next-to-leading order differential cross sections, and their matching to parton shower simulations*, [JHEP **07** \(2014\) 079](#), arXiv: [1405.0301 \[hep-ph\]](#).
- [111] M. Aliev et al., *HATHOR – HAdronic Top and Heavy quarks crOss section calculatoR*, [Comput. Phys. Commun. **182** \(2011\) 1034](#), arXiv: [1007.1327 \[hep-ph\]](#).
- [112] P. Kant et al., *HatHor for single top-quark production: Updated predictions and uncertainty estimates for single top-quark production in hadronic collisions*, [Comput. Phys. Commun. **191** \(2015\) 74](#), arXiv: [1406.4403 \[hep-ph\]](#).
- [113] D. de Florian et al., *Handbook of LHC Higgs Cross Sections: 4. Deciphering the Nature of the Higgs Sector*, (2017), arXiv: [1610.07922 \[hep-ph\]](#).
- [114] ATLAS Collaboration, *Luminosity determination in pp collisions at $\sqrt{s} = 13$ TeV using the ATLAS detector at the LHC*, [Eur. Phys. J. C **83** \(2023\) 982](#), arXiv: [2212.09379 \[hep-ex\]](#).
- [115] ATLAS Collaboration, *ATLAS data quality operations and performance for 2015–2018 data-taking*, [JINST **15** \(2020\) P04003](#), arXiv: [1911.04632 \[physics.ins-det\]](#).
- [116] ATLAS Collaboration, *Performance of electron and photon triggers in ATLAS during LHC Run 2*, [Eur. Phys. J. C **80** \(2020\) 47](#), arXiv: [1909.00761 \[hep-ex\]](#).
- [117] ATLAS Collaboration, *Performance of the ATLAS muon triggers in Run 2*, [JINST **15** \(2020\) P09015](#), arXiv: [2004.13447 \[physics.ins-det\]](#).
- [118] ATLAS Collaboration, *Vertex Reconstruction Performance of the ATLAS Detector at $\sqrt{s} = 13$ TeV*, ATL-PHYS-PUB-2015-026, 2015, URL: <https://cds.cern.ch/record/2037717>.
- [119] S. Schmitt, *Data Unfolding Methods in High Energy Physics*, [EPJ Web Conf. **137** \(2017\) 11008](#), ed. by Y. Foka, N. Brambilla and V. Kovalenko, arXiv: [1611.01927 \[physics.data-an\]](#).
- [120] V. Blobel, *Unfolding Methods in Particle Physics*, [PHYSTAT 2011 \(2011\) 240](#).
- [121] S. Schmitt, *TUnfold: an algorithm for correcting migration effects in high energy physics*, [JINST **7** \(2012\) T10003](#), arXiv: [1205.6201 \[physics.data-an\]](#).
- [122] A. N. Tikhonov, A. V. Goncharsky, V. V. Stepanov and A. G. Yagola, *Numerical Methods for the Solution of Ill-Posed Problems*, Springer, 1990, ISBN: 978-94-015-8480-7.
- [123] D. L. Phillips, *A Technique for the Numerical Solution of Certain Integral Equations of the First Kind*, [Journal of the ACM \(JACM\) **9** \(1962\) 84](#).

- [124] ATLAS Collaboration, *Tools for estimating fake/non-prompt lepton backgrounds with the ATLAS detector at the LHC*, [JINST **18** \(2023\) T11004](#), arXiv: [2211.16178 \[hep-ex\]](#).
- [125] ATLAS Collaboration, *ATLAS b-jet identification performance and efficiency measurement with $t\bar{t}$ events in pp collisions at $\sqrt{s} = 13$ TeV*, [Eur. Phys. J. C **79** \(2019\) 970](#), arXiv: [1907.05120 \[hep-ex\]](#).
- [126] ATLAS Collaboration, *Measurement of the c-jet mistagging efficiency in $t\bar{t}$ events using pp collision data at $\sqrt{s} = 13$ TeV collected with the ATLAS detector*, [Eur. Phys. J. C **82** \(2022\) 95](#), arXiv: [2109.10627 \[hep-ex\]](#).
- [127] ATLAS Collaboration, *Calibration of the light-flavour jet mistagging efficiency of the b-tagging algorithms with Z+jets events using 139 fb^{-1} of ATLAS proton–proton collision data at $\sqrt{s} = 13$ TeV*, [Eur. Phys. J. C **83** \(2023\) 728](#), arXiv: [2301.06319 \[hep-ex\]](#).
- [128] P. Artoisenet, R. Frederix, O. Mattelaer and R. Rietkerk, *Automatic spin-entangled decays of heavy resonances in Monte Carlo simulations*, [JHEP **03** \(2013\) 015](#), arXiv: [1212.3460 \[hep-ph\]](#).
- [129] ATLAS Collaboration, *ATLAS Computing Acknowledgements*, ATL-SOFT-PUB-2025-001, 2025, URL: <https://cds.cern.ch/record/2922210>.

The ATLAS Collaboration

G. Aad [ID103](#), E. Aakvaag [ID17](#), B. Abbott [ID122](#), S. Abdelhameed [ID118a](#), K. Abeling [ID55](#), N.J. Abicht [ID49](#), S.H. Abidi [ID30](#), M. Aboeela [ID45](#), A. Aboulhorma [ID36e](#), H. Abramowicz [ID156](#), Y. Abulaiti [ID119](#), B.S. Acharya [ID69a,69b,m](#), A. Ackermann [ID63a](#), C. Adam Bourdarios [ID4](#), L. Adamczyk [ID86a](#), S.V. Addepalli [ID148](#), M.J. Addison [ID102](#), J. Adelman [ID117](#), A. Adiguzel [ID22c](#), T. Adye [ID136](#), A.A. Affolder [ID138](#), Y. Afik [ID40](#), M.N. Agaras [ID13](#), A. Aggarwal [ID101](#), C. Agheorghiesei [ID28c](#), F. Ahmadov [ID39,ad](#), S. Ahuja [ID96](#), S. Ahuja [ID168](#), X. Ai [ID142b](#), G. Aielli [ID76a,76b](#), A. Aikot [ID168](#), M. Ait Tamliah [ID36e](#), B. Aitbenkikh [ID36a](#), T.P.A. Åkesson [ID99](#), A.V. Akimov [ID150](#), D. Akiyama [ID173](#), N.N. Akolkar [ID25](#), S. Aktas [ID171](#), G.L. Alberghi [ID24b](#), J. Albert [ID170](#), U. Alberti [ID20](#), P. Albicocco [ID53](#), G.L. Albouy [ID60](#), S. Alderweireldt [ID52](#), Z.L. Alegria [ID123](#), M. Aleksa [ID37](#), I.N. Aleksandrov [ID39](#), C. Alexa [ID28b](#), T. Alexopoulos [ID10](#), F. Alfonsi [ID24b](#), M. Algren [ID56](#), M. Alhroob [ID172](#), B. Ali [ID134](#), H.M.J. Ali [ID92,w](#), S. Ali [ID32](#), S.W. Alibocus [ID93](#), M. Aliev [ID34c](#), G. Alimonti [ID71a](#), W. Alkakh [ID55](#), C. Allaire [ID66](#), B.M.M. Allbrooke [ID151](#), D.R. Allen [ID123](#), J.S. Allen [ID102](#), J.F. Allen [ID52](#), P.P. Allport [ID21](#), A. Aloisio [ID72a,72b](#), F. Alonso [ID91](#), C. Alpigiani [ID141](#), Z.M.K. Alsolami [ID92](#), A. Alvarez Fernandez [ID101](#), M. Alves Cardoso [ID56](#), M.G. Alviggi [ID72a,72b](#), M. Aly [ID102](#), Y. Amaral Coutinho [ID82b](#), A. Ambler [ID105](#), C. Amelung [ID37](#), M. Amerl [ID102](#), C.G. Ames [ID110](#), T. Amezza [ID129](#), D. Amidei [ID107](#), B. Amini [ID54](#), K. Amirie [ID160](#), A. Amirkhanov [ID39](#), S.P. Amor Dos Santos [ID132a](#), K.R. Amos [ID168](#), D. Amperiadou [ID157](#), S. An [ID83](#), C. Anastopoulos [ID144](#), T. Andeen [ID11](#), J.K. Anders [ID93](#), A.C. Anderson [ID59](#), A. Andreatta [ID71a,71b](#), S. Angelidakis [ID9](#), A. Angerami [ID42](#), A.V. Anisenkov [ID39](#), A. Annovi [ID74a](#), C. Antel [ID37](#), E. Antipov [ID150](#), M. Antonelli [ID53](#), F. Anulli [ID75a](#), M. Aoki [ID83](#), T. Aoki [ID158](#), M.A. Aparo [ID151](#), L. Aperio Bella [ID48](#), M. Apicella [ID31](#), C. Appelt [ID156](#), A. Apyan [ID27](#), M. Arampatzi [ID10](#), S.J. Arbiol Val [ID87](#), C. Arcangeletti [ID53](#), A.T.H. Arce [ID51](#), J-F. Arguin [ID109](#), S. Argyropoulos [ID157](#), J.-H. Arling [ID48](#), O. Arnaez [ID4](#), H. Arnold [ID150](#), G. Artoni [ID75a,75b](#), H. Asada [ID112](#), K. Asai [ID120](#), S. Asatryan [ID178](#), N.A. Asbah [ID37](#), R.A. Ashby Pickering [ID172](#), A.M. Aslam [ID96](#), K. Assamagan [ID30](#), R. Astalos [ID29a](#), K.S.V. Astrand [ID99](#), S. Atashi [ID164](#), R.J. Atkin [ID34a](#), H. Atmani [ID36f](#), P.A. Atlasiddha [ID130](#), K. Augsten [ID134](#), A.D. Auriol [ID41](#), V.A. Austrup [ID102](#), A.S. Avad [ID95](#), G. Avolio [ID37](#), K. Axiotis [ID56](#), A. Azzam [ID13](#), D. Babal [ID29b](#), H. Bachacou [ID137](#), K. Bachas [ID157,q](#), A. Bachiu [ID35](#), E. Bachmann [ID50](#), M.J. Backes [ID63a](#), A. Badea [ID40](#), T.M. Baer [ID107](#), P. Bagnaia [ID75a,75b](#), M. Bahmani [ID19](#), D. Bahner [ID54](#), K. Bai [ID125](#), J.T. Baines [ID136](#), L. Baines [ID95](#), O.K. Baker [ID177](#), E. Bakos [ID16](#), D. Bakshi Gupta [ID8](#), L.E. Balabram Filho [ID82b](#), V. Balakrishnan [ID122](#), R. Balasubramanian [ID4](#), E.M. Baldin [ID38](#), P. Balek [ID86a](#), E. Ballabene [ID24b,24a](#), F. Balli [ID137](#), L.M. Baltes [ID63a](#), W.K. Balunas [ID33](#), J. Balz [ID101](#), I. Bamwidhi [ID118b](#), E. Banas [ID87](#), M. Bandieramonte [ID131](#), A. Bandyopadhyay [ID25](#), S. Bansal [ID25](#), L. Barak [ID156](#), M. Barakat [ID48](#), E.L. Barberio [ID106](#), D. Barberis [ID18b](#), M. Barbero [ID103](#), M.Z. Barel [ID116](#), T. Barillari [ID111](#), M-S. Barisits [ID37](#), T. Barklow [ID148](#), P. Baron [ID135](#), D.A. Baron Moreno [ID102](#), A. Baroncelli [ID62](#), A.J. Barr [ID128](#), J.D. Barr [ID97](#), F. Barreiro [ID100](#), J. Barreiro Guimarães da Costa [ID14](#), M.G. Barros Teixeira [ID132a](#), S. Barsov [ID38](#), F. Bartels [ID63a](#), R. Bartoldus [ID148](#), A.E. Barton [ID92](#), P. Bartos [ID29a](#), M. Baselga [ID49](#), S. Bashiri [ID87](#), A. Bassalat [ID66,b](#), M.J. Basso [ID161a](#), S. Bataju [ID45](#), R. Bate [ID169](#), R.L. Bates [ID59](#), S. Batlamous [ID100](#), M. Battaglia [ID138](#), D. Battulga [ID19](#), M. Baucé [ID75a,75b](#), M. Bauer [ID79](#), P. Bauer [ID25](#), L.T. Bayer [ID48](#), L.T. Bazzano Hurrell [ID31](#), J.B. Beacham [ID111](#), T. Beau [ID129](#), J.Y. Beauchamp [ID91](#), P.H. Beauchemin [ID163](#), P. Bechtel [ID25](#), H.P. Beck [ID20,p](#), K. Becker [ID172](#), A.J. Beddall [ID81](#), V.A. Bednyakov [ID39](#), C.P. Bee [ID150](#), L.J. Beemster [ID16](#), M. Begalli [ID82d](#), M. Begel [ID30](#), J.K. Behr [ID48](#), J.F. Beirer [ID37](#), F. Beisiegel [ID25](#), M. Belfkir [ID118b](#), G. Bella [ID156](#), L. Bellagamba [ID24b](#), A. Bellerive [ID35](#), C.D. Bellgraph [ID68](#), P. Bellos [ID21](#), K. Beloborodov [ID38](#), I. Benaoumeur [ID21](#), D. Benckroun [ID36a](#), F. Bendebba [ID36a](#), Y. Benhammou [ID156](#), K.C. Benkendorfer [ID61](#), L. Beresford [ID48](#),

M. Beretta ⁵³, E. Bergeaas Kuutmann ¹⁶⁶, N. Berger ⁴, B. Bergmann ¹³⁴, J. Beringer ^{18a},
G. Bernardi ⁵, C. Bernius ¹⁴⁸, F.U. Bernlochner ²⁵, A. Berrocal Guardia ¹³, T. Berry ⁹⁶,
P. Berta ¹³⁵, A. Berti ^{132a}, R. Bertrand ¹⁰³, S. Bethke ¹¹¹, A. Betti ^{75a,75b}, A.J. Bevan ⁹⁵,
L. Bezio ⁵⁶, N.K. Bhalla ⁵⁴, S. Bharthuar ¹¹¹, S. Bhatta ¹⁵⁰, P. Bhattacharai ¹⁴⁸, Z.M. Bhatti ¹¹⁹,
K.D. Bhide ⁵⁴, V.S. Bhopatkar ¹²³, R.M. Bianchi ¹³¹, G. Bianco ^{24b,24a}, O. Biebel ¹¹⁰,
M. Biglietti ^{77a}, C.S. Billingsley ⁴⁵, Y. Bimgdi ^{36f}, M. Bindi ⁵⁵, A. Bingham ¹⁷⁶, A. Bingul ^{22b},
C. Bini ^{75a,75b}, G.A. Bird ³³, M. Birman ¹⁷⁴, M. Biros ¹³⁵, S. Biryukov ¹⁵¹, T. Bisanz ⁴⁹,
E. Bisceglie ^{24b,24a}, J.P. Biswal ¹³⁶, D. Biswas ¹⁴⁶, I. Bloch ⁴⁸, A. Blue ⁵⁹, U. Blumenschein ⁹⁵,
V.S. Bobrovnikov ³⁹, L. Boccardo ^{57b,57a}, M. Boehler ⁵⁴, B. Boehm ¹⁷¹, D. Bogavac ¹³,
A.G. Bogdanchikov ³⁸, L.S. Boggia ¹²⁹, V. Boisvert ⁹⁶, P. Bokan ³⁷, T. Bold ^{86a}, M. Bomben ⁵,
M. Bona ⁹⁵, M. Boonekamp ¹³⁷, A.G. Borbély ⁵⁹, I.S. Bordulev ³⁸, G. Borissov ⁹²,
D. Bortoletto ¹²⁸, D. Boscherini ^{24b}, M. Bosman ¹³, K. Bouaouda ^{36a}, N. Bouchhar ¹⁶⁸,
L. Boudet ⁴, J. Boudreau ¹³¹, E.V. Bouhova-Thacker ⁹², D. Boumediene ⁴¹, R. Bouquet ^{57b,57a},
A. Boveia ¹²¹, J. Boyd ³⁷, D. Boye ³⁰, I.R. Boyko ³⁹, L. Bozianu ⁵⁶, J. Bracnik ²¹,
N. Brahimi ⁴, G. Brandt ¹⁷⁶, O. Brandt ³³, B. Brau ¹⁰⁴, J.E. Brau ¹²⁵, R. Brenner ¹⁷⁴,
L. Brenner ¹¹⁶, R. Brenner ¹⁶⁶, S. Bressler ¹⁷⁴, G. Brianti ^{78a,78b}, D. Britton ⁵⁹, D. Britzger ¹¹¹,
I. Brock ²⁵, R. Brock ¹⁰⁸, G. Brooijmans ⁴², A.J. Brooks ⁶⁸, E.M. Brooks ^{161b}, E. Brost ³⁰,
L.M. Brown ^{170,161a}, L.E. Bruce ⁶¹, T.L. Bruckler ¹²⁸, P.A. Bruckman de Renstrom ⁸⁷,
B. Brüers ⁴⁸, A. Bruni ^{24b}, G. Bruni ^{24b}, D. Brunner ^{47a,47b}, M. Bruschi ^{24b}, N. Bruscino ^{75a,75b},
T. Buanes ¹⁷, Q. Buat ¹⁴¹, D. Buchin ¹¹¹, A.G. Buckley ⁵⁹, O. Bulekov ⁸¹, B.A. Bullard ¹⁴⁸,
S. Burdin ⁹³, C.D. Burgard ⁴⁹, A.M. Burger ⁹⁰, B. Burghgrave ⁸, O. Burlayenko ⁵⁴,
J. Bureson ¹⁶⁷, J.C. Burzynski ¹⁴⁷, E.L. Busch ⁴², V. Büscher ¹⁰¹, P.J. Bussey ⁵⁹, O. But ²⁵,
J.M. Butler ²⁶, C.M. Buttar ⁵⁹, J.M. Butterworth ⁹⁷, P. Butti ³⁷, W. Buttinger ¹³⁶,
C.J. Buxo Vázquez ¹⁰⁸, A.R. Buzykaev ³⁹, S. Cabrera Urbán ¹⁶⁸, L. Cadamuro ⁶⁶, H. Cai ³⁷,
Y. Cai ^{24b,113c,24a}, Y. Cai ^{113a}, V.M.M. Cairo ³⁷, O. Cakir ^{3a}, N. Calace ³⁷, P. Calafiura ^{18a},
G. Calderini ¹²⁹, P. Calfayan ³⁵, L. Calic ⁹⁹, G. Callea ⁵⁹, L.P. Caloba ^{82b}, D. Calvet ⁴¹,
S. Calvet ⁴¹, R. Camacho Toro ¹²⁹, S. Camarda ³⁷, D. Camarero Munoz ²⁷, P. Camarri ^{76a,76b},
C. Camincher ¹⁷⁰, M. Campanelli ⁹⁷, A. Camplani ⁴³, V. Canale ^{72a,72b}, A.C. Canbay ^{3a},
E. Canonero ⁹⁶, J. Cantero ¹⁶⁸, Y. Cao ¹⁶⁷, F. Capocasa ²⁷, M. Capua ^{44b,44a}, A. Carbone ^{71a,71b},
R. Cardarelli ^{76a}, J.C.J. Cardenas ⁸, M.P. Cardiff ²⁷, G. Carducci ^{44b,44a}, T. Carli ³⁷,
G. Carlino ^{72a}, J.I. Carlotto ¹³, B.T. Carlson ^{131,r}, E.M. Carlson ¹⁷⁰, J. Carmignani ⁹³,
L. Carminati ^{71a,71b}, A. Carnelli ⁴, M. Carnesale ³⁷, S. Caron ¹¹⁵, E. Carquin ^{139g}, I.B. Carr ¹⁰⁶,
S. Carrá ^{73a,73b}, G. Carratta ^{24b,24a}, C. Carrion Martinez ¹⁶⁸, A.M. Carroll ¹²⁵, M.P. Casado ^{13,h},
P. Casolaro ^{72a,72b}, M. Caspar ⁴⁸, W.R. Castiglioni ⁴⁰, F.L. Castillo ⁴, L. Castillo Garcia ¹³,
V. Castillo Gimenez ¹⁶⁸, N.F. Castro ^{132a,132e}, A. Catinaccio ³⁷, J.R. Catmore ¹²⁷, T. Cavaliere ⁴,
V. Cavaliere ³⁰, L.J. Cavedes Betancourt ^{23b}, E. Celebi ⁸¹, S. Cella ³⁷, V. Cepaitis ⁵⁶,
K. Cerny ¹²⁴, A.S. Cerqueira ^{82a}, A. Cerri ^{74a,74b,am}, L. Cerrito ^{76a,76b}, F. Cerutti ^{18a},
B. Cervato ^{71a,71b}, A. Cervelli ^{24b}, G. Cesarini ⁵³, S.A. Cetin ⁸¹, P.M. Chabrilat ¹²⁹,
R. Chakkappai ⁵⁶, S. Chakraborty ¹⁷², A. Chambers ⁶¹, J. Chan ^{18a}, W.Y. Chan ¹⁵⁸,
J.D. Chapman ³³, E. Chapon ¹³⁷, B. Chargeishvili ^{154b}, D.G. Charlton ²¹, C. Chauhan ¹³⁵,
Y. Che ^{113a}, S. Chekanov ⁶, G.A. Chelkov ^{39,a}, B. Chen ¹⁵⁶, B. Chen ¹⁷⁰, H. Chen ³⁰,
J. Chen ^{143a}, J. Chen ¹⁴⁷, M. Chen ¹²⁸, S. Chen ⁸⁸, S.J. Chen ^{113a}, X. Chen ^{143a}, X. Chen ^{15,ah},
Z. Chen ⁶², C.L. Cheng ¹⁷⁵, H.C. Cheng ^{64a}, S. Cheong ¹⁴⁸, A. Cheplakov ³⁹,
E. Cherepanova ¹¹⁶, R. Cherkaoui El Moursli ^{36e}, E. Cheu ⁷, K. Cheung ⁶⁵, L. Chevalier ¹³⁷,
V. Chiarella ⁵³, G. Chiarelli ^{74a}, G. Chiodini ^{70a}, A.S. Chisholm ²¹, A. Chitan ^{28b},
M. Chitishvili ¹⁶⁸, M.V. Chizhov ^{39,s}, K. Choi ¹¹, Y. Chou ¹⁴¹, E.Y.S. Chow ¹¹⁵, K.L. Chu ¹⁷⁴,
M.C. Chu ^{64a}, X. Chu ^{14,113c}, Z. Chubinidze ⁵³, J. Chudoba ¹³³, J.J. Chwastowski ⁸⁷,

D. Cieri ¹¹¹, K.M. Ciesla ^{86a}, V. Cindro ⁹⁴, A. Ciocio ^{18a}, F. Cirotto ^{72a,72b}, Z.H. Citron ¹⁷⁴,
 M. Citterio ^{71a}, D.A. Ciubotaru ^{28b}, A. Clark ⁵⁶, P.J. Clark ⁵², N. Clarke Hall ⁹⁷, C. Clarry ¹⁶⁰,
 S.E. Clawson ⁴⁸, C. Clement ^{47a,47b}, L. Clissa ^{24b,24a}, Y. Coadou ¹⁰³, M. Cobal ^{69a,69c},
 A. Coccaro ^{57b}, R.F. Coelho Barrue ^{132a}, R. Coelho Lopes De Sa ¹⁰⁴, S. Coelli ^{71a}, M.M. Cohen ¹³⁰,
 L.S. Colangeli ¹⁶⁰, B. Cole ⁴², P. Collado Soto ¹⁰⁰, J. Collot ⁶⁰, R. Coluccia ^{70a,70b},
 P. Conde Muiño ^{132a,132g}, M.P. Connell ^{34c}, S.H. Connell ^{34c}, E.I. Conroy ¹²⁸,
 M. Contreras Cossio ¹¹, F. Conventi ^{72a,aj}, A.M. Cooper-Sarkar ¹²⁸, L. Corazzina ^{75a,75b},
 F.A. Corchia ^{24b,24a}, A. Cordeiro Oudot Choi ¹⁴¹, L.D. Corpe ⁴¹, M. Corradi ^{75a,75b},
 F. Corriveau ^{105,ab}, A. Cortes-Gonzalez ¹⁵⁸, M.J. Costa ¹⁶⁸, F. Costanza ⁴, D. Costanzo ¹⁴⁴,
 J. Couthures ⁴, G. Cowan ⁹⁶, K. Cranmer ¹⁷⁵, L. Cremer ⁴⁹, D. Cremonini ^{24b,24a},
 S. Crépe-Renaudin ⁶⁰, F. Crescioli ¹²⁹, T. Cresta ^{73a,73b}, M. Cristinziani ¹⁴⁶,
 M. Cristoforetti ^{78a,78b}, E. Critelli ⁹⁷, V. Croft ¹¹⁶, G. Crosetti ^{44b,44a}, A. Cueto ¹⁰⁰, H. Cui ⁹⁷,
 Z. Cui ⁷, B.M. Cunnett ¹⁵¹, W.R. Cunningham ⁵⁹, F. Curcio ¹⁶⁸, J.R. Curran ⁵²,
 M.J. Da Cunha Sargedas De Sousa ^{57b,57a}, J.V. Da Fonseca Pinto ^{82b}, C. Da Via ¹⁰²,
 W. Dabrowski ^{86a}, T. Dado ³⁷, S. Dahbi ¹⁵³, T. Dai ¹⁰⁷, D. Dal Santo ²⁰, C. Dallapiccola ¹⁰⁴,
 M. Dam ⁴³, G. D'amen ³⁰, V. D'Amico ¹¹⁰, J.R. Dandoy ³⁵, M. D'Andrea ^{57b,57a},
 D. Dannheim ³⁷, G. D'anniballe ^{74a,74b}, M. Danninger ¹⁴⁷, V. Dao ¹⁵⁰, G. Darbo ^{57b},
 S.J. Das ³⁰, F. Dattola ⁴⁸, S. D'Auria ^{71a,71b}, A. D'Avanzo ^{72a,72b}, T. Davidek ¹³⁵,
 J. Davidson ¹⁷², I. Dawson ⁹⁵, K. De ⁸, C. De Almeida Rossi ¹⁶⁰, R. De Asmundis ^{72a},
 N. De Biase ⁴⁸, S. De Castro ^{24b,24a}, N. De Groot ¹¹⁵, P. de Jong ¹¹⁶, H. De la Torre ¹¹⁷,
 A. De Maria ^{113a}, A. De Salvo ^{75a}, U. De Sanctis ^{76a,76b}, F. De Santis ^{70a,70b}, A. De Santo ¹⁵¹,
 J.B. De Vivie De Regie ⁶⁰, J. Debevc ⁹⁴, D.V. Dedovich ³⁹, J. Degens ⁹³, A.M. Deiana ⁴⁵,
 J. Del Peso ¹⁰⁰, L. Delagrangé ¹²⁹, F. Deliot ¹³⁷, C.M. Delitzsch ⁴⁹, M. Della Pietra ^{72a,72b},
 D. Della Volpe ⁵⁶, A. Dell'Acqua ³⁷, L. Dell'Asta ^{71a,71b}, M. Delmastro ⁴, C.C. Delogu ^{57b,57a},
 P.A. Delsart ⁶⁰, S. Demers ¹⁷⁷, M. Demichev ³⁹, S.P. Denisov ³⁸, H. Denizli ^{22a,1}, M.G. Depala ⁹³,
 L. D'Eramo ⁴¹, D. Derendarz ⁸⁷, F. Derue ¹²⁹, P. Dervan ^{93,*}, A.M. Desai ¹, K. Desch ²⁵,
 F.A. Di Bello ^{74a,74b}, A. Di Ciaccio ^{76a,76b}, L. Di Ciaccio ⁴, A. Di Domenico ^{75a,75b},
 C. Di Donato ^{72a,72b}, A. Di Girolamo ³⁷, G. Di Gregorio ⁶⁶, A. Di Luca ^{78a,78b},
 B. Di Micco ^{77a,77b}, R. Di Nardo ^{77a,77b}, K.F. Di Petrillo ⁴⁰, M. Diamantopoulou ³⁵, F.A. Dias ¹¹⁶,
 M.A. Diaz ^{139a,139b}, A.R. Didenko ³⁹, M. Didenko ¹⁶⁸, S.D. Diefenbacher ^{18a}, E.B. Diehl ¹⁰⁷,
 S. Díez Cornell ⁴⁸, C. Diez Pardos ¹⁴⁶, C. Dimitriadi ¹⁴⁹, A. Dimitrievska ²¹, A. Dimri ¹⁵⁰,
 Y. Ding ⁶², J. Dingfelder ²⁵, T. Dingley ¹²⁸, I-M. Dinu ^{28b}, S.J. Dittmeier ^{63b}, F. Dittus ³⁷,
 M. Divisek ¹³⁵, B. Dixit ⁹³, F. Djama ¹⁰³, T. Djobava ^{154b}, C. Doglioni ^{102,99}, A. Dohnalova ^{29a},
 Z. Dolezal ¹³⁵, K. Domijan ^{86a}, K.M. Dona ⁴⁰, M. Donadelli ^{82d}, B. Dong ¹⁰⁸, J. Donini ⁴¹,
 A. D'Onofrio ^{72a,72b}, M. D'Onofrio ⁹³, J. Dopke ¹³⁶, A. Doria ^{72a}, N. Dos Santos Fernandes ^{132a},
 I.A. Dos Santos Luz ^{82e}, P. Dougan ¹⁰², M.T. Dova ⁹¹, A.T. Doyle ⁵⁹, M.P. Drescher ⁵⁵,
 E. Dreyer ¹⁷⁴, I. Drivas-koulouris ¹⁰, M. Drnevich ¹¹⁹, D. Du ⁶², T.A. du Pree ¹¹⁶, Z. Duan ^{113a},
 M. Dubau ⁴, F. Dubinin ³⁹, M. Dubovsky ^{29a}, E. Duchovni ¹⁷⁴, G. Duckeck ¹¹⁰, P.K. Duckett ⁹⁷,
 O.A. Ducu ^{28b}, D. Duda ⁵², A. Dudarev ³⁷, M.M. Dudek ⁸⁷, E.R. Duden ²⁷, M. D'uffizi ¹⁰²,
 L. Duflot ⁶⁶, M. Dührssen ³⁷, I. Duminica ^{28g}, A.E. Dumitriu ^{28b}, M. Dunford ^{63a},
 K. Dunne ^{47a,47b}, A. Duperrin ¹⁰³, H. Duran Yildiz ^{3a}, A. Durglishvili ^{154b}, G.I. Dyckes ^{18a},
 M. Dyndal ^{86a}, B.S. Dziedzic ³⁷, Z.O. Earnshaw ¹⁵¹, G.H. Eberwein ¹²⁸, B. Eckerova ^{29a},
 S. Eggebrecht ⁵⁵, E. Egidio Purcino De Souza ^{82e}, G. Eigen ¹⁷, K. Einsweiler ^{18a}, T. Ekelof ¹⁶⁶,
 P.A. Ekman ⁹⁹, S. El Farkh ^{36b}, Y. El Ghazali ⁶², H. El Jarrari ¹⁰⁵, A. El Moussaouy ^{36a},
 D. Elitez ³⁷, M. Ellert ¹⁶⁶, F. Ellinghaus ¹⁷⁶, T.A. Elliot ⁹⁶, N. Ellis ³⁷, J. Elmsheuser ³⁰,
 M. Elsayy ^{118a}, M. Elsing ³⁷, D. Emeliyanov ¹³⁶, Y. Enari ⁸³, S. Epari ¹⁰⁹,
 D. Ernani Martins Neto ⁸⁷, F. Ernst ³⁷, M. Escalier ⁶⁶, C. Escobar ¹⁶⁸, E. Etzion ¹⁵⁶,

G. Evans [id](#)^{132a,132b}, H. Evans [id](#)⁶⁸, L.S. Evans [id](#)⁴⁸, A. Ezhilov [id](#)³⁸, S. Ezzarqtouni [id](#)^{36a}, F. Fabbri [id](#)^{24b,24a}, L. Fabbri [id](#)^{24b,24a}, G. Facini [id](#)⁹⁷, V. Fadeyev [id](#)¹³⁸, R.M. Fakhruddinov [id](#)³⁸, D. Fakoudis [id](#)¹⁰¹, S. Falciano [id](#)^{75a}, L.F. Falda Ulhoa Coelho [id](#)²⁷, F. Fallavollita [id](#)¹¹¹, G. Falsetti [id](#)^{44b,44a}, J. Faltova [id](#)¹³⁵, C. Fan [id](#)¹⁶⁷, K.Y. Fan [id](#)^{64b}, Y. Fan [id](#)¹⁴, Y. Fang [id](#)^{14,113c}, M. Fanti [id](#)^{71a,71b}, M. Faraj [id](#)^{69a,69b}, Z. Farazpay [id](#)⁹⁸, A. Farbin [id](#)⁸, A. Farilla [id](#)^{77a}, K. Farman [id](#)¹⁵³, T. Farooque [id](#)¹⁰⁸, J.N. Farr [id](#)¹⁷⁷, M.S. Farrington⁶¹, S.M. Farrington [id](#)^{136,52}, F. Fassi [id](#)^{36e}, D. Fassouliotis [id](#)⁹, L. Fayard [id](#)⁶⁶, P. Federic [id](#)¹³⁵, P. Federicova [id](#)¹³³, O.L. Fedin [id](#)^{38,a}, M. Feickert [id](#)¹⁷⁵, L. Feligioni [id](#)¹⁰³, D.E. Fellers [id](#)^{18a}, C. Feng [id](#)^{142a}, Y. Feng¹⁴, Z. Feng [id](#)¹¹⁶, M.J. Fenton [id](#)¹⁶⁴, L. Ferencz [id](#)⁴⁸, B. Fernandez Barbadillo [id](#)⁹², P. Fernandez Martinez [id](#)⁶⁷, M.J.V. Fernoux [id](#)¹⁰³, J. Ferrando [id](#)⁹², A. Ferrari [id](#)¹⁶⁶, P. Ferrari [id](#)^{116,115}, R. Ferrari [id](#)^{73a}, D. Ferrere [id](#)⁵⁶, C. Ferretti [id](#)¹⁰⁷, M.P. Fewell [id](#)¹, D. Fiacco [id](#)^{75a,75b}, F. Fiedler [id](#)¹⁰¹, P. Fiedler [id](#)¹³⁴, S. Filimonov [id](#)³⁹, M.S. Filip [id](#)^{28b,t}, A. Filipčič [id](#)⁹⁴, E.K. Filmer [id](#)^{161a}, F. Filthaut [id](#)¹¹⁵, M.C.N. Fiolhais [id](#)^{132a,132c,c}, L. Fiorini [id](#)¹⁶⁸, W.C. Fisher [id](#)¹⁰⁸, T. Fitschen [id](#)¹⁰², P.M. Fitzhugh¹³⁷, I. Fleck [id](#)¹⁴⁶, P. Fleischmann [id](#)¹⁰⁷, T. Flick [id](#)¹⁷⁶, M. Flores [id](#)^{34d,ag}, L.R. Flores Castillo [id](#)^{64a}, M. Foll [id](#)¹²⁷, F.M. Follega [id](#)^{78a,78b}, N. Fomin [id](#)³³, J.H. Foo [id](#)¹⁶⁰, A. Formica [id](#)¹³⁷, A.C. Forti [id](#)¹⁰², E. Fortin [id](#)³⁷, A.W. Fortman [id](#)^{18a}, L. Foster [id](#)^{18a}, L. Fountas [id](#)^{9,i}, D. Fournier [id](#)⁶⁶, H. Fox [id](#)⁹², P. Francavilla [id](#)^{74a,74b}, S. Francescato [id](#)⁶¹, S. Franchellucci [id](#)⁵⁶, M. Franchini [id](#)^{24b,24a}, S. Franchino [id](#)^{63a}, D. Francis³⁷, L. Franco [id](#)⁴⁸, L. Franconi [id](#)⁴⁸, M. Franklin [id](#)⁶¹, G. Frattari [id](#)²⁷, Y.Y. Frid [id](#)¹⁵⁶, J. Friend [id](#)⁵⁹, N. Fritzsche [id](#)³⁷, A. Froch [id](#)⁵⁶, D. Froidevaux [id](#)³⁷, J.A. Frost [id](#)¹³⁶, Y. Fu [id](#)¹⁰⁸, S. Fuenzalida Garrido [id](#)^{139g}, M. Fujimoto [id](#)¹⁵⁰, K.Y. Fung [id](#)^{64a}, E. Furtado De Simas Filho [id](#)^{82e}, M. Furukawa [id](#)¹⁵⁸, M. Fuste Costa⁴⁸, J. Fuster [id](#)¹⁶⁸, A. Gaa [id](#)⁵⁵, A. Gabrielli [id](#)^{24b,24a}, A. Gabrielli [id](#)¹⁶⁰, P. Gadow [id](#)³⁷, G. Gagliardi [id](#)^{57b,57a}, L.G. Gagnon [id](#)^{18a}, S. Gaid [id](#)^{84b}, S. Galantzan [id](#)¹⁵⁶, J. Gallagher [id](#)¹, E.J. Gallas [id](#)¹²⁸, A.L. Gallen [id](#)¹⁶⁶, B.J. Gallop [id](#)¹³⁶, K.K. Gan [id](#)¹²¹, S. Ganguly [id](#)¹⁵⁸, Y. Gao [id](#)⁵², A. Garabaglu [id](#)¹⁴¹, F.M. Garay Walls [id](#)^{139a,139b}, C. García [id](#)¹⁶⁸, A. Garcia Alonso [id](#)¹¹⁶, A.G. Garcia Caffaro [id](#)¹⁷⁷, J.E. García Navarro [id](#)¹⁶⁸, M.A. Garcia Ruiz [id](#)^{23b}, M. Garcia-Sciveres [id](#)^{18a}, G.L. Gardner [id](#)¹³⁰, R.W. Gardner [id](#)⁴⁰, N. Garelli [id](#)¹⁶³, R.B. Garg [id](#)¹⁴⁸, J.M. Gargan [id](#)³³, C.A. Garner¹⁶⁰, C.M. Garvey [id](#)^{34a}, V.K. Gassmann¹⁶³, G. Gaudio [id](#)^{73a}, V. Gautam¹³, P. Gauzzi [id](#)^{75a,75b}, J. Gavranovic [id](#)⁹⁴, I.L. Gavrilenko [id](#)^{132a}, A. Gavriyuk [id](#)³⁸, C. Gay [id](#)¹⁶⁹, G. Gaycken [id](#)¹²⁵, E.N. Gazis [id](#)¹⁰, A. Gekow¹²¹, C. Gemme [id](#)^{57b}, M.H. Genest [id](#)⁶⁰, A.D. Gentry [id](#)¹¹⁴, S. George [id](#)⁹⁶, T. Geralis [id](#)⁴⁶, A.A. Gerwin [id](#)¹²², P. Gessinger-Befurt [id](#)³⁷, M. Ghani [id](#)¹⁷², K. Ghorbanian [id](#)⁹⁵, A. Ghosal [id](#)¹⁴⁶, A. Ghosh [id](#)¹⁶⁴, A. Ghosh [id](#)⁷, B. Giacobbe [id](#)^{24b}, S. Giagu [id](#)^{75a,75b}, T. Giani [id](#)¹¹⁶, A. Giannini [id](#)⁶², S.M. Gibson [id](#)⁹⁶, M. Gignac [id](#)¹³⁸, D.T. Gil [id](#)^{86b}, A.K. Gilbert [id](#)^{86a}, B.J. Gilbert [id](#)⁴², D. Gillberg [id](#)³⁵, G. Gilles [id](#)¹¹⁶, D.M. Gingrich [id](#)^{2,ai}, M.P. Giordani [id](#)^{69a,69c}, P.F. Giraud [id](#)¹³⁷, G. Giugliarelli [id](#)^{69a,69c}, D. Giugni [id](#)^{71a}, F. Giuli [id](#)^{76a,76b}, I. Gkialas [id](#)^{9,i}, L.K. Gladilin [id](#)³⁸, C. Glasman [id](#)¹⁰⁰, M. Glazewska [id](#)²⁰, R.M. Gleason [id](#)¹⁶⁴, G. Glemža [id](#)⁴⁸, M. Glisic¹²⁵, I. Gnesi [id](#)^{44b}, Y. Go [id](#)³⁰, M. Goblirsch-Kolb [id](#)³⁷, B. Gocke [id](#)⁴⁹, D. Godin¹⁰⁹, B. Gokturk [id](#)^{22a}, S. Goldfarb [id](#)¹⁰⁶, T. Golling [id](#)⁵⁶, M.G.D. Gololo [id](#)^{34c}, A. Golub [id](#)¹⁴¹, D. Golubkov [id](#)³⁸, J.P. Gombas [id](#)¹⁰⁸, A. Gomes [id](#)^{132a,132b}, G. Gomes Da Silva [id](#)¹⁴⁶, A.J. Gomez Delegido [id](#)³⁷, R. Gonçalves [id](#)^{132a}, L. Gonella [id](#)²¹, A. Gongadze [id](#)^{154c}, F. Gonnella [id](#)²¹, J.L. Gonski [id](#)¹⁴⁸, R.Y. González Andana [id](#)⁵², S. González de la Hoz [id](#)¹⁶⁸, M.V. Gonzalez Rodrigues [id](#)⁴⁸, R. Gonzalez Suarez [id](#)¹⁶⁶, S. Gonzalez-Sevilla [id](#)⁵⁶, L. Goossens [id](#)³⁷, B. Gorini [id](#)³⁷, E. Gorini [id](#)^{70a,70b}, A. Gorišek [id](#)⁹⁴, T.C. Gosart [id](#)¹³⁰, A.T. Goshaw [id](#)⁵¹, M.I. Gostkin [id](#)³⁹, S. Goswami [id](#)¹²³, C.A. Gottardo [id](#)³⁷, S.A. Gotz [id](#)¹¹⁰, M. Goughri [id](#)^{36b}, A.G. Goussiou [id](#)¹⁴¹, N. Govender [id](#)^{34c}, R.P. Grabarczyk [id](#)¹²⁸, I. Grabowska-Bold [id](#)^{86a}, K. Graham [id](#)³⁵, E. Gramstad [id](#)¹²⁷, S. Grancagnolo [id](#)^{70a,70b}, C.M. Grant¹, P.M. Gravila [id](#)^{28f}, F.G. Gravili [id](#)^{70a,70b}, H.M. Gray [id](#)^{18a}, M. Greco [id](#)¹¹¹, M.J. Green [id](#)¹, C. Grefe [id](#)²⁵, A.S. Grefsrud [id](#)¹⁷, I.M. Gregor [id](#)⁴⁸, K.T. Greif [id](#)¹⁶⁴, P. Grenier [id](#)¹⁴⁸, S.G. Grewe¹¹¹, A.A. Grillo [id](#)¹³⁸, K. Grimm [id](#)³², S. Grinstein [id](#)^{13,x}, J.-F. Grivaz [id](#)⁶⁶, E. Gross [id](#)¹⁷⁴, J. Grosse-Knetter [id](#)⁵⁵, L.H. Grossman [id](#)^{18b}, L. Guan [id](#)¹⁰⁷, G. Guerrieri [id](#)³⁷,

R. Guevara ¹²⁷, R. Gugel ¹⁰¹, J.A.M. Guhit ¹⁰⁷, A. Guida ¹⁹, E. Guilloton ¹⁷², S. Guindon ³⁷,
 F. Guo ^{14,113c}, J. Guo ^{143a}, L. Guo ⁴⁸, L. Guo ^{113b,v}, Y. Guo ¹⁰⁷, Y. Guo ⁴², A. Gupta ⁴⁹,
 R. Gupta ¹³¹, S. Gupta ²⁷, S. Gurbuz ²⁵, S.S. Gurdasani ⁴⁸, G. Gustavino ^{75a,75b},
 P. Gutierrez ¹²², L.F. Gutierrez Zagazeta ¹³⁰, M. Gutsche ⁵⁰, C. Gutschow ⁹⁷, C. Gwenlan ¹²⁸,
 C.B. Gwilliam ⁹³, E.S. Haaland ¹²⁷, A. Haas ¹¹⁹, M. Habedank ⁵⁹, C. Haber ^{18a},
 H.K. Hadavand ⁸, A. Haddad ⁴¹, A. Hadeef ⁵⁰, A.I. Hagan ⁹², J.J. Hahn ¹⁴⁶, E.H. Haines ⁹⁷,
 M. Haleem ¹⁷¹, J. Haley ¹²³, G.D. Hallewell ¹⁰³, J.A. Hallford ⁴⁸, K. Hamano ¹⁷⁰,
 H. Hamdaoui ¹⁶⁶, M. Hamer ²⁵, S.E.D. Hammoud ⁶⁶, E.J. Hampshire ⁹⁶, J. Han ^{142a},
 L. Han ^{113a}, L. Han ⁶², S. Han ¹⁴, K. Hanagaki ⁸³, M. Hance ¹³⁸, D.A. Hangal ⁴²,
 H. Hanif ¹⁴⁷, M.D. Hank ¹³⁰, J.B. Hansen ⁴³, P.H. Hansen ⁴³, T. Harenberg ¹⁷⁶,
 S. Harkusha ¹⁷⁸, M.L. Harris ¹⁰⁴, Y.T. Harris ²⁵, J. Harrison ¹³, P.F. Harrison ¹⁷², M.L.E. Hart ⁹⁷,
 N.M. Hartman ¹¹¹, N.M. Hartmann ¹¹⁰, R.Z. Hasan ^{96,136}, Y. Hasegawa ¹⁴⁵, F. Haslbeck ¹²⁸,
 S. Hassan ¹⁷, R. Hauser ¹⁰⁸, M. Haviernik ¹³⁵, C.M. Hawkes ²¹, R.J. Hawkings ³⁷,
 Y. Hayashi ¹⁵⁸, D. Hayden ¹⁰⁸, C. Hayes ¹⁰⁷, R.L. Hayes ¹¹⁶, C.P. Hays ¹²⁸, J.M. Hays ⁹⁵,
 H.S. Hayward ⁹³, M. He ^{14,113c}, Y. He ⁴⁸, Y. He ⁹⁷, N.B. Heatley ⁹⁵, V. Hedberg ⁹⁹,
 J. Heilman ³⁵, S. Heim ⁴⁸, T. Heim ^{18a}, J.J. Heinrich ¹²⁵, L. Heinrich ¹¹¹, J. Hejbal ¹³³,
 M. Helbig ⁵⁰, A. Held ¹⁷⁵, S. Hellesund ¹⁷, C.M. Helling ¹⁶⁹, S. Hellman ^{47a,47b},
 A.M. Henriques Correia ³⁷, H. Herde ⁹⁹, Y. Hernández Jiménez ¹⁵⁰, L.M. Herrmann ²⁵,
 T. Herrmann ⁵⁰, G. Herten ⁵⁴, R. Hertenberger ¹¹⁰, L. Hervas ³⁷, M.E. Hespings ¹⁰¹,
 N.P. Hessey ^{161a}, J. Hessler ¹¹¹, M. Hidaoui ^{36b}, N. Hidic ¹³⁵, E. Hill ¹⁶⁰, T.S. Hillersoy ¹⁷,
 S.J. Hillier ²¹, J.R. Hinds ¹⁰⁸, F. Hinterkeuser ²⁵, M. Hirose ¹²⁶, S. Hirose ¹⁶²,
 D. Hirschbuehl ¹⁷⁶, T.G. Hitchings ¹⁰², B. Hiti ⁹⁴, J. Hobbs ¹⁵⁰, R. Hobincu ^{28e}, N. Hod ¹⁷⁴,
 A.M. Hodges ¹⁶⁷, M.C. Hodgkinson ¹⁴⁴, B.H. Hodgkinson ¹²⁸, A. Hoecker ³⁷, D.D. Hofer ¹⁰⁷,
 J. Hofer ¹⁶⁸, J. Hofner ¹⁰¹, M. Holzbock ³⁷, L.B.A.H. Hommels ³³, V. Homsak ¹²⁸,
 J.J. Hong ⁶⁸, T.M. Hong ¹³¹, B.H. Hooberman ¹⁶⁷, W.H. Hopkins ⁶, M.C. Hoppesch ¹⁶⁷,
 Y. Horii ¹¹², M.E. Horstmann ¹¹¹, S. Hou ¹⁵³, M.R. Housenga ¹⁶⁷, J. Howarth ⁵⁹, J. Hoya ⁶,
 M. Hrabovsky ¹²⁴, T. Hryn'ova ⁴, P.J. Hsu ⁶⁵, S.-C. Hsu ¹⁴¹, T. Hsu ⁶⁶, M. Hu ^{18a}, Q. Hu ⁶²,
 S. Huang ³³, X. Huang ^{14,113c}, Y. Huang ¹³⁵, Y. Huang ^{113b}, Y. Huang ¹⁴, Z. Huang ⁶⁶,
 Z. Hubacek ¹³⁴, F. Huegging ²⁵, T.B. Huffman ¹²⁸, M. Hufnagel Maranha De Faria ^{82a},
 C.A. Hugli ⁴⁸, M. Huhtinen ³⁷, S.K. Huiberts ¹²⁷, R. Hulsken ¹⁰⁵, C.E. Hultquist ^{18a},
 D.L. Humphreys ¹⁰⁴, N. Huseynov ¹², J. Huston ¹⁰⁸, J. Huth ⁶¹, L. Huth ⁴⁸, R. Hyneman ⁷,
 G. Iacobucci ⁵⁶, G. Iakovidis ³⁰, L. Iconomidou-Fayard ⁶⁶, J.P. Iddon ³⁷, P. Iengo ^{72a,72b},
 Y. Iiyama ¹⁵⁸, T. Iizawa ¹⁵⁸, Y. Ikegami ⁸³, D. Iliadis ¹⁵⁷, N. Ilic ¹⁶⁰, H. Imam ^{36a},
 G. Inacio Goncalves ^{82d}, S.A. Infante Cabanas ^{139c}, T. Ingebretsen Carlson ^{47a,47b}, J.M. Inglis ⁹⁵,
 G. Introzzi ^{73a,73b}, M. Iodice ^{77a}, V. Ippolito ^{75a,75b}, R.K. Irwin ⁹³, M. Ishino ¹⁵⁸, W. Islam ¹⁷⁵,
 C. Issever ¹⁹, S. Istin ^{22a,ao}, K. Itabashi ¹²⁶, H. Ito ¹⁷³, R. Iuppa ^{78a,78b}, A. Ivina ¹⁷⁴,
 S. Izumiyama ¹¹², V. Izzo ^{72a}, P. Jacka ¹³⁴, P. Jackson ¹, P. Jain ⁴⁸, K. Jakobs ⁵⁴, T. Jakoubek ¹⁷⁴,
 J. Jamieson ⁵⁹, W. Jang ¹⁵⁸, S. Jankovych ¹³⁵, M. Javurkova ¹⁰⁴, P. Jawahar ¹⁰², L. Jeanty ¹²⁵,
 J. Jejelava ^{154a,ae}, P. Jenni ^{54,f}, C.E. Jessiman ³⁵, C. Jia ^{142a}, H. Jia ¹⁶⁹, J. Jia ¹⁵⁰,
 X. Jia ^{111,113c}, Z. Jia ^{113a}, C. Jiang ⁵², Q. Jiang ^{64b}, S. Jiggins ⁴⁸, M. Jimenez Ortega ¹⁶⁸,
 J. Jimenez Pena ¹³, S. Jin ^{113a}, A. Jinaru ^{28b}, O. Jinnouchi ¹⁴⁰, P. Johansson ¹⁴⁴, K.A. Johns ⁷,
 J.W. Johnson ¹³⁸, F.A. Jolly ⁴⁸, D.M. Jones ¹⁵¹, E. Jones ⁴⁸, K.S. Jones ⁸, P. Jones ³³,
 R.W.L. Jones ⁹², T.J. Jones ⁹³, H.L. Joos ⁵⁵, R. Joshi ¹²¹, J. Jovicevic ¹⁶, X. Ju ^{18a},
 J.J. Junggeburth ³⁷, T. Junkermann ^{63a}, A. Juste Rozas ^{13,x}, M.K. Juzek ⁸⁷, S. Kabana ^{139f},
 A. Kaczmarska ⁸⁷, S.A. Kadir ¹⁴⁸, M. Kado ¹¹¹, H. Kagan ¹²¹, M. Kagan ¹⁴⁸, A. Kahn ¹³⁰,
 C. Kahra ¹⁰¹, T. Kaji ¹⁵⁸, E. Kajomovitz ¹⁵⁵, N. Kakati ¹⁷⁴, N. Kakoty ¹³, I. Kalaitzidou ⁵⁴,
 S. Kandel ⁸, N. Kanellos ¹⁰, N.J. Kang ¹³⁸, D. Kar ^{34j}, E. Karentzos ²⁵, K. Karki ⁸,

O. Karkout ¹¹⁶, S.N. Karpov ³⁹, Z.M. Karpova ³⁹, V. Kartvelishvili ^{92,154b}, A.N. Karyukhin ³⁸, E. Kasimi ¹⁵⁷, J. Katzy ⁴⁸, S. Kaur ³⁵, K. Kawade ¹⁴⁵, M.P. Kawale ¹²², C. Kawamoto ⁸⁸, T. Kawamoto ⁶², E.F. Kay ³⁷, S. Kazakos ¹⁰⁸, V.F. Kazanin ³⁸, J.M. Keaveney ^{34a}, R. Keeler ¹⁷⁰, G.V. Kehris ⁶¹, J.S. Keller ³⁵, J.M. Kelly ¹⁷⁰, J.J. Kempster ¹⁵¹, O. Kepka ¹³³, J. Kerr ^{161b}, B.P. Kerridge ¹³⁶, B.P. Kerševan ⁹⁴, L. Keszeghova ^{29a}, R.A. Khan ¹³¹, A. Khanov ¹²³, A.G. Kharlamov ³⁸, T. Kharlamova ³⁸, E.E. Khoda ¹⁴¹, M. Kholodenko ^{132a}, T.J. Khoo ¹⁹, G. Khorauli ¹⁷¹, Y. Khoulaki ^{36a}, Y.A.R. Khwaira ¹²⁹, B. Kibirige ^{34j}, D. Kim ⁶, D.W. Kim ^{18b}, Y.K. Kim ⁴⁰, N. Kimura ⁹⁷, M.K. Kingston ⁵⁵, A. Kirchhoff ⁵⁵, C. Kirfel ²⁵, F. Kirfel ²⁵, J. Kirk ¹³⁶, A.E. Kiryunin ¹¹¹, S. Kita ¹⁶², O. Kivernyk ²⁵, M. Klassen ¹⁶³, C. Klein ³⁵, L. Klein ¹⁷¹, M.H. Klein ⁴⁵, S.B. Klein ⁵⁶, U. Klein ⁹³, A. Klimentov ³⁰, T. Klioutchnikova ³⁷, P. Kluit ¹¹⁶, S. Kluth ¹¹¹, E. Kneringer ⁷⁹, T.M. Knight ¹⁶⁰, A. Knue ⁴⁹, M. Kobel ⁵⁰, D. Kobylanski ¹⁷⁴, S.F. Koch ¹²⁸, M. Kocian ¹⁴⁸, P. Kodyš ¹³⁵, D.M. Koeck ¹²⁵, T. Koffas ³⁵, O. Kolay ⁵⁰, I. Koletsou ⁴, T. Komarek ⁸⁷, K. Köneke ⁵⁵, A.X.Y. Kong ¹, T. Kono ¹²⁰, N. Konstantinidis ⁹⁷, P. Kontaxakis ⁵⁶, B. Konya ⁹⁹, R. Kopeliansky ⁴², S. Koperny ^{86a}, R. Koppenhofer ⁵⁴, K. Korcyl ⁸⁷, K. Kordas ^{157,d}, A. Korn ⁹⁷, S. Korn ⁵⁵, I. Korolkov ¹³, N. Korotkova ³⁸, B. Kortman ¹¹⁶, O. Kortner ¹¹¹, S. Kortner ¹¹¹, W.H. Kostecka ¹¹⁷, M. Kostov ^{29a}, V.V. Kostyukhin ¹⁴⁶, A. Kotsokechagia ³⁷, A. Kotwal ⁵¹, A. Koulouris ³⁷, A. Kourkoumeli-Charalampidi ^{73a,73b}, C. Kourkoumelis ⁹, E. Kourlitis ¹¹¹, O. Kovanda ¹²⁵, R. Kowalewski ¹⁷⁰, W. Kozanecki ¹²⁵, A.S. Kozhin ³⁸, V.A. Kramarenko ³⁸, G. Kramberger ⁹⁴, P. Kramer ²⁵, M.W. Krasny ¹²⁹, A. Krasznahorkay ¹⁰⁴, A.C. Kraus ¹¹⁷, J.W. Kraus ¹⁷⁶, J.A. Kremer ⁴⁸, N.B. Krenkel ¹⁴⁶, T. Kresse ⁵⁰, L. Kretschmann ¹⁷⁶, J. Kretzschmar ⁹³, P. Krieger ¹⁶⁰, K. Krizka ²¹, K. Kroeninger ⁴⁹, H. Kroha ¹¹¹, J. Kroll ¹³³, J. Kroll ¹³⁰, K.S. Krowpman ¹⁰⁸, U. Kruchonak ³⁹, H. Krüger ²⁵, N. Krumnack ⁸⁰, M.C. Kruse ⁵¹, O. Kuchinskaia ³⁹, S. Kuday ^{3a}, S. Kuehn ³⁷, R. Kuesters ⁵⁴, T. Kuhl ⁴⁸, V. Kukhtin ³⁹, Y. Kulchitsky ³⁹, S. Kuleshov ^{139d,139b}, J. Kull ¹, E.V. Kumar ¹¹⁰, M. Kumar ^{34j}, N. Kumari ⁴⁸, P. Kumari ^{161b}, A. Kupco ¹³³, A. Kupich ³⁸, O. Kuprash ⁵⁴, H. Kurashige ⁸⁵, L.L. Kurchaninov ^{161a}, O. Kurdysh ⁴, A. Kurova ³⁸, M. Kuze ¹⁴⁰, A.K. Kvam ¹⁰⁴, J. Kvitá ¹²⁴, N.G. Kyriacou ¹⁴¹, M. Laassiri ³⁰, C. Lacasta ¹⁶⁸, F. Lacava ^{75a,75b}, H. Lacker ¹⁹, D. Lacour ¹²⁹, N.N. Lad ⁹⁷, E. Ladygin ³⁹, A. Lafarge ⁴¹, B. Laforge ¹²⁹, T. Lagouri ¹⁷⁷, F.Z. Lahbabi ^{36a}, S. Lai ^{55,37}, W.S. Lai ⁹⁷, I.K. Lakomic ⁵⁵, J.E. Lambert ¹⁷⁰, S. Lammers ⁶⁸, W. Lampl ⁷, C. Lampoudis ^{157,d}, G. Lamprinoudis ¹⁷¹, A.N. Lancaster ¹¹⁷, E. Lançon ³⁰, U. Landgraf ⁵⁴, M.P.J. Landon ⁹⁵, V.S. Lang ⁵⁴, A.J. Lankford ¹⁶⁴, F. Lanni ³⁷, C.S. Lantz ¹⁶⁷, K. Lantzsch ²⁵, A. Lanza ^{73a}, M. Lanzac Berrocal ¹⁶⁸, J.F. Laporte ¹³⁷, T. Lari ^{71a}, D. Larsen ¹⁷, L. Larson ¹¹, F. Lasagni Manghi ^{24b}, M. Lassnig ³⁷, S.D. Lawlor ¹⁴⁴, R. Lazaridou ¹⁶⁴, M. Lazzaroni ^{71a,71b}, E.T.T. Le ¹⁶⁴, H.D.M. Le ¹⁰⁸, E.M. Le Boulicaut ¹⁷⁷, L.T. Le Pottier ^{18a}, B. Leban ^{24b,24a}, F. Ledroit-Guillon ⁶⁰, T.F. Lee ^{161b}, L.L. Leeuw ^{34c}, M. Lefebvre ¹⁷⁰, C. Leggett ^{18a}, G. Lehmann Miotto ³⁷, M. Leigh ⁵⁶, W.A. Leight ¹⁰⁴, W. Leinonen ¹¹⁵, A. Leisos ^{157,u}, M.A.L. Leite ^{82c}, C.E. Leitgeb ¹⁹, R. Leitner ¹³⁵, K.J.C. Leney ⁴⁵, T. Lenz ²⁵, S. Leone ^{74a}, C. Leonidopoulos ⁵², A. Leopold ¹⁴⁹, J.H. Lepage Bourbonnais ³⁵, R. Les ¹⁰⁸, C.G. Lester ³³, M. Levchenko ³⁸, J. Levêque ⁴, L.J. Levinson ¹⁷⁴, G. Levrini ^{24b,24a}, M.P. Lewicki ⁸⁷, C. Lewis ¹⁴¹, D.J. Lewis ⁴, L. Lewitt ¹⁴⁴, A. Li ³⁰, B. Li ^{142a}, C. Li ¹⁰⁷, C-Q. Li ¹¹¹, H. Li ^{142a}, H. Li ¹⁰², H. Li ¹⁵, H. Li ⁶², H. Li ^{142a}, J. Li ^{143a}, K. Li ¹⁴, L. Li ^{143a}, R. Li ¹⁷⁷, S. Li ^{14,113c}, S. Li ^{143b,143a}, T. Li ⁵, X. Li ¹⁰⁵, Y. Li ¹⁴, Z. Li ¹⁵⁸, Z. Li ^{14,113c}, Z. Li ⁶², S. Liang ^{14,113c}, Z. Liang ¹⁴, M. Liberatore ¹³⁷, B. Liberti ^{76a}, G.B. Libotte ^{82d}, K. Lie ^{64c}, J. Lieber Marin ^{82e}, H. Lien ⁶⁸, H. Lin ¹⁰⁷, S.F. Lin ¹⁵⁰, L. Linden ¹¹⁰, R.E. Lindley ⁷, J.H. Lindon ³⁷, J. Ling ⁶¹, E. Lipeles ¹³⁰, A. Lipniacka ¹⁷, A. Lister ¹⁶⁹, J.D. Little ⁶⁸, B. Liu ¹⁴, B.X. Liu ^{113b}, D. Liu ¹⁵⁵, D. Liu ¹³⁸, E.H.L. Liu ²¹, J.K.K. Liu ¹¹⁹, K. Liu ^{143b}, K. Liu ^{143b,143a}, M. Liu ⁶²,

M.Y. Liu ⁶², P. Liu ¹⁴, Q. Liu ¹⁴⁸, S. Liu ¹⁵⁰, X. Liu ^{142a}, Y. Liu ^{113b,113c}, Y. Liu ¹⁶⁷,
Y.L. Liu ^{142a}, Y.W. Liu ⁶², Z. Liu ^{66,k}, S.L. Lloyd ⁹⁵, E.M. Lobodzinska ⁴⁸, P. Loch ⁷,
E. Lodhi ¹⁶⁰, K. Lohwasser ¹⁴⁴, E. Loiacono ⁴⁸, J.D. Lomas ²¹, J.D. Long ⁴², I. Longarini ¹⁶⁴,
R. Longo ¹⁶⁷, A. Lopez Solis ¹³, N.A. Lopez-canelas ⁷, N. Lorenzo Martinez ⁴, A.M. Lory ¹¹⁰,
M. Losada ^{118a}, G. Löschcke Centeno ⁴, X. Lou ^{47a,47b}, X. Lou ^{14,113c}, A. Lounis ⁶⁶,
P.A. Love ⁹², M. Lu ⁶⁶, S. Lu ¹³⁰, Y.J. Lu ¹⁵³, H.J. Lubatti ¹⁴¹, C. Luci ^{75a,75b},
F.L. Lucio Alves ^{113a}, F. Luehring ⁶⁸, B.S. Lunday ¹³⁰, O. Lundberg ¹⁴⁹, J. Lunde ³⁷,
N.A. Luongo ⁶, M.S. Lutz ³⁷, A.B. Lux ²⁶, D. Lynn ³⁰, R. Lysak ¹³³, V. Lysenko ¹³⁴,
E. Lytken ⁹⁹, V. Lyubushkin ³⁹, T. Lyubushkina ³⁹, M.M. Lyukova ¹⁵⁰, H. Ma ³⁰, K. Ma ⁶²,
L.L. Ma ^{142a}, W. Ma ⁶², Y. Ma ¹²³, J.C. MacDonald ¹⁰¹, P.C. Machado De Abreu Farias ^{82c},
D. Macina ³⁷, R. Madar ⁴¹, T. Madula ⁹⁷, J. Maeda ⁸⁵, T. Maeno ³⁰, P.T. Mafa ^{34c,j},
H. Maguire ¹⁴⁴, M. Maheshwari ³³, V. Maiboroda ⁶⁶, A. Maio ^{132a,132b,132d}, K. Maj ^{86a},
O. Majersky ⁴⁸, S. Majewski ¹²⁵, R. Makhmanazarov ³⁸, N. Makovec ⁶⁶, V. Maksimovic ¹⁶,
B. Malaescu ¹²⁹, J. Malamant ¹²⁷, Pa. Malecki ⁸⁷, V.P. Maleev ³⁸, F. Malek ^{60,o}, M. Mali ⁹⁴,
D. Malito ⁹⁶, A. Maloizel ⁵, S. Maltezos ¹⁰, A. Malvezzi Lopes ^{82d}, S. Malyukov ³⁹, J. Mamuzic ⁹⁴,
G. Mancini ⁵³, M.N. Mancini ²⁷, G. Manco ^{73a,73b}, J.P. Mandalia ⁹⁵, S.S. Mandarri ¹⁵¹,
I. Mandić ⁹⁴, L. Manhaes de Andrade Filho ^{82a}, I.M. Maniatis ¹⁷⁴, J. Manjarres Ramos ⁹⁰,
D.C. Mankad ¹⁷⁴, A. Mann ¹¹⁰, T. Manoussos ³⁷, M.N. Mantinan ⁴⁰, S. Manzoni ³⁷,
L. Mao ^{143a}, X. Mapekula ^{34c}, A. Marantis ¹⁵⁷, R.R. Marcelo Gregorio ⁹⁵, G. Marchiori ⁵,
C. Marcon ^{71a}, E. Maricic ¹⁶, M. Marinescu ⁴⁸, S. Marium ⁴⁸, M. Marjanovic ¹²²,
A. Markhoos ⁵⁴, M. Markovitch ⁶⁶, M.K. Maroun ¹⁰⁴, M.C. Marr ¹⁴⁷, G.T. Marsden ¹⁰²,
E.J. Marshall ⁹², Z. Marshall ^{18a}, S. Marti-Garcia ¹⁶⁸, J. Martin ⁹⁷, T.A. Martin ¹³⁶,
V.J. Martin ⁵², B. Martin dit Latour ¹⁷, L. Martinelli ^{75a,75b}, M. Martinez ^{13,x},
P. Martinez Agullo ¹⁶⁸, V.I. Martinez Outschoorn ¹⁰⁴, P. Martinez Suarez ³⁷, S. Martin-Haugh ¹³⁶,
G. Martinovicova ¹³⁵, V.S. Martoiu ^{28b}, A.C. Martyniuk ⁹⁷, A. Marzin ³⁷, D. Mascione ^{78a,78b},
L. Masetti ¹⁰¹, J. Masik ¹⁰², A.L. Maslennikov ³⁹, S.L. Mason ⁴², P. Massarotti ^{72a,72b},
P. Mastrandrea ^{74a,74b}, A. Mastroberardino ^{44b,44a}, T. Masubuchi ¹²⁶, T.T. Mathew ¹²⁵,
J. Matousek ¹³⁵, D.M. Mattern ⁴⁹, K. Mauer ⁴⁸, J. Maurer ^{28b}, T. Maurin ⁵⁹, A.J. Maury ⁶⁶,
B. Maček ⁹⁴, C. Mavungu Tsava ¹⁰³, D.A. Maximov ³⁸, A.E. May ¹⁰², E. Mayer ⁴¹,
R. Mazini ^{34j}, I. Maznas ¹¹⁷, S.M. Mazza ¹³⁸, E. Mazzeo ³⁷, J.P. Mc Gowan ¹⁷⁰,
S.P. Mc Kee ¹⁰⁷, C.A. Mc Lean ⁶, C.C. McCracken ¹⁶⁹, E.F. McDonald ¹⁰⁶, A.E. McDougall ¹¹⁶,
L.F. Mcelhinney ⁹², J.A. Mcfayden ¹⁵¹, R.P. McGovern ¹³⁰, R.P. Mckenzie ^{34j}, T.C. Mclachlan ⁴⁸,
D.J. McLaughlin ⁹⁷, S.J. McMahan ¹³⁶, C.M. Mcpartland ⁹³, R.A. McPherson ^{170,ab},
S. Mehlhase ¹¹⁰, A. Mehta ⁹³, D. Melini ¹⁶⁸, B.R. Mellado Garcia ^{34j}, A.H. Melo ⁵⁵,
F. Meloni ⁴⁸, A.M. Mendes Jacques Da Costa ¹⁰², L. Meng ⁹², S. Menke ¹¹¹, M. Mentink ³⁷,
E. Meoni ^{44b,44a}, G. Mercado ¹¹⁷, S. Merianos ¹⁵⁷, C. Merlassino ^{69a,69c}, C. Meroni ^{71a,71b},
J. Metcalfe ⁶, A.S. Mete ⁶, E. Meuser ¹⁰¹, C. Meyer ⁶⁸, J-P. Meyer ¹³⁷, Y. Miao ^{113a},
R.P. Middleton ¹³⁶, M. Mihovilovic ⁶⁶, L. Mijović ⁵², G. Mikenberg ¹⁷⁴, M. Mikestikova ¹³³,
M. Mikuž ⁹⁴, H. Mildner ¹⁰¹, A. Milic ³⁷, D.W. Miller ⁴⁰, E.H. Miller ¹⁴⁸, A. Milov ¹⁷⁴,
D.A. Milstead ^{47a,47b}, T. Min ^{113a}, A.A. Minaenko ³⁸, I.A. Minashvili ^{154b}, A.I. Mincer ¹¹⁹,
B. Mindur ^{86a}, M. Mineev ³⁹, Y. Mino ⁸⁸, L.M. Mir ¹³, M. Miralles Lopez ⁵⁹, M. Mironova ^{18a},
M. Missio ⁴¹, A. Mitra ¹⁷², V.A. Mitsou ¹⁶⁸, Y. Mitsumori ¹¹², O. Miu ¹⁶⁰, P.S. Miyagawa ⁹⁵,
T. Mkrtychyan ³⁷, M. Mlinarevic ⁹⁷, T. Mlinarevic ⁹⁷, M. Mlynarikova ¹³⁵, L. Mlynarska ^{86a},
C. Mo ^{143a}, S. Mobius ²⁰, M.H. Mohamed Farook ¹¹⁴, S. Mohapatra ⁴², M.F. Mohd Soberi ⁵²,
S. Mohiuddin ¹²³, G. Mokgatitswane ^{34j}, L. Moleri ¹⁷⁴, U. Molinatti ¹²⁸, L.G. Mollier ²⁰,
B. Mondal ¹³³, S. Mondal ¹³⁴, K. Mönig ⁴⁸, E. Monnier ¹⁰³, L. Monsonis Romero ¹⁶⁸,
J. Montejo Berlingen ¹³, A. Montella ^{47a,47b}, M. Montella ¹²¹, F. Montekali ^{77a,77b},

F. Monticelli ⁹¹, S. Monzani ^{69a,69c}, A. Morancho Tarda ⁴³, N. Morange ⁶⁶,
A.L. Moreira De Carvalho ⁴⁸, M. Moreno Llácer ¹⁶⁸, C. Moreno Martinez ⁵⁶, J.M. Moreno Perez ^{23b},
P. Morettini ^{57b}, S. Morgenstern ³⁷, M. Morii ⁶¹, M. Morinaga ¹⁵⁸, M. Moritsu ⁸⁹,
F. Morodei ^{75a,75b}, P. Moschovakos ³⁷, B. Moser ⁵⁴, M. Mosidze ^{154b}, T. Moskalets ⁴⁵,
P. Moskvitina ¹¹⁵, J. Moss ³², P. Moszkowicz ^{86a}, T. Motta Quirino ^{82d}, A. Moussa ^{36d},
Y. Moyal ¹⁷⁴, H. Moyano Gomez ¹³, E.J.W. Moyse ¹⁰⁴, T.G. Mroz ⁸⁷, S. Muanza ¹⁰³,
M. Mucha ²⁵, J. Mueller ¹³¹, R. Müller ³⁷, G.A. Mullier ¹⁶⁶, A.J. Mullin ³³, J.J. Mullin ⁵¹,
A.C. Mullins ⁴⁵, A.E. Mulski ⁶¹, D.P. Mungo ¹⁶⁰, D. Munoz Perez ¹⁶⁸, F.J. Munoz Sanchez ¹⁰²,
W.J. Murray ^{172,136}, M. Muškinja ⁹⁴, C. Mwewa ⁴⁸, A.G. Myagkov ^{38,a}, A.J. Myers ⁸,
G. Myers ¹⁰⁷, M. Myska ¹³⁴, B.P. Nachman ¹⁴⁸, K. Nagai ¹²⁸, K. Nagano ⁸³, R. Nagasaka ¹⁵⁸,
J.L. Nagle ^{30,al}, E. Nagy ¹⁰³, A.M. Nairz ³⁷, Y. Nakahama ⁸³, K. Nakamura ⁸³, K. Nakkalil ⁵,
A. Nandi ^{63b}, H. Nanjo ¹²⁶, E.A. Narayanan ⁴⁵, Y. Narukawa ¹⁵⁸, I. Naryshkin ³⁸,
L. Nasella ^{71a,71b}, S. Nasri ^{118b}, C. Nass ²⁵, G. Navarro ^{23a}, A. Nayaz ¹⁹, P.Y. Nechaeva ³⁸,
S. Nechaeva ^{24b,24a}, F. Nechansky ¹³³, L. Nedic ¹²⁸, T.J. Neep ²¹, A. Negri ^{73a,73b},
M. Negrini ^{24b}, C. Nellist ¹¹⁶, C. Nelson ¹⁰⁵, K. Nelson ¹⁰⁷, S. Nemecek ¹³³, M. Nessi ^{37,g},
M.S. Neubauer ¹⁶⁷, J. Newell ⁹³, P.R. Newman ²¹, Y.W.Y. Ng ¹⁶⁷, B. Ngair ^{118a},
H.D.N. Nguyen ¹⁰⁹, J.D. Nichols ¹²², R.B. Nickerson ¹²⁸, R. Nicolaidou ¹³⁷, J. Nielsen ¹³⁸,
M. Niemeyer ⁵⁵, J. Niermann ³⁷, N. Nikiforou ³⁷, V. Nikolaenko ^{38,a}, I. Nikolic-Audit ¹²⁹,
P. Nilsson ³⁰, I. Ninca ⁴⁸, G. Ninio ¹⁵⁶, A. Nisati ^{75a}, R. Nisius ¹¹¹, N. Nitika ¹⁷⁴,
E.K. Nkadimeng ^{34b}, T. Nobe ¹⁵⁸, D. Noll ¹⁴⁸, T. Nommensen ¹⁵², M.B. Norfolk ¹⁴⁴,
B.J. Norman ³⁵, L.C. Nosler ^{18a}, M. Noury ^{36a}, J. Novak ⁹⁴, T. Novak ⁹⁴, P. Novotny ¹⁷⁴,
R. Novotny ¹³⁴, L. Nozka ¹²⁴, K. Ntekas ¹⁶⁴, D. Ntounis ¹⁴⁸, N.M.J. Nunes De Moura Junior ^{82b},
J. Ocariz ¹²⁹, I. Ochoa ^{132a}, A. Odella Rodriguez ¹³, S. Oerdek ^{48,y}, J.T. Offermann ⁴⁰,
A. Ogrodnik ⁸⁷, A. Oh ¹⁰², C.C. Ohm ¹⁴⁹, H. Oide ⁸³, M.L. Ojeda ³⁷, Y. Okumura ¹⁵⁸,
L.F. Oleiro Seabra ^{132a}, I. Oleksiyuk ⁵⁶, G. Oliveira Correa ¹³, D. Oliveira Damazio ³⁰,
J.L. Oliver ¹, R. Omar ⁶⁸, Ö.O. Öncel ⁵⁴, A.P. O'Neill ²⁰, A. Onofre ^{132a,132e,e}, P.U.E. Onyisi ¹¹,
M.J. Oreglia ⁴⁰, D. Orestano ^{77a,77b}, R. Orlandini ^{77a,77b}, R.S. Orr ¹⁶⁰, L.M. Osojnak ⁴²,
Y. Osumi ¹¹², G. Otero y Garzon ³¹, H. Otono ⁸⁹, M. Ouchrif ^{36d}, F. Ould-Saada ¹²⁷,
T. Ovsiannikova ¹⁴¹, M. Owen ⁵⁹, R.E. Owen ¹³⁶, V.E. Ozcan ^{22a}, F. Ozturk ⁸⁷, N. Ozturk ⁸,
S. Ozturk ⁸¹, H.A. Pacey ¹²⁸, K. Pachal ^{161a}, A. Pacheco Pages ¹³, C. Padilla Aranda ¹³,
G. Padovano ^{75a,75b}, S. Pagan Griso ^{18a}, J. Pampel ²⁵, J. Pan ¹⁷⁷, D.K. Panchal ¹¹,
C.E. Pandini ⁶⁰, J.G. Panduro Vazquez ¹³⁶, H.D. Pandya ¹, H. Pang ¹³⁷, P. Pani ⁴⁸,
G. Panizzo ^{69a,69c}, L. Panwar ¹²⁹, L. Paolozzi ⁵⁶, S. Parajuli ¹⁶⁷, A. Paramonov ⁶,
C. Paraskevopoulos ⁵³, D. Paredes Hernandez ^{64b}, S.R. Paredes Saenz ⁵², A. Pareti ^{73a,73b},
K.R. Park ⁴², T.H. Park ¹¹¹, F. Parodi ^{57b,57a}, J.A. Parsons ⁴², U. Parzefall ⁵⁴, B. Pascual Dias ⁴¹,
L. Pascual Dominguez ¹⁰⁰, E. Pasqualucci ^{75a}, S. Passaggio ^{57b}, F. Pastore ⁹⁶, P. Patel ⁸⁷,
U.M. Patel ⁵¹, J.R. Pater ¹⁰², T. Pauly ³⁷, F. Pauwels ¹³⁵, C.I. Pazos ¹⁶³, M. Pedersen ¹²⁷,
R. Pedro ^{132a}, S.V. Peleganchuk ³⁸, O. Penc ¹³³, S. Peng ¹⁵, G.D. Penn ¹⁷⁷, K.E. Pensi ¹¹⁰,
M. Penzin ³⁸, B.S. Peralva ^{82d}, A.P. Pereira Peixoto ¹⁴¹, L. Pereira Sanchez ¹⁴⁸,
D.V. Perpelitsa ^{30,al}, G. Perera ¹⁰⁴, E. Perez Codina ³⁷, M. Perganti ¹⁰, H. Pernegger ³⁷,
S. Perrella ^{75a,75b}, K. Peters ⁴⁸, R.F.Y. Peters ¹⁰², B.A. Petersen ³⁷, T.C. Petersen ⁴³, E. Petit ¹⁰³,
V. Petousis ¹³⁴, A.R. Petri ^{71a,71b}, C. Petridou ^{157,d}, T. Petru ¹³⁵, M. Pettee ^{18a}, A. Petukhov ⁸¹,
K. Petukhova ³⁷, R. Pezoa ^{139g}, L. Pezzotti ^{24b,24a}, G. Pezzullo ¹⁷⁷, L. Pfaffenbichler ³⁷,
A.J. Pflieger ⁷⁹, T.M. Pham ¹⁷⁵, T. Pham ¹⁰⁶, P.W. Phillips ¹³⁶, G. Piacquadio ¹⁵⁰, E. Pianori ^{18a},
F. Piazza ¹²⁵, R. Piegai ³¹, D. Pietreanu ^{28b}, A.D. Pilkington ¹⁰², M. Pinamonti ^{69a,69c},
J.L. Pinfeld ², G. Pinheiro Matos ⁴², B.C. Pinheiro Pereira ^{132a}, J. Pinol Bel ¹³,
A.E. Pinto Pinoargote ¹²⁹, L. Pintucci ^{69a,69c}, K.M. Piper ¹⁵¹, A. Pirttikoski ⁵⁶, D.A. Pizzi ³⁵,

L. Pizzimento ^{64b}, A. Plebani ³³, M.-A. Pleier ³⁰, V. Pleskot ¹³⁵, E. Plotnikova ³⁹, G. Poddar ⁹⁵,
 R. Poettgen ⁹⁹, L. Poggioli ¹²⁹, S. Polacek ¹³⁵, G. Polesello ^{73a}, A. Poley ¹⁴⁷, A. Polini ^{24b},
 C.S. Pollard ¹⁷², Z.B. Pollock ¹²¹, E. Pompa Pacchi ¹²², N.I. Pond ⁹⁷, D. Ponomarenko ⁶⁸,
 L. Pontecorvo ³⁷, S. Popa ^{28a}, G.A. Popeneciu ^{28d}, A. Poreba ³⁷, D.M. Portillo Quintero ^{161a},
 S. Pospisil ¹³⁴, M.A. Postill ¹⁴⁴, P. Postolache ^{28c}, K. Potamianos ¹⁷², P.A. Potepa ^{86a},
 I.N. Potrap ³⁹, C.J. Potter ³³, H. Potti ¹⁵², J. Poveda ¹⁶⁸, M.E. Pozo Astigarraga ³⁷, R. Pozzi ³⁷,
 A. Prades Ibanez ^{76a,76b}, S.R. Pradhan ¹⁴⁴, J. Pretel ¹⁷⁰, D. Price ¹⁰², M. Primavera ^{70a},
 L. Primomo ^{69a,69c}, M.A. Principe Martin ¹⁰⁰, R. Privara ¹²⁴, T. Procter ^{86b}, M.L. Proffitt ¹⁴¹,
 N. Proklova ¹³⁰, K. Prokofiev ^{64c}, G. Proto ¹¹¹, J. Proudfoot ⁶, M. Przybycien ^{86a},
 W.W. Przygoda ^{86b}, A. Psallidas ⁴⁶, J.E. Puddefoot ¹⁴⁴, D. Pudzha ⁵³, H.I. Purnell ¹,
 D. Pyatiizbyantseva ¹¹⁵, J. Qian ¹⁰⁷, R. Qian ¹⁰⁸, D. Qichen ¹²⁸, Y. Qin ¹³, T. Qiu ⁵²,
 A. Quadt ⁵⁵, M. Queitsch-Maitland ¹⁰², G. Quetant ⁵⁶, R.P. Quinn ¹⁶⁹, G. Rabanal Bolanos ⁶¹,
 D. Rafanoharana ¹¹¹, F. Raffaelli ^{76a,76b}, F. Ragusa ^{71a,71b}, J.L. Rainbolt ⁴⁰, S. Rajagopalan ³⁰,
 E. Ramakoti ³⁹, L. Rambelli ^{57b,57a}, I.A. Ramirez-Berend ³⁵, K. Ran ^{107,113c}, D.S. Rankin ¹³⁰,
 N.P. Rapheeha ^{34j}, H. Rasheed ^{28b}, A. Rastogi ^{18a}, S. Rave ¹⁰¹, S. Ravera ^{57b,57a}, B. Ravina ³⁷,
 I. Ravinovich ¹⁷⁴, M. Raymond ³⁷, A.L. Read ¹²⁷, N.P. Radioff ¹⁴⁴, D.M. Rebutti ^{73a,73b},
 A.S. Reed ⁵⁹, K. Reeves ²⁷, D. Reikher ³⁷, A. Rej ⁴⁹, C. Rembser ³⁷, H. Ren ⁶², M. Renda ^{28b},
 F. Renner ⁴⁸, A.G. Rennie ⁵⁹, M. Repik ⁵⁶, A.L. Rescia ^{57b,57a}, S. Resconi ^{71a},
 M. Ressegotti ^{57b,57a}, S. Rettie ¹¹⁶, W.F. Rettie ³⁵, M.M. Revering ³³, E. Reynolds ^{18a},
 O.L. Rezanova ³⁹, P. Reznicek ¹³⁵, H. Riani ^{36d}, N. Ribaric ⁵¹, B. Ricci ^{69a,69c}, E. Ricci ^{78a,78b},
 R. Richter ¹¹¹, S. Richter ^{47a,47b}, E. Richter-Was ^{86b}, M. Ridel ¹²⁹, S. Ridouani ^{36d}, P. Rieck ¹¹⁹,
 P. Riedler ³⁷, E.M. Riefel ^{47a,47b}, J.O. Rieger ¹¹⁶, M. Rijssenbeek ¹⁵⁰, M. Rimoldi ^{34c},
 L. Rinaldi ^{24b,24a}, P. Rincke ^{166,55}, G. Ripellino ¹⁶⁶, I. Riu ¹³, J.C. Rivera Vergara ¹⁷⁰,
 F. Rizatdinova ¹²³, E. Rizvi ⁹⁵, B.R. Roberts ⁴⁰, S.S. Roberts ¹³⁸, D. Robinson ³³, A. Robson ⁵⁹,
 A. Rocchi ^{76a,76b}, C. Roda ^{74a,74b}, F.A. Rodriguez ¹¹⁷, S. Rodriguez Bosca ³⁷,
 Y. Rodriguez Garcia ^{23a}, A.M. Rodríguez Vera ¹¹⁷, S. Roe ³⁷, J.T. Roemer ³⁷, O. Røhne ¹²⁷,
 R.A. Rojas ³⁷, C.P.A. Roland ¹²⁹, A. Romaniouk ⁷⁹, E. Romano ^{73a,73b}, M. Romano ^{24b},
 A.C. Romero Hernandez ¹⁶⁷, N. Rompotis ⁹³, L. Roos ¹²⁹, S. Rosati ^{75a}, B.J. Rosser ⁴⁰,
 E. Rossi ¹²⁸, E. Rossi ^{72a,72b}, L.P. Rossi ⁶¹, L. Rossini ⁵⁴, R. Rosten ¹²¹, M. Rotaru ^{28b},
 D. Rousseau ⁶⁶, D. Rousso ⁴⁸, S. Roy-Garand ¹⁶⁰, A. Rozanov ¹⁰³, Z.M.A. Rozario ⁵⁹,
 Y. Rozen ¹⁵⁵, A. Rubio Jimenez ¹⁶⁸, V.H. Ruelas Rivera ¹⁹, T.A. Ruggeri ¹, A. Ruggiero ¹²⁸,
 A. Ruiz-Martinez ¹⁶⁸, A. Rummler ³⁷, G.B. Rupnik Boero ³⁷, Z. Rurikova ⁵⁴,
 N.A. Rusakovich ³⁹, S. Ruscelli ⁴⁹, H.L. Russell ¹⁷⁰, G. Russo ^{75a,75b}, J.P. Rutherford ⁷,
 S. Rutherford Colmenares ³³, M. Rybar ¹³⁵, P. Rybczynski ^{86a}, A. Ryzhov ⁴⁵,
 H.F.W. Sadrozinski ¹³⁸, F. Safai Tehrani ^{75a}, S. Saha ¹, M. Sahinsoy ⁸¹, B. Sahoo ¹⁷⁴,
 A. Saibel ¹⁶⁸, B.T. Saifuddin ¹²², M. Saimpert ¹³⁷, G.T. Saito ^{82c}, M. Saito ¹⁵⁸, T. Saito ¹⁵⁸,
 A. Sala ^{71a,71b}, A. Salnikov ¹⁴⁸, J. Salt ¹⁶⁸, A. Salvador Salas ¹⁵⁶, F. Salvatore ¹⁵¹,
 A. Salzburger ³⁷, D. Sammel ⁵⁴, E. Sampson ⁹², D. Sampsonidis ^{157,d}, D. Sampsonidou ¹²⁵,
 M.A.A. Samy ⁵⁹, J. Sánchez ¹⁶⁸, V. Sanchez Sebastian ¹⁶⁸, H. Sandaker ¹²⁷, C.O. Sander ⁴⁸,
 J.A. Sandesara ¹⁷⁵, M. Sandhoff ¹⁷⁶, C. Sandoval ^{23b}, L. Sanfilippo ^{63a}, D.P.C. Sankey ¹³⁶,
 T. Sano ⁸⁸, A. Sansoni ⁵³, M. Santana Queiroz ^{18b}, L. Santi ³⁷, C. Santoni ⁴¹,
 H. Santos ^{132a,132b}, A. Santra ¹⁷⁴, E. Sanzani ^{24b,24a}, K.A. Saoucha ^{84b}, J.G. Saraiva ^{132a,132d},
 J. Sardain ⁷, O. Sasaki ⁸³, K. Sato ¹⁶², C. Sauer ³⁷, E. Sauvan ⁴, P. Savard ^{160,ai}, R. Sawada ¹⁵⁸,
 C. Sawyer ¹³⁶, L. Sawyer ⁹⁸, A.M. Sayed ²⁷, C. Sbarra ^{24b}, A. Sbrizzi ^{24b,24a}, T. Scanlon ⁹⁷,
 J. Schaarschmidt ¹⁴¹, U. Schäfer ¹⁰¹, A.C. Schaffer ^{66,45}, D. Schaile ¹¹⁰, R.D. Schamberger ¹⁵⁰,
 C. Scharf ¹⁹, M.M. Schefer ²⁰, V.A. Schegelsky ³⁸, D. Scheirich ¹³⁵, M. Schernau ^{139f},
 C. Scheulen ⁵⁶, C. Schiavi ^{57b,57a}, M. Schioppa ^{44b,44a}, B. Schlag ¹⁴⁸, S. Schlenker ³⁷,

J. Schmeing ¹⁷⁶, E. Schmidt ¹¹¹, M.A. Schmidt ¹⁷⁶, K. Schmieden ²⁵, C. Schmitt ¹⁰¹,
 N. Schmitt ¹⁰¹, S. Schmitt ⁴⁸, N.A. Schneider ¹¹⁰, L. Schoeffel ¹³⁷, A. Schoening ^{63b},
 P.G. Scholer ³⁵, E. Schopf ¹⁴⁶, M. Schott ²⁵, S. Schramm ⁵⁶, T. Schroer ⁵⁶,
 H-C. Schultz-Coulon ^{63a}, M. Schumacher ⁵⁴, B.A. Schumm ¹³⁸, Ph. Schune ¹³⁷, H.R. Schwartz ⁷,
 A. Schwartzman ¹⁴⁸, T.A. Schwarz ¹⁰⁷, Ph. Schwemling ¹³⁷, R. Schwienhorst ¹⁰⁸, F.G. Sciacca ²⁰,
 A. Sciandra ³⁰, G. Sciolla ²⁷, F. Scuri ^{74a}, C.D. Sebastiani ³⁷, K. Sedlaczek ¹¹⁷, S.C. Seidel ¹¹⁴,
 A. Seiden ¹³⁸, B.D. Seidlitz ⁴², C. Seitz ⁴⁸, J.M. Seixas ^{82b}, G. Sekhniaidze ^{72a}, L. Selem ⁶⁰,
 N. Semprini-Cesari ^{24b,24a}, A. Semushin ¹⁷⁸, D. Sengupta ⁵⁶, V. Senthilkumar ¹⁶⁸, L. Serin ⁶⁶,
 M. Sessa ^{72a,72b}, H. Severini ¹²², F. Sforza ^{57b,57a}, A. Sfyrla ⁵⁶, Q. Sha ¹⁴, H. Shaddix ¹¹⁷,
 A.H. Shah ³³, R. Shaheen ¹⁴⁹, J.D. Shahinian ¹³⁰, M. Shamim ³⁷, L.Y. Shan ¹⁴, M. Shapiro ^{18a},
 A. Sharma ³⁷, A.S. Sharma ¹⁶⁹, P. Sharma ³⁰, P.B. Shatalov ³⁸, K. Shaw ¹⁵¹, S.M. Shaw ¹⁰²,
 Q. Shen ¹⁴, D.J. Sheppard ¹⁴⁷, P. Sherwood ⁹⁷, L. Shi ⁹⁷, X. Shi ¹⁴, S. Shimizu ⁸³,
 I.P.J. Shipsey ^{128,*}, S. Shirabe ⁸⁹, M. Shiyakova ^{39,z}, M.J. Shochet ⁴⁰, D.R. Shope ¹²⁷,
 B. Shrestha ¹²², S. Shrestha ^{121,an}, I. Shreyber ³⁹, M.J. Shroff ¹⁷⁰, P. Sicho ¹³³, A.M. Sickles ¹⁶⁷,
 E. Sideras Haddad ^{34j,165}, A.C. Sidley ¹¹⁶, A. Sidoti ^{24b}, F. Siegert ⁵⁰, Dj. Sijacki ¹⁶, F. Sili ⁶²,
 J.M. Silva ⁵², I. Silva Ferreira ^{82b}, M.V. Silva Oliveira ³⁰, S.B. Silverstein ^{47a}, S. Simion ⁶⁶,
 R. Simoniello ³⁷, E.L. Simpson ¹⁰², H. Simpson ¹⁵¹, L.R. Simpson ⁶, S. Simsek ⁸¹,
 S. Sindhu ⁵⁵, P. Sinervo ¹⁶⁰, S.N. Singh ²⁷, S. Singh ³⁰, S. Sinha ⁴⁸, S. Sinha ¹⁰²,
 M. Sioli ^{24b,24a}, K. Sioulas ⁹, I. Siral ³⁷, E. Sitnikova ⁴⁸, J. Sjölin ^{47a,47b}, A. Skaf ⁵⁵,
 E. Skorda ²¹, P. Skubic ¹²², M. Slawinska ⁸⁷, I. Slazyk ¹⁷, I. Sliusar ¹²⁷, V. Smakhtin ¹⁷⁴,
 B.H. Smart ¹³⁶, S.Yu. Smirnov ^{139b}, Y. Smirnov ^{34c}, L.N. Smirnova ^{38,a}, O. Smirnova ⁹⁹,
 A.C. Smith ⁴², D.R. Smith ¹⁶⁴, J.L. Smith ¹⁰², M.B. Smith ³⁵, R. Smith ¹⁴⁸, H. Smitmanns ¹⁰¹,
 M. Smizanska ⁹², K. Smolek ¹³⁴, P. Smolyanskiy ¹³⁴, A.A. Snesarev ³⁹, H.L. Snoek ¹¹⁶,
 R.M. Snyder ⁵¹, S. Snyder ³⁰, R. Sobie ^{170,ab}, A. Soffer ¹⁵⁶, C.A. Solans Sanchez ³⁷,
 E.Yu. Soldatov ³⁹, U. Soldevila ¹⁶⁸, A.A. Solodkov ^{34j}, S. Solomon ²⁷, A. Soloshenko ³⁹,
 K. Solovieva ⁵⁴, O.V. Solovyanov ⁴¹, P. Sommer ⁵⁰, A. Sonay ¹³, A. Sopczak ¹³⁴,
 A.L. Sopio ⁵², F. Sopkova ^{29b}, J.D. Sorenson ¹¹⁴, I.R. Sotarriva Alvarez ¹⁴⁰, V. Sothilingam ^{63a},
 O.J. Soto Sandoval ^{139c,139b}, S. Sottocornola ⁶⁸, R. Soualah ^{84a}, Z. Soumami ^{36e}, D. South ⁴⁸,
 N. Soybelman ¹⁷⁴, S. Spagnolo ^{70a,70b}, D. Sperlich ⁵⁴, B. Spisso ^{72a,72b}, D.P. Spiteri ⁵⁹,
 L. Splendori ¹⁰³, M. Spousta ¹³⁵, E.J. Staats ³⁵, R. Stamen ^{63a}, E. Stanecka ⁸⁷,
 W. Stanek-Maslouska ⁴⁸, M.V. Stange ⁵⁰, B. Stanislaus ^{18a}, M.M. Stanitzki ⁴⁸, E.A. Starchenko ³⁸,
 G.H. Stark ¹³⁸, J. Stark ⁹⁰, P. Staroba ¹³³, P. Starovoitov ^{84b}, R. Staszewski ⁸⁷, C. Stauch ¹¹⁰,
 G. Stavropoulos ⁴⁶, A. Stefl ³⁷, A. Stein ¹⁰¹, P. Steinberg ³⁰, B. Stelzer ^{147,161a}, H.J. Stelzer ¹³¹,
 O. Stelzer ^{161a}, H. Stenzel ⁵⁸, T.J. Stevenson ¹⁵¹, G.A. Stewart ³⁷, J.R. Stewart ¹²³,
 G. Stoicea ^{28b}, M. Stolarski ^{132a}, S. Stonjek ¹¹¹, A. Straessner ⁵⁰, J. Strandberg ¹⁴⁹,
 S. Strandberg ^{47a,47b}, M. Stratmann ¹⁷⁶, M. Strauss ¹²², T. Streblner ¹⁰³, P. Strizened ^{29b},
 R. Ströhmer ¹⁷¹, D.M. Strom ¹²⁵, R. Stroynowski ⁴⁵, A. Strubig ^{47a,47b}, S.A. Stucci ³⁰,
 B. Stugu ¹⁷, J. Stupak ¹²², N.A. Styles ⁴⁸, D. Su ¹⁴⁸, S. Su ⁶², X. Su ⁶², D. Suchy ^{29a},
 A.D. Sudhakar Ponnu ⁵⁵, L. Sudit ¹⁷⁴, K. Sugizaki ¹³⁰, V.V. Sulin ³⁸, D.M.S. Sultan ¹²⁸,
 L. Sultaniyeva ²⁵, S. Sultansoy ^{3b}, S. Sun ¹⁷⁵, W. Sun ¹⁴, N. Sur ⁹⁹, N. Suri Jr ¹⁷⁷,
 M.R. Sutton ¹⁵¹, M. Svatos ¹³³, P.N. Swallow ³³, M. Swiatlowski ^{161a}, A. Swoboda ³⁷,
 I. Sykora ^{29a}, M. Sykora ¹³⁵, T. Sykora ¹³⁵, D. Ta ¹⁰¹, K. Tackmann ^{48,y}, A. Taffard ¹⁶⁴,
 R. Tafirout ^{161a}, Y. Takubo ⁸³, M. Talby ¹⁰³, A.A. Talyshev ³⁸, K.C. Tam ^{64b}, N.M. Tamir ¹⁵⁶,
 A. Tanaka ¹⁵⁸, J. Tanaka ¹⁵⁸, R. Tanaka ⁶⁶, M. Tanasini ¹⁵⁰, Z. Tao ¹⁶⁹, S. Tapia Araya ^{139g},
 S. Tapprogge ¹⁰¹, A. Tarek Abouelfadl Mohamed ³⁷, S. Tarem ¹⁵⁵, K. Tariq ¹⁴, G. Tarna ³⁷,
 G.F. Tartarelli ^{71a}, M.J. Tartarin ⁹⁰, P. Tas ¹³⁵, M. Tasevsky ¹³³, E. Tassi ^{44b,44a}, A.C. Tate ¹⁶⁷,
 Y. Tayalati ^{36e,aa}, G.N. Taylor ¹⁰⁶, W. Taylor ^{161b}, R.J. Taylor Vara ¹⁶⁸, A.S. Tegetmeier ⁹⁰,

P. Teixeira-Dias ⁹⁶, J.J. Teoh ¹⁶⁰, K. Terashi ¹⁵⁸, J. Terron ¹⁰⁰, S. Terzo ¹³, M. Testa ⁵³,
 R.J. Teuscher ^{160,ab}, A. Thaler ⁷⁹, O. Theiner ⁵⁶, T. Theveneaux-Pelzer ¹⁰³, D.W. Thomas ⁹⁶,
 J.P. Thomas ²¹, E.A. Thompson ^{18a}, P.D. Thompson ²¹, E. Thomson ¹³⁰, R.E. Thornberry ⁴⁵,
 C. Tian ⁶², Y. Tian ⁵⁶, V. Tikhomirov ⁸¹, Yu.A. Tikhonov ³⁹, S. Timoshenko ³⁸, D. Timoshyn ¹³⁵,
 E.X.L. Ting ¹, P. Tipton ¹⁷⁷, A. Tishelman-Charny ³⁰, K. Todome ¹⁴⁰, S. Todorova-Nova ¹³⁵,
 L. Toffolin ^{69a,69c}, M. Togawa ⁸³, J. Tojo ⁸⁹, S. Tokár ^{29a}, O. Toldaiev ⁶⁸, G. Tolkachev ¹⁰³,
 M. Tomoto ⁸³, L. Tompkins ^{148,n}, E. Torrence ¹²⁵, H. Torres ⁹⁰, D.I. Torres Arza ^{139g},
 E. Torró Pastor ¹⁶⁸, M. Toscani ³¹, C. Toscirci ⁴⁰, M. Tost ¹¹, D.R. Tovey ¹⁴⁴, T. Trefzger ¹⁷¹,
 P.M. Tricarico ¹³, A. Tricoli ³⁰, I.M. Trigger ^{161a}, S. Trincaz-Duvoid ¹²⁹, D.A. Trischuk ¹⁷⁰,
 A. Tropina ³⁹, D. Truncali ^{76a,76b}, L. Truong ^{34c}, M. Trzebinski ⁸⁷, A. Trzupiek ⁸⁷, F. Tsai ¹⁵⁰,
 M. Tsai ¹⁰⁷, A. Tsiamis ¹⁵⁷, P.V. Tsiareshka ³⁹, S. Tsigaridas ^{161a}, A. Tsigiriotis ^{157,u},
 V. Tsiskaridze ^{154a}, E.G. Tskhadadze ^{154a}, Y. Tsujikawa ⁸⁸, I.I. Tsukerman ³⁸, V. Tsulaia ^{18a},
 S. Tsuno ⁸³, K. Tsuru ¹²⁰, D. Tsybychev ¹⁵⁰, Y. Tu ^{64b}, A. Tudorache ^{28b}, V. Tudorache ^{28b},
 S.B. Tuncay ¹²⁸, S. Turchikhin ^{57b,57a}, I. Turk Cakir ^{3a}, R. Turra ^{71a}, T. Turtuvshin ^{39,ac},
 P.M. Tuts ⁴², S. Tzamarias ^{157,d}, Y. Uematsu ⁸³, F. Ukegawa ¹⁶², P.A. Ulloa Poblete ^{139c,139b},
 E.N. Umaka ³⁰, G. Unal ³⁷, A. Undrus ³⁰, G. Unel ¹⁶⁴, J. Urban ^{29b}, P. Urrejola ^{139e},
 G. Usai ⁸, R. Ushioda ¹⁵⁹, M. Usman ¹⁰⁹, F. Ustuner ⁵², Z. Uysal ⁸¹, V. Vacek ¹³⁴,
 B. Vachon ¹⁰⁵, T. Vafeiadis ³⁷, A. Vaitkus ⁹⁷, C. Valderanis ¹¹⁰, E. Valdes Santurio ^{47a,47b},
 M. Valente ³⁷, S. Valentinetti ^{24b,24a}, A. Valero ¹⁶⁸, E. Valiente Moreno ¹⁶⁸, A. Vallier ⁹⁰,
 J.A. Valls Ferrer ¹⁶⁸, D.R. Van Arneman ¹¹⁶, A. Van Der Graaf ⁴⁹, H.Z. Van Der Schyf ^{34j},
 P. Van Gemmeren ⁶, M. Van Rijnbach ³⁷, S. Van Stroud ⁹⁷, I. Van Vulpen ¹¹⁶, P. Vana ¹³⁵,
 M. Vanadia ^{76a,76b}, U.M. Vande Voorde ¹⁴⁹, W. Vandelli ³⁷, E.R. Vandewall ¹⁴⁸, D. Vannicola ¹⁵⁶,
 L. Vannoli ⁵³, R. Vari ^{75a}, M. Varma ¹⁷⁷, E.W. Varnes ⁷, C. Varni ⁷⁹, D. Varouchas ⁶⁶,
 L. Varriale ¹⁶⁸, K.E. Varvell ¹⁵², M.E. Vasile ^{28b}, L. Vaslin ⁸³, M.D. Vassilev ¹⁴⁸, A. Vasyukov ³⁹,
 L.M. Vaughan ¹²³, R. Vavricka ¹³⁵, T. Vazquez Schroeder ¹³, J. Veatch ³², V. Vecchio ¹⁰²,
 M.J. Veen ¹⁰⁴, I. Veliscek ³⁰, I. Velkovska ⁹⁴, L.M. Veloce ¹⁶⁰, F. Veloso ^{132a,132c},
 A.G. Veltman ⁵², S. Veneziano ^{75a}, A. Ventura ^{70a,70b}, A. Verbytskyi ¹¹¹, M. Verducci ^{74a,74b},
 C. Vergis ⁹⁵, M. Verissimo De Araujo ^{82b}, W. Verkerke ¹¹⁶, J.C. Vermeulen ¹¹⁶, C. Vernieri ¹⁴⁸,
 M. Vessella ¹⁶⁴, M.C. Vetterli ^{147,ai}, A. Vgenopoulos ¹⁰¹, N. Viaux Maira ^{139g,af}, T. Vickey ¹⁴⁴,
 O.E. Vickey Boeriu ¹⁴⁴, G.H.A. Viehhauser ¹²⁸, L. Vigani ^{63b}, M. Vigl ¹¹¹, M. Villa ^{24b,24a},
 M. Villaplana Perez ¹⁶⁸, E.M. Villhauer ⁴⁰, E. Vilucchi ⁵³, M. Vincent ¹⁶⁸, M.G. Vincter ³⁵,
 A. Visibile ¹¹⁶, A. Visive ¹¹⁶, C. Vittori ³⁷, I. Vivarelli ^{24b,24a}, M.I. Vivas Albornoz ⁴⁸,
 E. Voevodina ¹¹¹, F. Vogel ¹¹⁰, J.C. Voigt ⁵⁰, P. Vokac ¹³⁴, Yu. Volkotrub ^{86b}, L. Vomberg ²⁵,
 E. Von Toerne ²⁵, B. Vormwald ³⁷, K. Vorobev ⁵¹, M. Vos ¹⁶⁸, K. Voss ¹⁴⁶, M. Vozak ³⁷,
 L. Vozdecky ¹²², N. Vranjes ¹⁶, M. Vranjes Milosavljevic ¹⁶, M. Vreeswijk ¹¹⁶, N.K. Vu ^{143b,143a},
 R. Vuillermet ³⁷, O. Vujinovic ¹⁰¹, I. Vukotic ⁴⁰, I.K. Vyas ³⁵, J.F. Wack ³³, S. Wada ¹⁶²,
 C. Wagner ¹⁴⁸, J.M. Wagner ^{18a}, W. Wagner ¹⁷⁶, S. Wahdan ¹⁷⁶, H. Wahlberg ⁹¹, C.H. Waits ¹²²,
 J. Walder ¹³⁶, R. Walker ¹¹⁰, K. Walkingshaw Pass ⁵⁹, W. Walkowiak ¹⁴⁶, A. Wall ¹³⁰,
 E.J. Wallin ⁹⁹, T. Wamorkar ^{18a}, K. Wandall-Christensen ¹⁶⁸, A. Wang ⁶², A.Z. Wang ¹³⁸,
 C. Wang ⁴⁸, C. Wang ¹¹, H. Wang ^{18a}, J. Wang ^{64c}, P. Wang ¹⁰², P. Wang ⁹⁷, R. Wang ⁶¹,
 R. Wang ⁶, S.M. Wang ¹⁵³, S. Wang ¹⁴, T. Wang ¹¹⁵, T. Wang ⁶², W.T. Wang ¹²⁸, W. Wang ¹⁴,
 X. Wang ¹⁶⁷, X. Wang ^{143a}, X. Wang ⁴⁸, Y. Wang ¹⁵⁰, Y. Wang ¹¹⁴, Z. Wang ¹⁰⁷,
 Z. Wang ^{143b}, Z. Wang ¹⁰⁷, C. Wanotayaroj ⁸³, A. Warburton ¹⁰⁵, A.L. Warnerbring ¹⁴⁶,
 S. Waterhouse ⁹⁶, A.T. Watson ²¹, H. Watson ⁵², M.F. Watson ²¹, E. Watton ³⁷, G. Watts ¹⁴¹,
 B.M. Waugh ⁹⁷, J.M. Webb ⁵⁴, C. Weber ³⁰, M.S. Weber ²⁰, S.M. Weber ^{63a}, C. Wei ⁶²,
 Y. Wei ⁵⁴, A.R. Weidberg ¹²⁸, E.J. Weik ¹¹⁹, J. Weingarten ⁴⁹, C. Weiser ⁵⁴, C.J. Wells ⁴⁸,
 T. Wenaus ³⁰, T. Wengler ³⁷, N.S. Wenke ¹¹¹, N. Wermes ²⁵, M. Wessels ^{63a}, A.M. Wharton ⁹²,

A.S. White ⁶¹, A. White ⁸, M.J. White ¹, D. Whiteson ¹⁶⁴, L. Wickremasinghe ¹²⁶,
W. Wiedenmann ¹⁷⁵, M. Wielers ¹³⁶, R. Wierda ¹⁴⁹, C. Wigglesworth ⁴³, H.G. Wilkens ³⁷,
J.J.H. Wilkinson ³³, D.M. Williams ⁴², H.H. Williams ¹³⁰, S. Williams ³³, S. Willocq ¹⁰⁴,
B.J. Wilson ¹⁰², D.J. Wilson ¹⁰², P.J. Windischhofer ⁴⁰, F.I. Winkel ³¹, F. Winklmeier ¹²⁵,
B.T. Winter ⁵⁴, M. Wittgen ¹⁴⁸, M. Wobisch ⁹⁸, T. Wojtkowski ⁶⁰, Z. Wolfs ¹¹⁶, J. Wollrath ³⁷,
M.W. Wolter ⁸⁷, H. Wolters ^{132a,132c}, M.C. Wong ¹³⁸, E.L. Woodward ⁴², S.D. Worm ⁴⁸,
B.K. Wosiek ⁸⁷, K.W. Woźniak ⁸⁷, S. Wozniowski ⁵⁵, K. Wraight ⁵⁹, C. Wu ¹⁶⁰, C. Wu ²¹,
J. Wu ¹⁵⁸, M. Wu ^{113b}, M. Wu ¹¹⁵, S.L. Wu ¹⁷⁵, S. Wu ^{14,ak}, X. Wu ⁶², Y.Q. Wu ¹⁶⁰,
Y. Wu ⁶², Z. Wu ⁴, Z. Wu ^{113a}, J. Wuerzinger ¹¹¹, T.R. Wyatt ¹⁰², B.M. Wynne ⁵², S. Xella ⁴³,
L. Xia ^{113a}, M. Xie ⁶², A. Xiong ¹²⁵, D. Xu ¹⁴, H. Xu ⁶², L. Xu ⁶², R. Xu ¹³⁰, T. Xu ¹⁰⁷,
W. Xu ^{113a}, Y. Xu ¹⁴¹, Z. Xu ⁵², R. Xue ¹³¹, B. Yabsley ¹⁵², S. Yacoob ^{34a}, Y. Yamaguchi ⁸³,
E. Yamashita ¹⁵⁸, H. Yamauchi ¹⁶², T. Yamazaki ^{18a}, Y. Yamazaki ⁸⁵, S. Yan ⁵⁹, Z. Yan ¹⁰⁴,
H.J. Yang ^{143a,143b}, H.T. Yang ⁶², S. Yang ⁶², T. Yang ^{64c}, X. Yang ³⁷, X. Yang ¹⁴,
Y. Yang ¹⁵⁸, Y. Yang ⁶², W.-M. Yao ^{18a}, C.L. Yardley ¹⁵¹, J. Ye ¹⁴, S. Ye ³⁰, X. Ye ⁶², Y. Yeh ⁹⁷,
I. Yeletsikh ³⁹, B. Yeo ^{18b}, M.R. Yexley ⁹⁷, T.P. Yildirim ¹²⁸, K. Yorita ¹⁷³, C.J.S. Young ³⁷,
C. Young ¹⁴⁸, I.N.L. Young ⁵⁹, N.D. Young ¹²⁵, Y. Yu ⁶², J. Yuan ^{14,113c}, M. Yuan ¹⁰⁷,
R. Yuan ^{143b}, L. Yue ⁹⁷, M. Zaazoua ⁶², B. Zabinski ⁸⁷, I. Zahir ^{36a}, A. Zaio ^{57b,57a}, Z.K. Zak ⁸⁷,
T. Zakareishvili ¹⁶⁸, S. Zambito ⁵⁶, J.A. Zamora Saa ^{139d}, J. Zang ¹⁵⁸, R. Zanzottera ^{71a,71b},
O. Zaplatilek ¹³⁴, C. Zeitnitz ¹⁷⁶, H. Zeng ¹⁴, D.T. Zenger Jr ²⁷, O. Zenin ³⁸, T. Ženiš ^{29a},
S. Zenz ⁹⁵, D. Zerwas ⁶⁶, B. Zhang ¹⁷², D.F. Zhang ¹⁴⁴, G. Zhang ^{14,ak}, J. Zhang ^{142a},
J. Zhang ⁶, L. Zhang ⁶², L. Zhang ^{113a}, P. Zhang ^{14,113c}, R. Zhang ^{113a}, S. Zhang ⁹⁰,
T. Zhang ¹⁵⁸, Y. Zhang ¹⁴¹, Y. Zhang ⁹⁷, Y. Zhang ⁶², Y. Zhang ^{113a}, Z. Zhang ^{18a},
Z. Zhang ^{142a}, Z. Zhang ⁶⁶, H. Zhao ¹⁴¹, T. Zhao ^{142a}, Y. Zhao ³⁵, Z. Zhao ⁶², Z. Zhao ⁶²,
A. Zhemchugov ³⁹, J. Zheng ^{113a}, K. Zheng ¹⁶⁷, X. Zheng ⁶², Z. Zheng ¹⁴⁸, D. Zhong ¹⁶⁷,
B. Zhou ¹⁰⁷, B. Zhou ^{143b}, H. Zhou ⁷, N. Zhou ^{143a}, Y. Zhou ¹⁵, Y. Zhou ^{113a}, Y. Zhou ⁷,
J. Zhu ¹⁰⁷, X. Zhu ^{143b}, Y. Zhu ^{143a}, Y. Zhu ⁶², X. Zhuang ¹⁴, K. Zhukov ⁶⁸, N.I. Zimine ³⁹,
J. Zinsser ^{53b}, M. Ziolkowski ¹⁴⁶, L. Živković ¹⁶, A. Zoccoli ^{24b,24a}, K. Zoch ⁶¹, A. Zografos ³⁷,
T.G. Zorbas ¹⁴⁴, O. Zormpa ⁴⁶, L. Zwalinski ³⁷.

¹Department of Physics, University of Adelaide, Adelaide; Australia.

²Department of Physics, University of Alberta, Edmonton AB; Canada.

³(^a)Department of Physics, Ankara University, Ankara; (^b)Division of Physics, TOBB University of Economics and Technology, Ankara; Türkiye.

⁴LAPP, Université Savoie Mont Blanc, CNRS/IN2P3, Annecy; France.

⁵APC, Université Paris Cité, CNRS/IN2P3, Paris; France.

⁶High Energy Physics Division, Argonne National Laboratory, Argonne IL; United States of America.

⁷Department of Physics, University of Arizona, Tucson AZ; United States of America.

⁸Department of Physics, University of Texas at Arlington, Arlington TX; United States of America.

⁹Physics Department, National and Kapodistrian University of Athens, Athens; Greece.

¹⁰Physics Department, National Technical University of Athens, Zografou; Greece.

¹¹Department of Physics, University of Texas at Austin, Austin TX; United States of America.

¹²Institute of Physics, Azerbaijan Academy of Sciences, Baku; Azerbaijan.

¹³Institut de Física d'Altes Energies (IFAE), Barcelona Institute of Science and Technology, Barcelona; Spain.

¹⁴Institute of High Energy Physics, Chinese Academy of Sciences, Beijing; China.

¹⁵Physics Department, Tsinghua University, Beijing; China.

¹⁶Institute of Physics, University of Belgrade, Belgrade; Serbia.

- ¹⁷Department for Physics and Technology, University of Bergen, Bergen; Norway.
- ¹⁸(^a)Physics Division, Lawrence Berkeley National Laboratory, Berkeley CA; (^b)University of California, Berkeley CA; United States of America.
- ¹⁹Institut für Physik, Humboldt Universität zu Berlin, Berlin; Germany.
- ²⁰Albert Einstein Center for Fundamental Physics and Laboratory for High Energy Physics, University of Bern, Bern; Switzerland.
- ²¹School of Physics and Astronomy, University of Birmingham, Birmingham; United Kingdom.
- ²²(^a)Department of Physics, Bogazici University, Istanbul; (^b)Department of Physics Engineering, Gaziantep University, Gaziantep; (^c)Department of Physics, Istanbul University, Istanbul; Türkiye.
- ²³(^a)Facultad de Ciencias y Centro de Investigaciones, Universidad Antonio Nariño, Bogotá; (^b)Departamento de Física, Universidad Nacional de Colombia, Bogotá; Colombia.
- ²⁴(^a)Dipartimento di Fisica e Astronomia A. Righi, Università di Bologna, Bologna; (^b)INFN Sezione di Bologna; Italy.
- ²⁵Physikalisches Institut, Universität Bonn, Bonn; Germany.
- ²⁶Department of Physics, Boston University, Boston MA; United States of America.
- ²⁷Department of Physics, Brandeis University, Waltham MA; United States of America.
- ²⁸(^a)Transilvania University of Brasov, Brasov; (^b)Horia Hulubei National Institute of Physics and Nuclear Engineering, Bucharest; (^c)Department of Physics, Alexandru Ioan Cuza University of Iasi, Iasi; (^d)National Institute for Research and Development of Isotopic and Molecular Technologies, Physics Department, Cluj-Napoca; (^e)National University of Science and Technology Politehnica, Bucharest; (^f)West University in Timisoara, Timisoara; (^g)Faculty of Physics, University of Bucharest, Bucharest; Romania.
- ²⁹(^a)Faculty of Mathematics, Physics and Informatics, Comenius University, Bratislava; (^b)Department of Subnuclear Physics, Institute of Experimental Physics of the Slovak Academy of Sciences, Kosice; Slovak Republic.
- ³⁰Physics Department, Brookhaven National Laboratory, Upton NY; United States of America.
- ³¹Universidad de Buenos Aires, Facultad de Ciencias Exactas y Naturales, Departamento de Física, y CONICET, Instituto de Física de Buenos Aires (IFIBA), Buenos Aires; Argentina.
- ³²California State University, CA; United States of America.
- ³³Cavendish Laboratory, University of Cambridge, Cambridge; United Kingdom.
- ³⁴(^a)Department of Physics, University of Cape Town, Cape Town; (^b)iThemba Labs, Western Cape; (^c)Department of Mechanical Engineering Science, University of Johannesburg, Johannesburg; (^d)National Institute of Physics, University of the Philippines Diliman (Philippines); (^e)Department of Physics, Stellenbosch University, Matieland; (^f)University of KwaZulu-Natal, School of Agriculture and Science, Mathematics, Westville; (^g)University of South Africa, Department of Physics, Pretoria; (^h)University of Pretoria, Department of Mechanical and Aeronautical Engineering, Pretoria; (ⁱ)University of Zululand, KwaDlangezwa; (^j)School of Physics, University of the Witwatersrand, Johannesburg; South Africa.
- ³⁵Department of Physics, Carleton University, Ottawa ON; Canada.
- ³⁶(^a)Faculté des Sciences Ain Chock, Université Hassan II de Casablanca; (^b)Faculté des Sciences, Université Ibn-Tofail, Kénitra; (^c)Faculté des Sciences Semlalia, Université Cadi Ayyad, LPHEA-Marrakech; (^d)LPMR, Faculté des Sciences, Université Mohamed Premier, Oujda; (^e)Faculté des sciences, Université Mohammed V, Rabat; (^f)Institute of Applied Physics, Mohammed VI Polytechnic University, Ben Guerir; Morocco.
- ³⁷CERN, Geneva; Switzerland.
- ³⁸Affiliated with an institute formerly covered by a cooperation agreement with CERN.
- ³⁹Affiliated with an international laboratory covered by a cooperation agreement with CERN.
- ⁴⁰Enrico Fermi Institute, University of Chicago, Chicago IL; United States of America.

- ⁴¹LPC, Université Clermont Auvergne, CNRS/IN2P3, Clermont-Ferrand; France.
- ⁴²Nevis Laboratory, Columbia University, Irvington NY; United States of America.
- ⁴³Niels Bohr Institute, University of Copenhagen, Copenhagen; Denmark.
- ⁴⁴(^a)Dipartimento di Fisica, Università della Calabria, Rende; (^b)INFN Gruppo Collegato di Cosenza, Laboratori Nazionali di Frascati; Italy.
- ⁴⁵Physics Department, Southern Methodist University, Dallas TX; United States of America.
- ⁴⁶National Centre for Scientific Research "Demokritos", Agia Paraskevi; Greece.
- ⁴⁷(^a)Department of Physics, Stockholm University; (^b)Oskar Klein Centre, Stockholm; Sweden.
- ⁴⁸Deutsches Elektronen-Synchrotron DESY, Hamburg and Zeuthen; Germany.
- ⁴⁹Fakultät Physik, Technische Universität Dortmund, Dortmund; Germany.
- ⁵⁰Institut für Kern- und Teilchenphysik, Technische Universität Dresden, Dresden; Germany.
- ⁵¹Department of Physics, Duke University, Durham NC; United States of America.
- ⁵²SUPA - School of Physics and Astronomy, University of Edinburgh, Edinburgh; United Kingdom.
- ⁵³INFN e Laboratori Nazionali di Frascati, Frascati; Italy.
- ⁵⁴Physikalisches Institut, Albert-Ludwigs-Universität Freiburg, Freiburg; Germany.
- ⁵⁵II. Physikalisches Institut, Georg-August-Universität Göttingen, Göttingen; Germany.
- ⁵⁶Département de Physique Nucléaire et Corpusculaire, Université de Genève, Genève; Switzerland.
- ⁵⁷(^a)Dipartimento di Fisica, Università di Genova, Genova; (^b)INFN Sezione di Genova; Italy.
- ⁵⁸II. Physikalisches Institut, Justus-Liebig-Universität Giessen, Giessen; Germany.
- ⁵⁹SUPA - School of Physics and Astronomy, University of Glasgow, Glasgow; United Kingdom.
- ⁶⁰LPSC, Université Grenoble Alpes, CNRS/IN2P3, Grenoble INP, Grenoble; France.
- ⁶¹Laboratory for Particle Physics and Cosmology, Harvard University, Cambridge MA; United States of America.
- ⁶²Department of Modern Physics and State Key Laboratory of Particle Detection and Electronics, University of Science and Technology of China, Hefei; China.
- ⁶³(^a)Kirchhoff-Institut für Physik, Ruprecht-Karls-Universität Heidelberg, Heidelberg; (^b)Physikalisches Institut, Ruprecht-Karls-Universität Heidelberg, Heidelberg; Germany.
- ⁶⁴(^a)Department of Physics, Chinese University of Hong Kong, Shatin, N.T., Hong Kong; (^b)Department of Physics, University of Hong Kong, Hong Kong; (^c)Department of Physics and Institute for Advanced Study, Hong Kong University of Science and Technology, Clear Water Bay, Kowloon, Hong Kong; China.
- ⁶⁵Department of Physics, National Tsing Hua University, Hsinchu; Taiwan.
- ⁶⁶IJCLab, Université Paris-Saclay, CNRS/IN2P3, 91405, Orsay; France.
- ⁶⁷Centro Nacional de Microelectrónica (IMB-CNM-CSIC), Barcelona; Spain.
- ⁶⁸Department of Physics, Indiana University, Bloomington IN; United States of America.
- ⁶⁹(^a)INFN Gruppo Collegato di Udine, Sezione di Trieste, Udine; (^b)ICTP, Trieste; (^c)Dipartimento Politecnico di Ingegneria e Architettura, Università di Udine, Udine; Italy.
- ⁷⁰(^a)INFN Sezione di Lecce; (^b)Dipartimento di Matematica e Fisica, Università del Salento, Lecce; Italy.
- ⁷¹(^a)INFN Sezione di Milano; (^b)Dipartimento di Fisica, Università di Milano, Milano; Italy.
- ⁷²(^a)INFN Sezione di Napoli; (^b)Dipartimento di Fisica, Università di Napoli, Napoli; Italy.
- ⁷³(^a)INFN Sezione di Pavia; (^b)Dipartimento di Fisica, Università di Pavia, Pavia; Italy.
- ⁷⁴(^a)INFN Sezione di Pisa; (^b)Dipartimento di Fisica E. Fermi, Università di Pisa, Pisa; Italy.
- ⁷⁵(^a)INFN Sezione di Roma; (^b)Dipartimento di Fisica, Sapienza Università di Roma, Roma; Italy.
- ⁷⁶(^a)INFN Sezione di Roma Tor Vergata; (^b)Dipartimento di Fisica, Università di Roma Tor Vergata, Roma; Italy.
- ⁷⁷(^a)INFN Sezione di Roma Tre; (^b)Dipartimento di Matematica e Fisica, Università Roma Tre, Roma; Italy.
- ⁷⁸(^a)INFN-TIFPA; (^b)Università degli Studi di Trento, Trento; Italy.

- ⁷⁹Universität Innsbruck, Department of Astro and Particle Physics, Innsbruck; Austria.
- ⁸⁰Department of Physics and Astronomy, Iowa State University, Ames IA; United States of America.
- ⁸¹Istinye University, Sariyer, Istanbul; Türkiye.
- ⁸²(^a) Departamento de Engenharia Elétrica, Universidade Federal de Juiz de Fora (UFJF), Juiz de Fora; (^b) Universidade Federal do Rio De Janeiro COPPE/EE/IF, Rio de Janeiro; (^c) Instituto de Física, Universidade de São Paulo, São Paulo; (^d) Rio de Janeiro State University, Rio de Janeiro; (^e) Federal University of Bahia, Bahia; Brazil.
- ⁸³KEK, High Energy Accelerator Research Organization, Tsukuba; Japan.
- ⁸⁴(^a) Khalifa University of Science and Technology, Abu Dhabi; (^b) University of Sharjah, Sharjah; United Arab Emirates.
- ⁸⁵Graduate School of Science, Kobe University, Kobe; Japan.
- ⁸⁶(^a) AGH University of Krakow, Faculty of Physics and Applied Computer Science, Krakow; (^b) Marian Smoluchowski Institute of Physics, Jagiellonian University, Krakow; Poland.
- ⁸⁷Institute of Nuclear Physics Polish Academy of Sciences, Krakow; Poland.
- ⁸⁸Faculty of Science, Kyoto University, Kyoto; Japan.
- ⁸⁹Research Center for Advanced Particle Physics and Department of Physics, Kyushu University, Fukuoka ; Japan.
- ⁹⁰L2IT, Université de Toulouse, CNRS/IN2P3, UPS, Toulouse; France.
- ⁹¹Instituto de Física La Plata, Universidad Nacional de La Plata and CONICET, La Plata; Argentina.
- ⁹²Physics Department, Lancaster University, Lancaster; United Kingdom.
- ⁹³Oliver Lodge Laboratory, University of Liverpool, Liverpool; United Kingdom.
- ⁹⁴Department of Experimental Particle Physics, Jožef Stefan Institute and Department of Physics, University of Ljubljana, Ljubljana; Slovenia.
- ⁹⁵Department of Physics and Astronomy, Queen Mary University of London, London; United Kingdom.
- ⁹⁶Department of Physics, Royal Holloway University of London, Egham; United Kingdom.
- ⁹⁷Department of Physics and Astronomy, University College London, London; United Kingdom.
- ⁹⁸Louisiana Tech University, Ruston LA; United States of America.
- ⁹⁹Fysiska institutionen, Lunds universitet, Lund; Sweden.
- ¹⁰⁰Departamento de Física Teórica C-15 and CIAFF, Universidad Autónoma de Madrid, Madrid; Spain.
- ¹⁰¹Institut für Physik, Universität Mainz, Mainz; Germany.
- ¹⁰²School of Physics and Astronomy, University of Manchester, Manchester; United Kingdom.
- ¹⁰³CPPM, Aix-Marseille Université, CNRS/IN2P3, Marseille; France.
- ¹⁰⁴Department of Physics, University of Massachusetts, Amherst MA; United States of America.
- ¹⁰⁵Department of Physics, McGill University, Montreal QC; Canada.
- ¹⁰⁶School of Physics, University of Melbourne, Victoria; Australia.
- ¹⁰⁷Department of Physics, University of Michigan, Ann Arbor MI; United States of America.
- ¹⁰⁸Department of Physics and Astronomy, Michigan State University, East Lansing MI; United States of America.
- ¹⁰⁹Group of Particle Physics, University of Montreal, Montreal QC; Canada.
- ¹¹⁰Fakultät für Physik, Ludwig-Maximilians-Universität München, München; Germany.
- ¹¹¹Max-Planck-Institut für Physik (Werner-Heisenberg-Institut), München; Germany.
- ¹¹²Graduate School of Science and Kobayashi-Maskawa Institute, Nagoya University, Nagoya; Japan.
- ¹¹³(^a) Department of Physics, Nanjing University, Nanjing; (^b) School of Science, Shenzhen Campus of Sun Yat-sen University; (^c) University of Chinese Academy of Science (UCAS), Beijing; China.
- ¹¹⁴Department of Physics and Astronomy, University of New Mexico, Albuquerque NM; United States of America.
- ¹¹⁵Institute for Mathematics, Astrophysics and Particle Physics, Radboud University/Nikhef, Nijmegen;

Netherlands.

¹¹⁶Nikhef National Institute for Subatomic Physics and University of Amsterdam, Amsterdam; Netherlands.

¹¹⁷Department of Physics, Northern Illinois University, DeKalb IL; United States of America.

¹¹⁸(^a)New York University Abu Dhabi, Abu Dhabi;(^b)United Arab Emirates University, Al Ain; United Arab Emirates.

¹¹⁹Department of Physics, New York University, New York NY; United States of America.

¹²⁰Ochanomizu University, Otsuka, Bunkyo-ku, Tokyo; Japan.

¹²¹Ohio State University, Columbus OH; United States of America.

¹²²Homer L. Dodge Department of Physics and Astronomy, University of Oklahoma, Norman OK; United States of America.

¹²³Department of Physics, Oklahoma State University, Stillwater OK; United States of America.

¹²⁴Palacký University, Joint Laboratory of Optics, Olomouc; Czech Republic.

¹²⁵Institute for Fundamental Science, University of Oregon, Eugene, OR; United States of America.

¹²⁶Graduate School of Science, University of Osaka, Osaka; Japan.

¹²⁷Department of Physics, University of Oslo, Oslo; Norway.

¹²⁸Department of Physics, Oxford University, Oxford; United Kingdom.

¹²⁹LPNHE, Sorbonne Université, Université Paris Cité, CNRS/IN2P3, Paris; France.

¹³⁰Department of Physics, University of Pennsylvania, Philadelphia PA; United States of America.

¹³¹Department of Physics and Astronomy, University of Pittsburgh, Pittsburgh PA; United States of America.

¹³²(^a)Laboratório de Instrumentação e Física Experimental de Partículas - LIP, Lisboa;(^b)Departamento de Física, Faculdade de Ciências, Universidade de Lisboa, Lisboa;(^c)Departamento de Física, Universidade de Coimbra, Coimbra;(^d)Centro de Física Nuclear da Universidade de Lisboa, Lisboa;(^e)Departamento de Física, Escola de Ciências, Universidade do Minho, Braga;(^f)Departamento de Física Teórica y del Cosmos, Universidad de Granada, Granada (Spain);(^g)Departamento de Física, Instituto Superior Técnico, Universidade de Lisboa, Lisboa; Portugal.

¹³³Institute of Physics of the Czech Academy of Sciences, Prague; Czech Republic.

¹³⁴Czech Technical University in Prague, Prague; Czech Republic.

¹³⁵Charles University, Faculty of Mathematics and Physics, Prague; Czech Republic.

¹³⁶Particle Physics Department, Rutherford Appleton Laboratory, Didcot; United Kingdom.

¹³⁷IRFU, CEA, Université Paris-Saclay, Gif-sur-Yvette; France.

¹³⁸Santa Cruz Institute for Particle Physics, University of California Santa Cruz, Santa Cruz CA; United States of America.

¹³⁹(^a)Departamento de Física, Pontificia Universidad Católica de Chile, Santiago;(^b)Millennium Institute for Subatomic physics at high energy frontier (SAPHIR), Santiago;(^c)Instituto de Investigación Multidisciplinario en Ciencia y Tecnología, y Departamento de Física, Universidad de La Serena;(^d)Universidad Andres Bello, Department of Physics, Santiago;(^e)Universidad San Sebastian, Recoleta;(^f)Instituto de Alta Investigación, Universidad de Tarapacá, Arica;(^g)Departamento de Física, Universidad Técnica Federico Santa María, Valparaíso; Chile.

¹⁴⁰Department of Physics, Institute of Science, Tokyo; Japan.

¹⁴¹Department of Physics, University of Washington, Seattle WA; United States of America.

¹⁴²(^a)Institute of Frontier and Interdisciplinary Science and Key Laboratory of Particle Physics and Particle Irradiation (MOE), Shandong University, Qingdao;(^b)School of Physics, Zhengzhou University; China.

¹⁴³(^a)State Key Laboratory of Dark Matter Physics, School of Physics and Astronomy, Shanghai Jiao Tong University, Key Laboratory for Particle Astrophysics and Cosmology (MOE), SKLPPC, Shanghai;(^b)State Key Laboratory of Dark Matter Physics, Tsung-Dao Lee Institute, Shanghai Jiao Tong University,

Shanghai; China.

¹⁴⁴Department of Physics and Astronomy, University of Sheffield, Sheffield; United Kingdom.

¹⁴⁵Department of Physics, Shinshu University, Nagano; Japan.

¹⁴⁶Department Physik, Universität Siegen, Siegen; Germany.

¹⁴⁷Department of Physics, Simon Fraser University, Burnaby BC; Canada.

¹⁴⁸SLAC National Accelerator Laboratory, Stanford CA; United States of America.

¹⁴⁹Department of Physics, Royal Institute of Technology, Stockholm; Sweden.

¹⁵⁰Departments of Physics and Astronomy, Stony Brook University, Stony Brook NY; United States of America.

¹⁵¹Department of Physics and Astronomy, University of Sussex, Brighton; United Kingdom.

¹⁵²School of Physics, University of Sydney, Sydney; Australia.

¹⁵³Institute of Physics, Academia Sinica, Taipei; Taiwan.

¹⁵⁴^(a)E. Andronikashvili Institute of Physics, Iv. Javakhishvili Tbilisi State University, Tbilisi; ^(b)High Energy Physics Institute, Tbilisi State University, Tbilisi; ^(c)University of Georgia, Tbilisi; Georgia.

¹⁵⁵Department of Physics, Technion, Israel Institute of Technology, Haifa; Israel.

¹⁵⁶Raymond and Beverly Sackler School of Physics and Astronomy, Tel Aviv University, Tel Aviv; Israel.

¹⁵⁷Department of Physics, Aristotle University of Thessaloniki, Thessaloniki; Greece.

¹⁵⁸International Center for Elementary Particle Physics and Department of Physics, University of Tokyo, Tokyo; Japan.

¹⁵⁹Graduate School of Science and Technology, Tokyo Metropolitan University, Tokyo; Japan.

¹⁶⁰Department of Physics, University of Toronto, Toronto ON; Canada.

¹⁶¹^(a)TRIUMF, Vancouver BC; ^(b)Department of Physics and Astronomy, York University, Toronto ON; Canada.

¹⁶²Division of Physics and Tomonaga Center for the History of the Universe, Faculty of Pure and Applied Sciences, University of Tsukuba, Tsukuba; Japan.

¹⁶³Department of Physics and Astronomy, Tufts University, Medford MA; United States of America.

¹⁶⁴Department of Physics and Astronomy, University of California Irvine, Irvine CA; United States of America.

¹⁶⁵University of West Attica, Athens; Greece.

¹⁶⁶Department of Physics and Astronomy, University of Uppsala, Uppsala; Sweden.

¹⁶⁷Department of Physics, University of Illinois, Urbana IL; United States of America.

¹⁶⁸Instituto de Física Corpuscular (IFIC), Centro Mixto Universidad de Valencia - CSIC, Valencia; Spain.

¹⁶⁹Department of Physics, University of British Columbia, Vancouver BC; Canada.

¹⁷⁰Department of Physics and Astronomy, University of Victoria, Victoria BC; Canada.

¹⁷¹Fakultät für Physik und Astronomie, Julius-Maximilians-Universität Würzburg, Würzburg; Germany.

¹⁷²Department of Physics, University of Warwick, Coventry; United Kingdom.

¹⁷³Waseda University, Tokyo; Japan.

¹⁷⁴Department of Particle Physics and Astrophysics, Weizmann Institute of Science, Rehovot; Israel.

¹⁷⁵Department of Physics, University of Wisconsin, Madison WI; United States of America.

¹⁷⁶Fakultät für Mathematik und Naturwissenschaften, Fachgruppe Physik, Bergische Universität Wuppertal, Wuppertal; Germany.

¹⁷⁷Department of Physics, Yale University, New Haven CT; United States of America.

¹⁷⁸Yerevan Physics Institute, Yerevan; Armenia.

^a Also at Affiliated with an institute formerly covered by a cooperation agreement with CERN.

^b Also at An-Najah National University, Nablus; Palestine.

^c Also at Borough of Manhattan Community College, City University of New York, New York NY; United States of America.

- d* Also at Center for Interdisciplinary Research and Innovation (CIRI-AUTH), Thessaloniki; Greece.
- e* Also at Centre of Physics of the Universities of Minho and Porto (CF-UM-UP); Portugal.
- f* Also at CERN, Geneva; Switzerland.
- g* Also at Département de Physique Nucléaire et Corpusculaire, Université de Genève, Genève; Switzerland.
- h* Also at Departament de Física de la Universitat Autònoma de Barcelona, Barcelona; Spain.
- i* Also at Department of Financial and Management Engineering, University of the Aegean, Chios; Greece.
- j* Also at Department of Mathematical Sciences, University of South Africa, Johannesburg; South Africa.
- k* Also at Department of Modern Physics and State Key Laboratory of Particle Detection and Electronics, University of Science and Technology of China, Hefei; China.
- l* Also at Department of Physics, Bolu Abant İzzet Baysal University, Bolu; Türkiye.
- m* Also at Department of Physics, King's College London, London; United Kingdom.
- n* Also at Department of Physics, Stanford University, Stanford CA; United States of America.
- o* Also at Department of Physics, Stellenbosch University; South Africa.
- p* Also at Department of Physics, University of Fribourg, Fribourg; Switzerland.
- q* Also at Department of Physics, University of Thessaly; Greece.
- r* Also at Department of Physics, Westmont College, Santa Barbara; United States of America.
- s* Also at Faculty of Physics, Sofia University, 'St. Kliment Ohridski', Sofia; Bulgaria.
- t* Also at Faculty of Physics, University of Bucharest ; Romania.
- u* Also at Hellenic Open University, Patras; Greece.
- v* Also at Henan University; China.
- w* Also at Imam Mohammad Ibn Saud Islamic University; Saudi Arabia.
- x* Also at Institutio Catalana de Recerca i Estudis Avancats, ICREA, Barcelona; Spain.
- y* Also at Institut für Experimentalphysik, Universität Hamburg, Hamburg; Germany.
- z* Also at Institute for Nuclear Research and Nuclear Energy (INRNE) of the Bulgarian Academy of Sciences, Sofia; Bulgaria.
- aa* Also at Institute of Applied Physics, Mohammed VI Polytechnic University, Ben Guerir; Morocco.
- ab* Also at Institute of Particle Physics (IPP); Canada.
- ac* Also at Institute of Physics and Technology, Mongolian Academy of Sciences, Ulaanbaatar; Mongolia.
- ad* Also at Institute of Physics, Azerbaijan Academy of Sciences, Baku; Azerbaijan.
- ae* Also at Institute of Theoretical Physics, Iliia State University, Tbilisi; Georgia.
- af* Also at Millennium Institute for Subatomic physics at high energy frontier (SAPHIR), Santiago; Chile.
- ag* Also at National Institute of Physics, University of the Philippines Diliman (Philippines); Philippines.
- ah* Also at The Collaborative Innovation Center of Quantum Matter (CICQM), Beijing; China.
- ai* Also at TRIUMF, Vancouver BC; Canada.
- aj* Also at Università di Napoli Parthenope, Napoli; Italy.
- ak* Also at University of Chinese Academy of Sciences (UCAS), Beijing; China.
- al* Also at University of Colorado Boulder, Department of Physics, Colorado; United States of America.
- am* Also at University of Sienna; Italy.
- an* Also at Washington College, Chestertown, MD; United States of America.
- ao* Also at Yeditepe University, Physics Department, Istanbul; Türkiye.
- * Deceased